

**LLNL Final Design for Thermal/Epithermal eXperiments
(TEX) with ZPPR Plutonium/Aluminum Plates with
Polyethylene and Tantalum**

IER-184 CED-2 Report



Catherine Percher
Soon Kim
David Heinrichs
Nuclear Criticality Safety Division

November 18, 2014

Auspices

This work performed under the auspices of the U.S. Department of Energy by Lawrence Livermore National Laboratory under Contract DE-AC52-07NA27344.

Disclaimer

This document was prepared as an account of work sponsored by an agency of the United States government. Neither the United States government nor Lawrence Livermore National Security, LLC, nor any of their employees makes any warranty, expressed or implied, or assumes any legal liability or responsibility for the accuracy, completeness, or usefulness of any information, apparatus, product, or process disclosed, or represents that its use would not infringe privately owned rights. Reference herein to any specific commercial product, process, or service by trade name, trademark, manufacturer, or otherwise does not necessarily constitute or imply its endorsement, recommendation, or favoring by the United States government or Lawrence Livermore National Security, LLC. The views and opinions of authors expressed herein do not necessarily state or reflect those of the United States government or Lawrence Livermore National Security, LLC, and shall not be used for advertising or product endorsement purposes.

0.0 Executive Summary

This report presents the results of final design (CED-2) for IER-184, Thermal/Epithermal experiments (TEX), and focuses on ten critical configurations with plutonium ZPPR plates moderated by polyethylene with and without a tantalum diluent. ^{239}Pu and ^{240}Pu were identified as being the number one and two nuclear data need at the original TEX meeting in Albuquerque, with special emphasis placed on performance issues of the Pu cross sections in the intermediate region. From the 2012 TEX preliminary design report, Ta was recommended as the first diluent to pursue for final design, as it represented a high priority data need, showed the highest sensitivity and largest contribution to uncertainty with the Pu ZPPR system, and the NCSP already owned a large amount of high quality Ta plates from the ZPPR inventory in Idaho.

A total of ten critical configurations were designed as part of CED-2. The universal critical assembly machine, Planet, will be used for the TEX experiments. Five TEX experiments (Experiments 1-5) were designed to establish baseline configurations with the Pu ZPPR plates covering the thermal, intermediate, and fast fission energy regimes. For all five experiments, the ZPPR plates will be arranged in layers of 24 plates (6 plates by 4 plates), resulting in approximately a 12 inch by 12 inch footprint. Multiple layers will be stacked together with varying thicknesses of interspersed polyethylene placed between the layers to fine tune the neutron spectrum of the assembly. The other five experiments (Experiments 6-10) will be similar to the five baseline experiments, except that a tantalum layer will be placed next to each plutonium plate layer, thus diluting the stack and allowing for tests of the neutron cross section for tantalum.

The assessment of experimental uncertainties gave very good results, especially considering the number of parts present in each configuration, with the total predicted uncertainty for the experiments as $0.0026 \Delta k_{\text{eff}}$. Due to the discovery of a large amount of historical information regarding the Pu/Al ZPPR plates at the Idaho National Laboratory Library Archives, the experimental uncertainties attributable to the ZPPR plates were very low. Uncertainties are dominated by assembly gaps and polyethylene dimensional tolerances, which will be further reduced by careful assembly and appropriate characterization measurements.

Due to the high plutonium loading of the TEX assemblies and the use of polyethylene, which has a low melting temperature, a thermal analysis was completed for the assemblies. While the calculations determined that the aluminum support structure used for the experiments transferred enough heat to keep temperatures well below any impact to the polyethylene, the addition of thin (0.01") aluminum heat transfer plates (fins) in contact with each plutonium layer was shown to flatten the temperature distribution over the entire assembly and keep all experiments at nearly the same low temperature. Therefore, fins were incorporated into the final design.

Fabrication costs are estimated to be \$21,800. Since the fissile material and diluent plates are existing, the remaining parts to be fabricated are polyethylene reflectors, polyethylene moderator sheets, aluminum heat dispersal plates, and the aluminum upper platen for use

with the Planet critical assembly machine. Composition and impurity analysis of the manufactured parts is estimated at \$20,000. Additionally, inspection, dimensional analysis, and contour measurements for a representative subset of all experimental parts (fissile and non-fissile) is estimated to be \$25,000.

NCERC is in possession of enough Pu ZPPR plates to complete two of the ten experiments in FY15. The remaining eight experiments will be completed once the remaining ZPPR inventory is transferred to NCERC in FY16.

Table of Contents

1.0 Introduction.....	7
2.0 Overview of CED-1	7
2.1 Justification of Need for Intermediate Energy Critical Experiments	7
2.2 TEX Meeting Summary.....	8
2.3 CED-1 Feasibility Results with Pu ZPPR Fuel.....	9
2.4 CED-1 Recommendations for Final Design.....	11
3.0 Experiment Description	12
3.1 Assembly Machine.....	12
3.2 Plutonium/Aluminum ZPPR Plates	13
3.2.1 ZPPR Plate Fabrication and Dimensional Information.....	13
3.2.2 ZPPR Plate Mass and Isotopic Information.....	22
3.3 Experimental Configurations.....	23
3.3.1 Plutonium Baseline Experiments.....	23
3.3.2 Tantalum Diluent Experiments.....	29
4.0 Calculational Models of the Experiments.....	37
4.1 Criticality and Spectrum Calculations	37
4.1.1 Methodology and Code Used	37
4.1.2 MCNP5 Model of Plutonium/Aluminum ZPPR Plates	38
4.1.3 MCNP5 Model of Experimental Configurations.....	45
4.1.4 MCNP5 Calculation Results	52
4.2 Uncertainty and Bias Characterization	61
4.2.1 Mass Uncertainties.....	61
4.2.2 Dimensional Uncertainties	62
4.2.3 Determination of Bias	63
4.2.4 Summary of Uncertainty and Bias Calculations.....	66
4.3 Thermal Analysis of ZPPR TEX Configurations.....	67
4.3.1 Methodology	67
4.3.2 ANSYS Model of ZPPR Stacks.....	68
4.3.3 Thermal Analysis Results.....	73
4.3.4 Thermal Analysis Conclusions.....	84
4.4 Structural Load Analysis for Aluminum Platen and Diaphragm.....	85
4.4.1 Load Analysis Methodology	85
4.4.2 SAP2000 FEA model	85
4.4.3 Load Analysis Results and Conclusions	86
5.0 Cost Estimates for Fabrication	88
6.0 Conclusions and Recommended Schedule for CED-3	89
6.1 Scheduling Considerations	89
6.1.1 NCSP Possession of ZPPR Plates	89
6.1.2 Fabrication of Moderators, Reflectors, and Fixturing.....	90
6.1.3 Subcritical Measurements to Confirm Temperature Calculations.....	90
6.1.4 Documented Safety Analysis MAR Limit for Planet.....	90

6.1.5 Characterization of ZPPR Plates	90
6.2 CED-3 Schedule	90
6.3 CED-4 Schedule	91
Appendix A: Sample MCNP5 Calculations	92
Appendix B: Design Drawings.....	113
Appendix C: Separation Distance Study for Estimating Critical Configurations	114
Appendix D: Partial Layer Study for Estimating Critical Configurations	117

1.0 Introduction

The need for epithermal and intermediate energy range critical benchmarks is an established international criticality safety data need. The goal of the Nuclear Criticality Safety Program's (NCSP) Thermal/Epithermal eXperiments (TEX) Project is to address this need by executing experiments with NCSP fissile assets that can be used to create critical assemblies that span a wide range of fission energy spectrums, from thermal (below 0.625 eV), through the intermediate energy range (0.625 eV to 100 keV), to fast (above 100 keV). An additional goal of the TEX project is to design critical assemblies that can be easily modified to include various high priority materials identified by the international criticality safety and nuclear data communities.

In FY2014, Lawrence Livermore National Laboratory was approved to complete final design for TEX experiments using plutonium Zero Power Research Reactor (ZPPR) fuel moderated with polyethylene and incorporating a high-priority diluent of interest, tantalum.

2.0 Overview of CED-1

Critical Experiment Preliminary Design (CED-1) for TEX was completed in FY2012¹. The NCSP national inventory was evaluated to find fissile material candidates that could be assembled into experimental configurations that would span a broad range of energies. Four candidate fissile materials were considered in CED-1, 7Up low enriched uranium oxide fuel, highly enriched uranium Jemima plates, plutonium/aluminum ZPPR fuel, and a new fissile fuel form, low enriched uranium molybdenum alloy. It was determined that the TEX goals could be met with all fuel forms besides the 7Up fuel. Due to the high priority of ²³⁹Pu and ²⁴⁰Pu cross section data needs and the results of sensitivity and uncertainty calculations presented in CED-1, it was recommended the first TEX experiments focus on the Pu/Al ZPPR fuel.

2.1 Justification of Need for Intermediate Energy Critical Experiments

During the half century of active criticality experimental programs around the world, the majority of the experimentation focused on thermal neutron systems (the energy regime of solutions and light water nuclear reactors) and fast neutron systems (the energy regime of nuclear weapons and fast nuclear reactors). The intermediate energy regime, between the 0.625 eV "thermal cutoff" and 100 keV, was not a major experimental focus due to the lack of driving intermediate energy nuclear applications. The 2011 edition of the International Criticality Safety Benchmark Evaluation Project (ICSBEP) handbook includes 96 intermediate energy critical and subcritical benchmarks (greater than 50% of

¹ Percher, C. and D. Heinrichs. *IER-184 CED-1 Report: LLNL Preliminary Design for Thermal/Epithermal eXperiments (TEX)*. Lawrence Livermore National Laboratory. September 15, 2012.

the fissions occur in the intermediate range) out of a total of 4550 configurations, or only 2.1%.²

With the reduction in critical experimental facilities and the higher reliance placed on ever-improving radiation transport codes, the lack of intermediate energy benchmarks poses a challenge to the modern-day nuclear criticality safety (NCS) practitioner. Nuclear operations encompass a wide range of fissionable, reflector, and moderator materials that are evaluated by NCS engineers under both normal and credible abnormal conditions, usually with the aid of computational codes. These computational models are relied upon to set safety limits, and can in some cases result in a system where greater than 50% of the fissions occur in the intermediate spectrum. Intermediate spectra are created when a system is under-moderated but contains enough moderator or scattering materials to partially slow originally fast fission neutrons. Since hydrogenous materials are often used for contamination control, vaults and storage arrays are prime configurations that can create an intermediate system. Additionally, abnormal conditions involving fire-suppression systems (the addition of water or sprinkler mists) to an operation can likewise result in an intermediate energy system. Further complexity is added to the problem of lack of experimental intermediate energy benchmarks due to the underlying nuclear data. Resonance effects dominate in the intermediate energy range, giving the underlying cross section data much more structure, in general, than the more well-behaved thermal and fast cross sections. These resonance effects show up as peaks and valleys in the cross sections and experimental cross section measurement data must be fit with calculational techniques. In the resolved resonance region, the experimental resolution is smaller than the width of the resonances, allowing for accurate fitting of the data using relatively simple techniques such as the generalized-least squares method. In the unresolved resonance region, unresolved multiplets of resonances overlap each other and make simple fitting of the cross section curve impossible. Much more involved fitting techniques involving average values of physical quantities obtained in the resolved range, statistical methods, and scientific judgment are used to try and calculate the unresolved region. High-quality intermediate energy critical benchmarks are also, therefore, important to the nuclear data community as a way to validate their fitting methods and data.³

2.2 TEX Meeting Summary

The U.S. Nuclear Criticality Safety Program (NCSP), a Department of Energy Headquarters Program under NA-16, convened a meeting in July of 2011 to discuss the intermediate energy data and experimental needs of criticality safety practitioners. The meeting was held at Sandia National Laboratories (SNL) in Albuquerque, NM with attendees from the U.S., the United Kingdom, and France. The meeting was convened

² NEA/NSC/DOC(95)03. *International Handbook of Evaluated Criticality Safety Benchmark Experiments*. September 2011 Edition. Nuclear Energy Agency. Organisation for Economic Cooperation and Development.

³ Leal, L.C. et al. "Nuclear Data for Criticality Safety- Current Issues." *Proceedings of the Nuclear Criticality Technology and Safety Project Embedded Topical Meeting*. San Diego, CA. May 17, 1995.

under the name “Thermal/Epithermal eXperiments (TEX) Feasibility Meeting,” but the focus of the meeting quickly shifted more generally to the lack of experimental data in the intermediate energy range. At the TEX meeting, the first day of the two day meeting was dedicated to representatives from the U.S., U.K., and France discussing their high priority needs for benchmark data. The consensus prioritization of data needs was published in the TEX meeting minutes, as follows: ^{239}Pu , ^{240}Pu , ^{238}U , ^{235}U , Temperature variations, Water density variations, Steel, Lead reflection, Hafnium, Tantalum, Tungsten, Nickel, Molybdenum, Chromium, Manganese, Copper, Vanadium, Titanium, and Concrete reflection (focusing on characterization and water content).

2.3 CED-1 Feasibility Results with Pu ZPPR Fuel

The TEX CED-1 report demonstrated with Scale/KENO calculations that it is feasible to create multiple critical systems with the Pu ZPPR plates and varying thicknesses of polyethylene with different fission energy spectrums, including a mixed spectrum that is largely intermediate. The critical system design was a simple, unreflected stack of homogenized Pu/Al ZPPR plates in approximately 12” by 12” layers (as if they were constructed of 24 2” by 3” by 1/8” thick ZPPR plates arranged in a square pattern) interspersed with varying amounts of polyethylene, as shown in Figure 2.1. The report also showed feasibility of creating critical, largely intermediate systems with the addition of diluent plates of nickel, iron, copper, tungsten, molybdenum, tantalum, and hafnium.

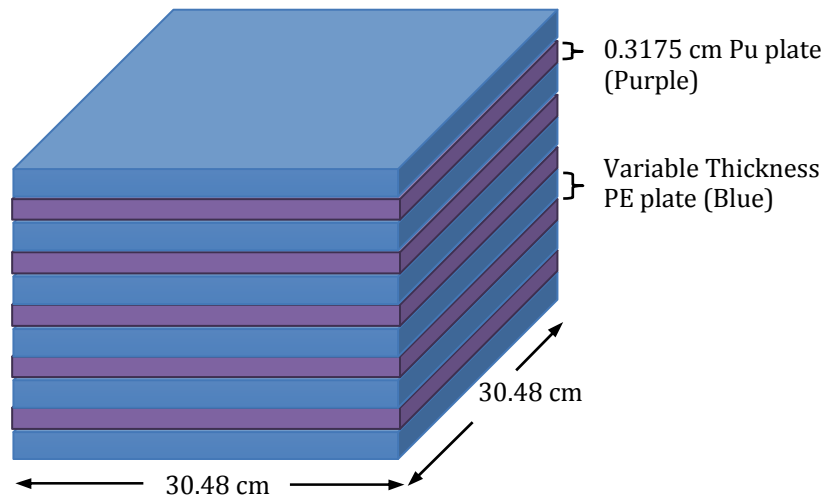


Figure 2.1: Representation of the Keno Geometry for Pu ZPPR Plates Moderated by Polyethylene. The homogenized Pu ZPPR plates are shown in purple and were kept a constant 0.3175 cm (1/8 in) thickness. The polyethylene (shown in blue) thickness was varied to increase the level of moderation and soften the neutron spectrum. The figure is not to scale.

Aside from simply having the right energy spectrum for a critical benchmark, a goal of

the CED-1 report was also to investigate the potential of the intermediate energy systems to test high priority cross sections as identified by the nuclear data and criticality safety international communities. To this end, TSUNAMI-3D was employed to examine the sensitivity of the SCALE/KENO models to a 1% change in the constituent materials' cross sections. Figure 2.2 summarizes the sensitivity data presented in the CED-1 report. The “Total Sensitivity”, shown as light blue bars, is reported as the positive sensitivity plus the absolute value of the negative sensitivity for the most important nuclides in the KENO models. The intermediate sensitivity (red bars) is only the portion of the sensitivity attributed to the intermediate energy region.

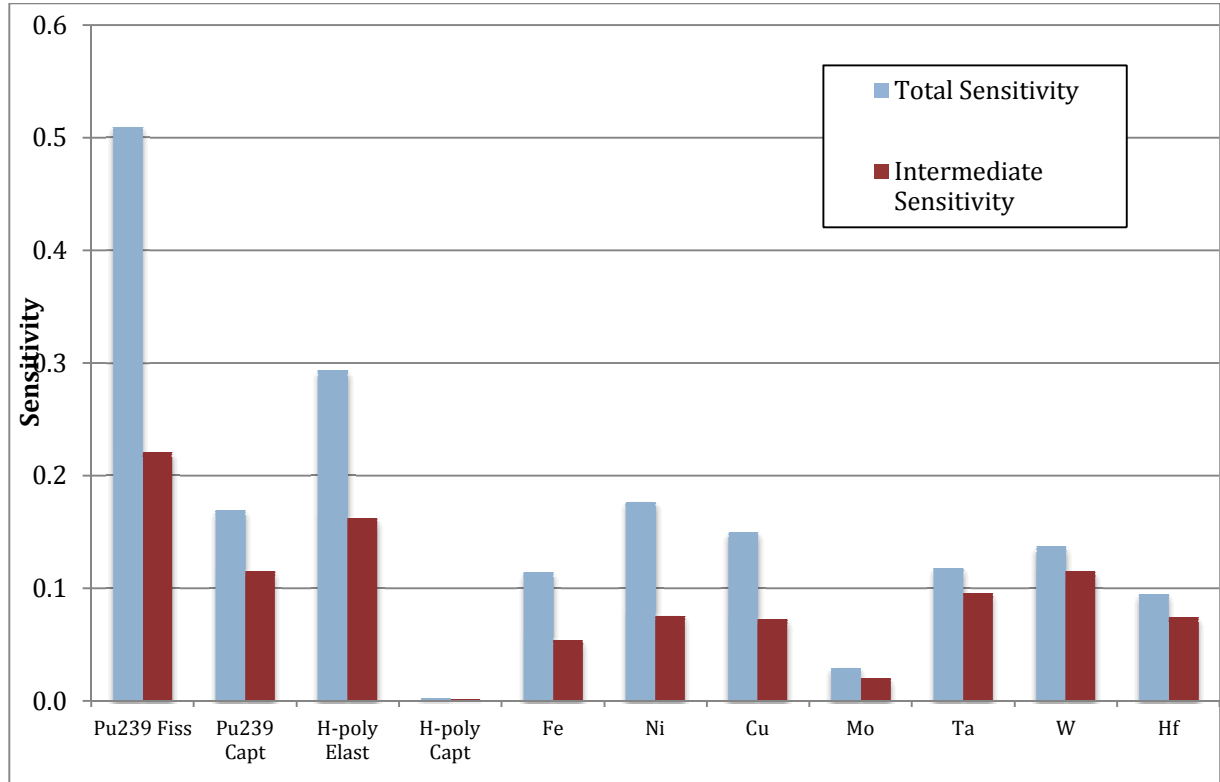


Figure 2.2: Total and Intermediate Energy Sensitivity Summary for Materials of Interest for the Pu ZPPR Plates. Sensitivities are reported as the positive sensitivity plus the absolute value of the negative sensitivity and include only the nuclides found to have the highest contribution to overall sensitivity.

As seen in the Figure 2.2, the Pu ZPPR/PE system was most sensitive to changes in the ^{239}Pu fission cross section, with just under half of the sensitivity attributable to the intermediate energy region. From the sensitivity data for the diluent materials (Fe, Ni, Cu, Mo, Ta, W, and Hf), the Pu ZPPR/PE system would be most useful in testing the tantalum and tungsten cross sections in the intermediate energy region, followed by hafnium, nickel, and copper. The molybdenum diluent thickness that would allow criticality in the intermediate energy region was too thin to have a high sensitivity effect. One limitation with the current version of TSUNAMI is that it does not examine differences in the angular distribution of the scattering cross sections, which could have a large effect on the k_{eff} for the cases with diluent materials.

As presented in the TEX CED-1 report and reproduced in Table 2-1, uncertainties in the cross sections for tantalum, tungsten, and hafnium play a large role in the total uncertainty, indicating an increased need for experiments to test these cross sections.

Table 2-1: Uncertainty Results Summary for Each Diluent Material of Interest with the Pu ZPPR Plates and Polyethylene Moderation

Diluent Material	Case ID	Total Uncertainty from All Sources (%$\Delta k/k$)	Percent Contribution from Diluent
Fe	zfepe2	0.9969	1.29
Ni	znipe2	1.0213	2.90
Cu	zcupe2	1.0115	2.42
Mo	zmope2	0.9889	1.10
Ta	ztape2	1.2917	25.47
W	zwpe2	1.1637	12.92
Hf	zhfpe2	1.0633	4.92

2.4 CED-1 Recommendations for Final Design

As documented in the TEX CED-1 report, configurations made with plutonium ZPPR fuel moderated by polyethylene systems with and without diluents showed the highest sensitivities of the systems studied to changes in the cross sections of interest as reported by TSUNAMI. Additionally, ^{239}Pu and ^{240}Pu were identified as being the number one and two nuclear data need at the original TEX meeting in Albuquerque, with special emphasis placed on performance issues of the Pu cross sections in the intermediate region. LLNL recommended that CED-2 for TEX focus on experiment designs based on Pu ZPPR plates.

Seven diluents were studied in CED-1, but Ta is recommended as the first diluent for final design. The highest priority diluents from the TEX meeting were Fe (major component of steel), Hf, and Ta. Of these three, Ta showed the highest cross section sensitivity when used as a diluent in the Pu/Al ZPPR and polyethylene system. Additionally, Ta provided the highest contribution to total system uncertainty of any diluent studied, as shown in Table 2-1. Finally, the NCSP owns a large amount of high quality Ta plates from the ZPPR inventory in Idaho, so diluent plates will not need to be fabricated.

3.0 Experiment Description

3.1 Assembly Machine

One of the two universal critical assembly machines, Planet or Comet, will be used for the TEX experiments. Planet and Comet are vertical lift machines that are used to separate a critical assembly into halves. The upper half of the assembly is supported on a stationary platen and the bottom half is supported by a movable platform. The bottom platform is raised to achieve or approach criticality and is raised until it contacts the top portion of the assembly. Figure 3.1 shows a picture of the Planet machine with a previously conducted experiment. The figure was taken from the ICSBEP Handbook, evaluation HEU-MET-THERM-001⁴. Comet and Planet are designed with a similar basic structure and can accept the same experimental fixturing.

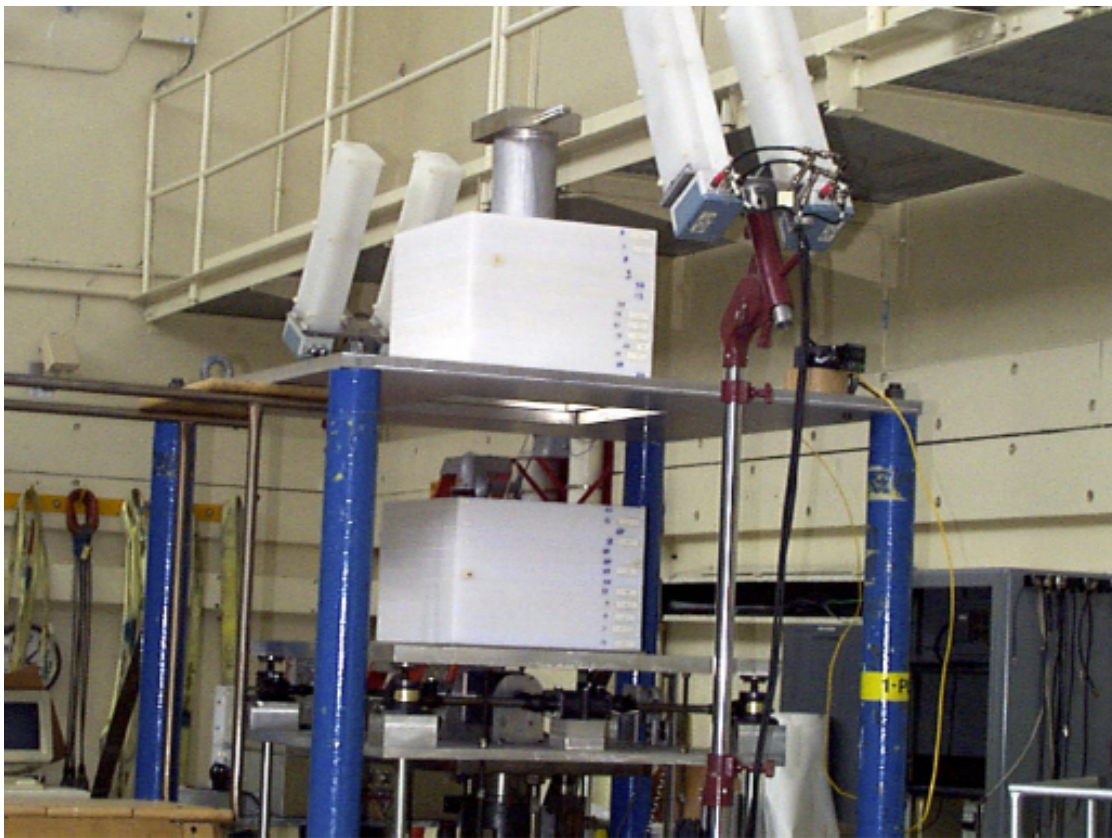


Figure 3.1: Planet Machine in 1998 Loaded with Polyethylene Reflected and Moderated Highly Enriched Uranium Experiment with Silicon (HEU-MET-THERM-001)

⁴ Brewer, R. HEU-MET-THERM-001, *Polyethylene Reflected and Moderated Highly Enriched Uranium System with Silicon*. International Handbook of Evaluated Criticality Safety Benchmark Experiments. NEA/NSC/DOC(95)03/I. September 2013.

The TEX experimental setup consists of layers of plutonium plates and polyethylene with an 18 in by 18 in footprint. The upper platen, with outer dimensions of 45 in by 45 in, will be rigidly attached to the Planet (or Comet) supports (shown in blue in Figure 3.1). A drawing of the platen design, which will need to be fabricated before use, is shown in Appendix B. The outer edge of the plate is 1" thick Aluminum 6061 and has a 19" square section in the middle of the plate with a thinner diaphragm (0.125" Al-6061). The experiment stack will be centered on the thin diaphragm. The lower half of the assembly will rest on an existing 1.5" aluminum plate that is 31" by 31" square (similar to the bottom platform shown in Figure 3.1). The drawing for this plate is also provided in Appendix B.

3.2 Plutonium/Aluminum ZPPR Plates

The Argonne National Laboratory procured many types of fissile material fuels for its ZPPR program. A subset of this fuel is stainless steel-clad plutonium plates that are delta-stabilized with approximately 1.1 weight percent aluminum. The Pu/Al plates of interest to the TEX program are the Plutonium Aluminum No Nickel (PANN) plates, fabricated by the Dow Chemical Company at Rocky Flats in 1960. There are three different sizes of the PANN plates, but the majority have nominal outer cladding dimensions of 1/8" (0.3175 cm) by 2" (5.08 cm) by 3" (7.62 cm).

3.2.1 ZPPR Plate Fabrication and Dimensional Information

Due to the limited amount of information regarding the dimensions of the Pu ZPPR plates available at the time, the calculations for CED-1 were greatly simplified. The plutonium, aluminum, air gaps, and 304 stainless steel cladding were homogenized over the entire plate for the Scale/KENO models. As part of final design, a large amount of historical information regarding the Pu/Al ZPPR plates was uncovered at the Idaho National Laboratory Library Archives. The following discussion is based on the original specification for the Pu/Al plates⁵, the original drawing of the plates⁶, and an ANL document that discusses the fabrication of the plates⁷. The cores were fabricated by rolling cast slabs of Pu/Al to the desired thickness, 0.084 to 0.086 in (2.13 to 2.18 mm), and strips were sheared and machined to a width of 1.763 to 1.767 in (4.478 to 4.488 cm). The cores were cut to a length of 2.923 to 2.937 in (7.424 to 7.460 cm) and the edges were radiused. The plutonium core with dimensions from the specification is shown in Figure 3.3 and the original drawing is provided in Appdenix A.

As detailed in the original specification, the ²³⁹Pu content of each plate had the most restrictive tolerance, with a target mass of 98.98 ± 0.5 g. As such, the specification allowed the weight of the core to be adjusted by drilling 3/32" to 1/4" diameter holes,

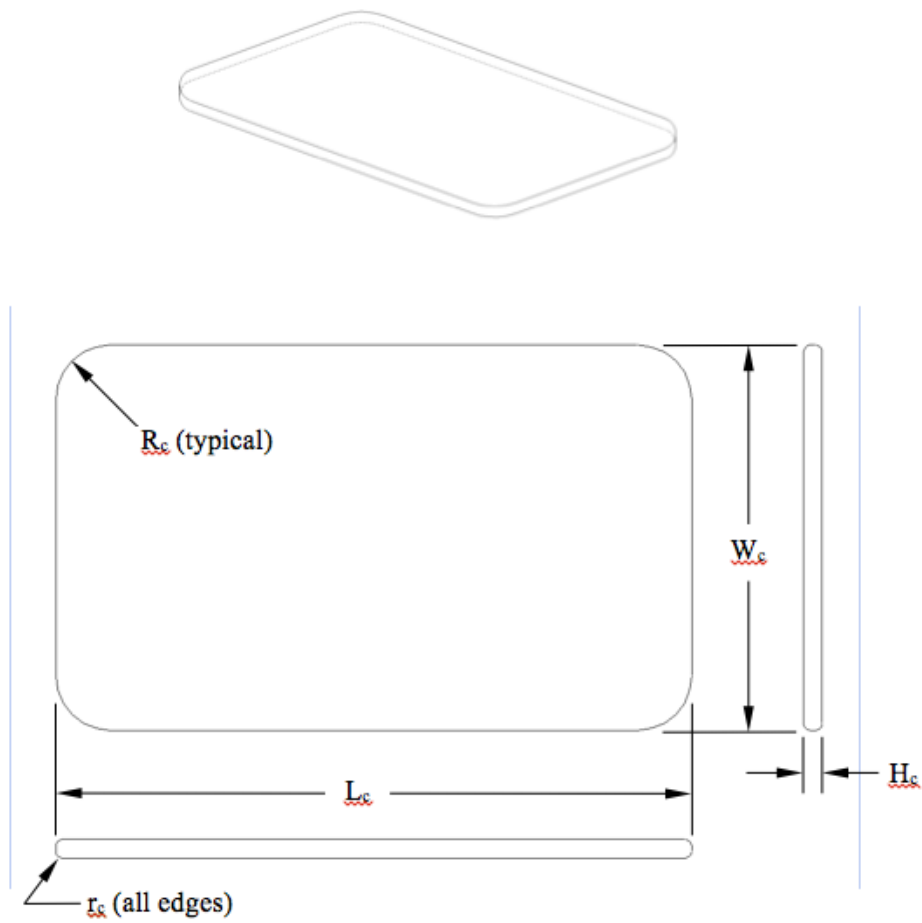
⁵ *Stainless Steel Jacketed, Nickel Plated Plutonium Aluminum Alloy Fuel Elements, Zero Power Reactor 3*. Argonne National Laboratory. August 15, 1960.

⁶ *3" Fuel Plate*. Argonne National Laboratory. Drawing No. PF-1303. August 1960.

⁷ Shuck, A.B et al. *The Development of a Design and Fabrication Method for Plutonium-Bearing Zero-Power Reactor Fuel Elements*. Argonne National Laboratory. ANL-7313. August 1967.

with a maximum of five holes in scattered locations in a single core. Alternatively, the edges and corners were allowed to be shaved as long as the dimensions did not fall below the minimum specifications. The original specification called for plutonium with 93.5 wt % ^{239}Pu to be used to make the plates. However, as detailed in Section 3.2.2 (below), the ^{239}Pu content of the plates was actually 95.02 wt %. This discrepancy is explained in a letter dated November 29, 1960 from Dow Chemical to ANL⁸. The letter states that the U.S. Atomic Energy Commission (AEC- precursor agency to the Department of Energy) had ruled that declassified material must be used for the fabrication of the fuel plates. The available material was 95.02% ^{239}Pu . Since higher ^{239}Pu content plutonium was used for the plates, the size of the cores will likely be closer to the minimums required by the specification to achieve the tight tolerances on the ^{239}Pu target mass.

⁸ Langell, F.H. Letter from F.H. Langell to Norman Hilberry. *ZPR-III Plutonium Alloy Fuel Elements*. November 29, 1960.



Dimension	inches	centimeters
L_c	$2.937 \frac{+0.000}{-0.014}$	$7.460 \frac{+0.000}{-0.036}$
W_c	$1.767 \frac{+0.000}{-0.004}$	$4.488 \frac{+0.000}{-0.013}$
H_c	$0.086 \frac{+0.000}{-0.002}$	$0.218 \frac{+0.000}{-0.005}$
R_c	1/16 to 1/4	0.158 to 0.635
r_c	1/64 to 1/32	0.040 to 0.079

Figure 3.3. Attributes of the Plutonium-Aluminum Alloy Core (PF-1301-1).

The construction of the stainless steel cladding and assembly of the plate is shown in Figures 3.4 and 3.5. The following discussion is largely taken from ANL 7313 (Reference 5), Section 1.B. Figure 3.6 shows the outer dimensions of the stainless steel cladding from the original specification and drawing. The cladding was fabricated by folding 12-mil, Type 304 stainless steel strips around a rectangular mandrel and welding one edge (Steps A-D of Figure 3.4). A flat plug was then welded into the bottom (Step E of Figure 3.5). The dimensions of the plug are shown in Figure 3.7. The cladding was made to a relatively loose fit to facilitate core loading. A flat spring was placed in one end of the cladding to hold the core plate against the opposite end of the cladding. The uncompressed spring dimensions are shown in Figure 3.8. According to the specification, the plates are marked with the core batch letter and core batch serial number along the short edge of the plate closest to the spring.

As detailed in the original specification for the Pu/Al plates, each plate was to be coated with nickel deposited from carbonyl to allow loading and welding without cladding contamination and to form a secondary oxidation barrier. The carbonyl-nickel coating was found to be impractical to apply and prohibitively costly. Dow Chemical Company personnel developed a method of loading that protected the cladding from contamination by means of a disposable, shim-stock loading funnel and sheath. This method was used for the PANN plates, which is why they do not have the nickel coating.

The side of the element through which the cladding was loaded was closed by a stainless steel plug strip (Step G in Figure 3.5). The welds were made at sub-atmospheric pressure of helium-argon gas mixture by means of a TIG welder developed at Argonne National Laboratory. The reduced-pressure welds were required to prevent inflation of the cladding at lower atmospheric pressure and by thermally expanded gas. The external atmospheric pressure forced the sides of the cladding against the core plate.

The final, fully assembled plate had to pass through a go-no-go gage, which effectively set the upper bound for the outer dimensions of the clad plate. Three gages were used: a 0.125" gage to check height, a 3.01" gage to check the length of the plate, and a 2.00" gage to check the width of the plate. Each plate was required to pass through the gages by the force of their own weight.

According to ANL-7313, the design of these plates provided a number of lessons learned incorporated in the designs of later ZPR fuel. The springs were not sufficiently strong to hold the core against one end of the cladding during thermal expansion and contractions and were abandoned for later designs. Also, the ratio of stainless steel volume to core volume was "objectionably high."

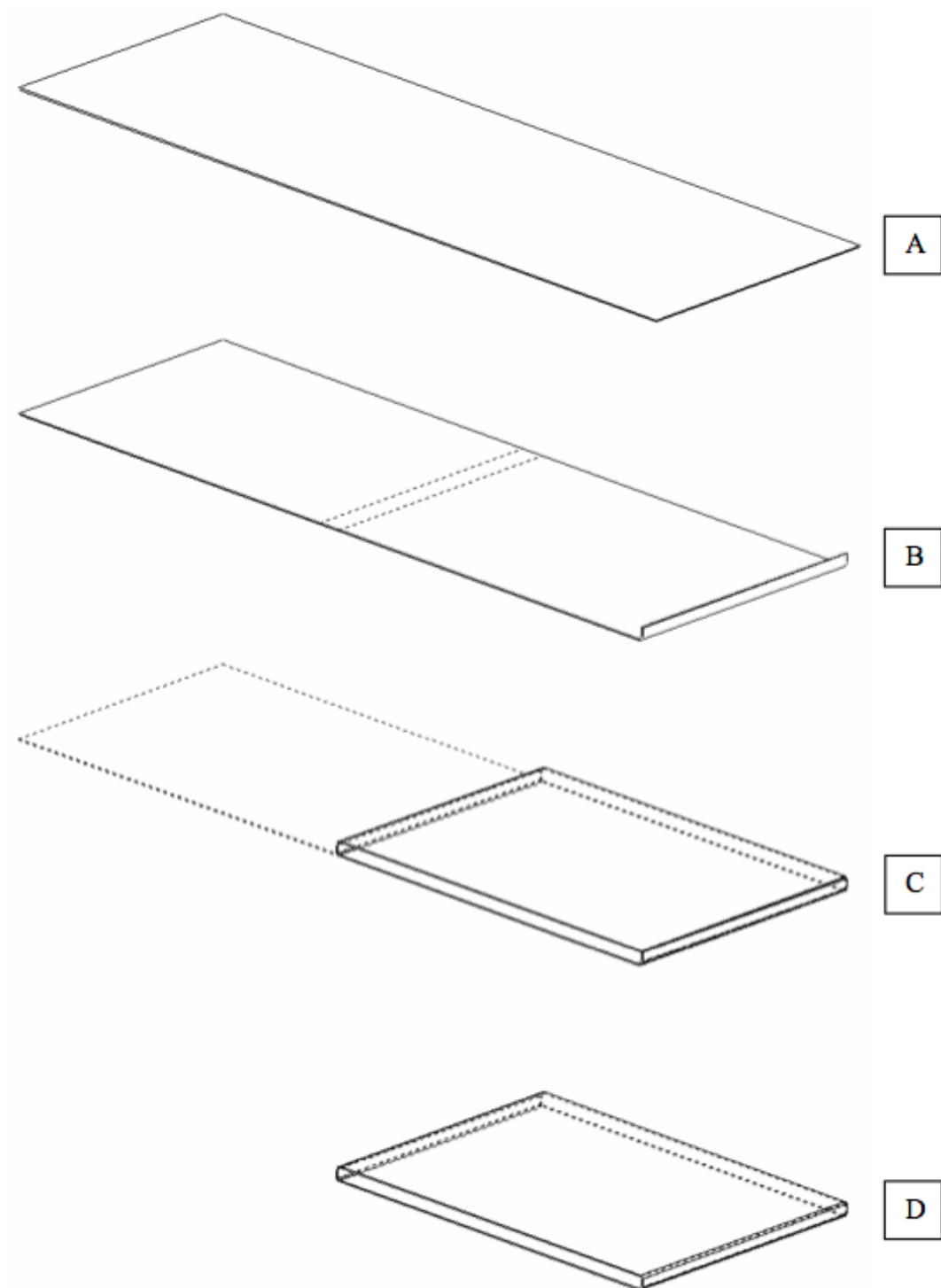


Figure 3.4. A strip of thin stainless steel sheet (A) is bent 90° at specified locations along its length (B) so that the opposite ends may be welded together (C) to form a narrow sleeve with open sides (D).

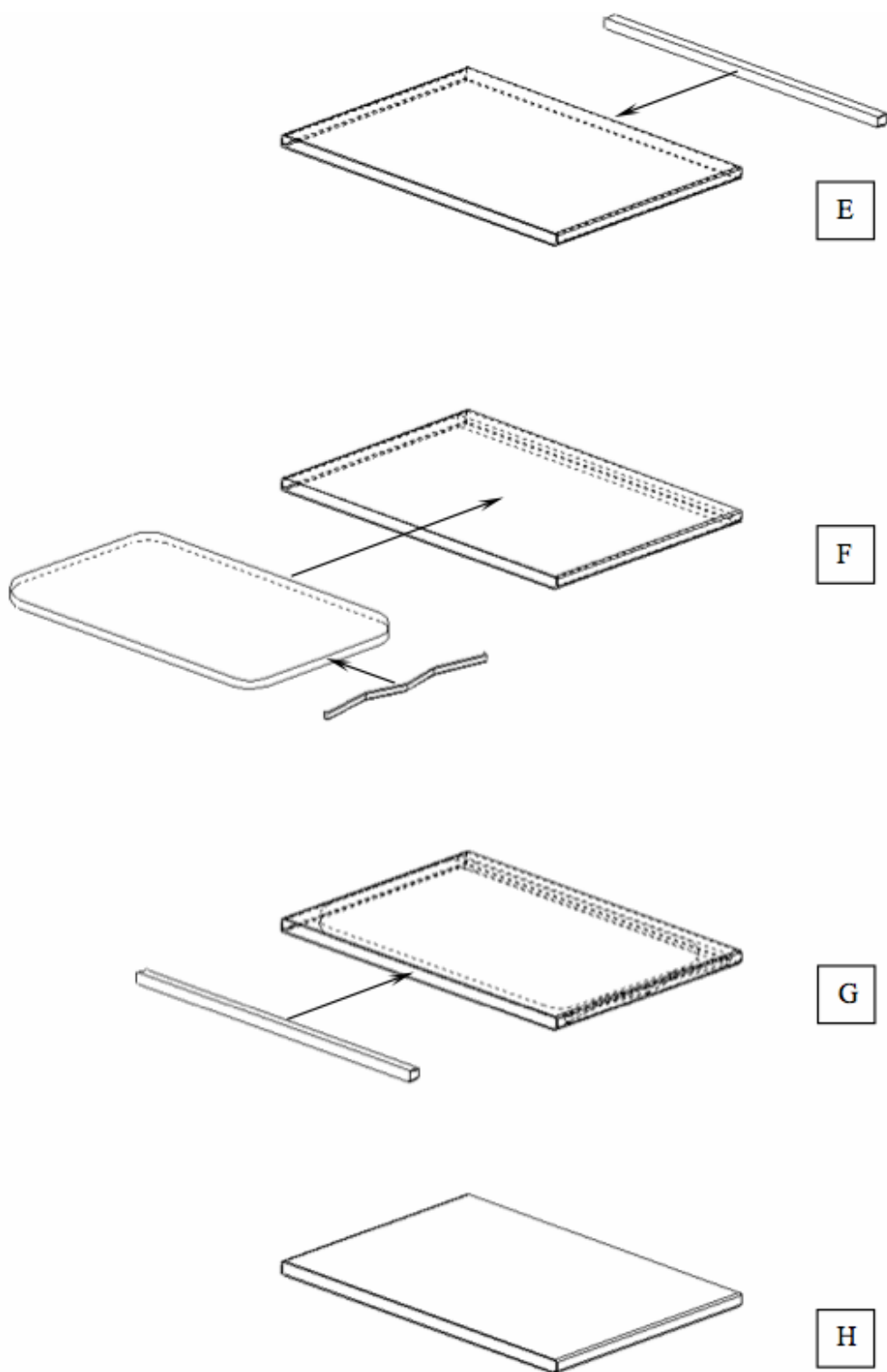
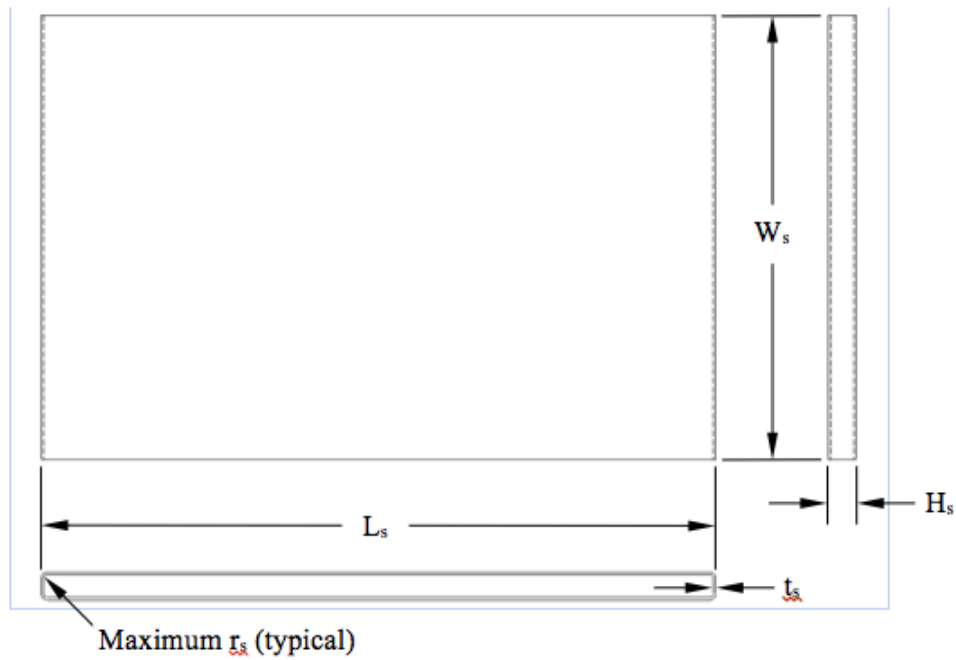
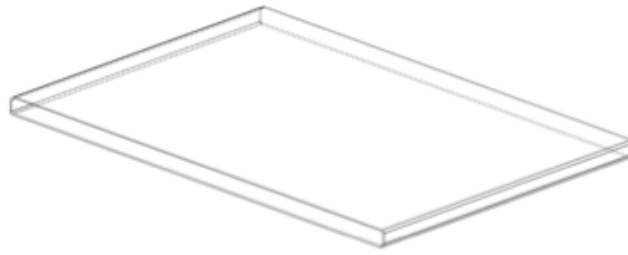
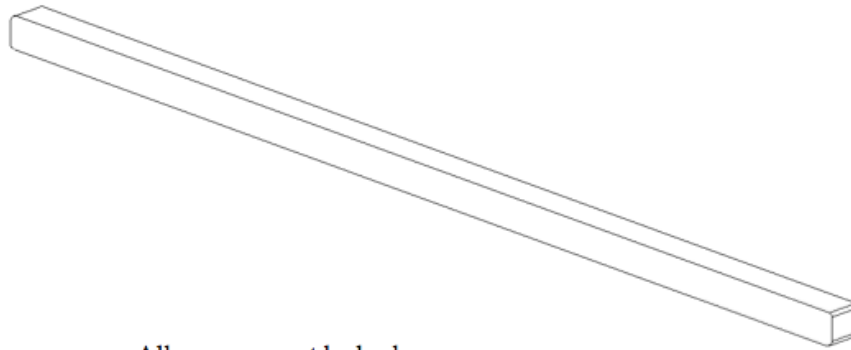


Figure 3.5. A stainless steel plug is welded to close one side of the sleeve (E), a carbon steel spring and an un-clad plutonium-aluminum alloy core are inserted through the open side of the sleeve (F), and a second plug is welded to close the other side of the sleeve (G) to yield a completely sealed plate (H).

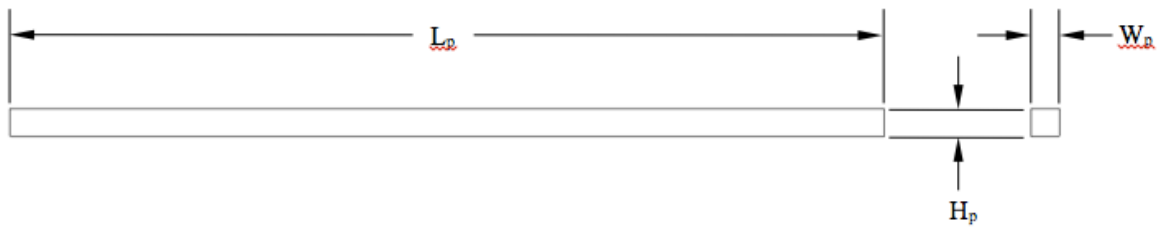


Dimension	inches	centimeters
L_s	$3.005 \frac{+ 0.000}{- 0.005}$	$7.6327 \frac{+ 0.0000}{- 0.0127}$
W_s	$1.975 \frac{+ 0.005}{- 0.005}$	$5.01565 \frac{+ 0.0127}{- 0.0127}$
H_s	$0.125 \frac{+ 0.000}{- 0.004}$	$0.3175 \frac{+ 0.00000}{- 0.01016}$
t_s	$0.012 \frac{+ 0.001}{- 0.001}$	$0.03048 \frac{+ 0.00254}{- 0.00254}$
r_s	1/64	0.0396875

Figure 3.6. Attributes of a stainless steel sleeve prior to plate assembly (PF-1301-2).

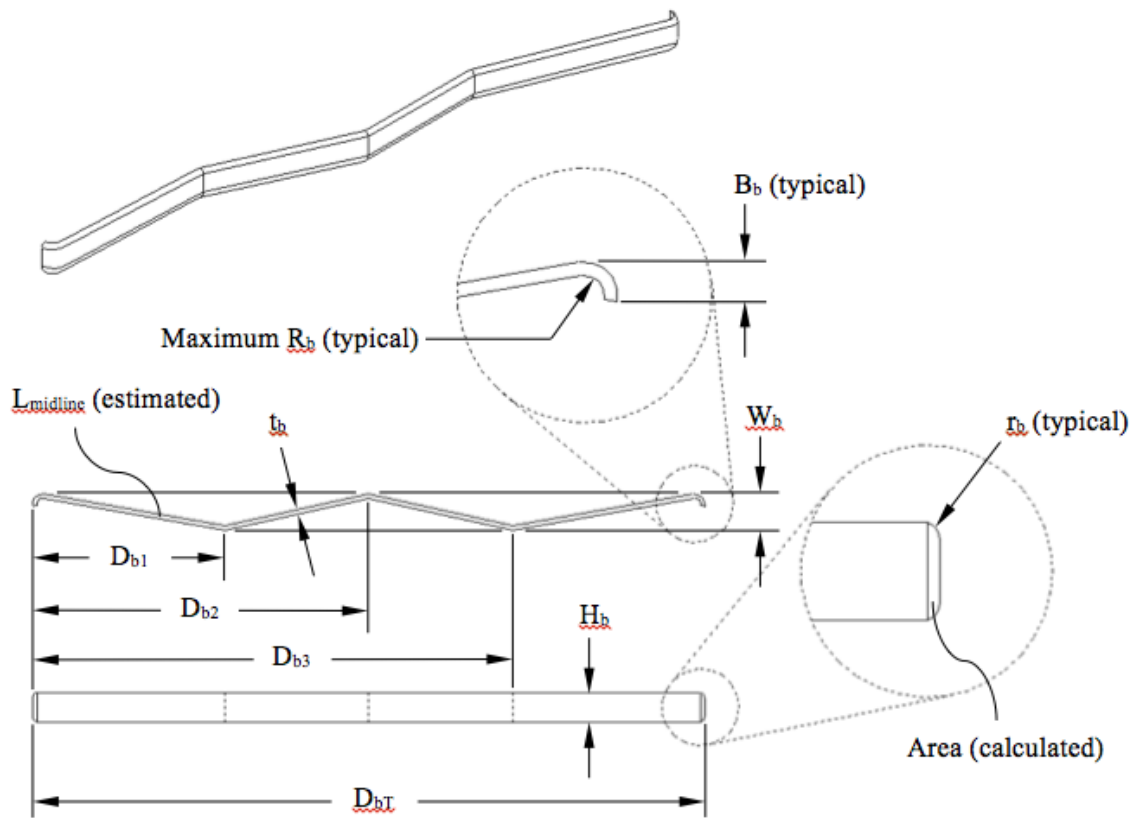


All corners must be broken



Dimension	inches	centimeters
L_p	$2.974 \begin{smallmatrix} + 0.000 \\ - 0.001 \end{smallmatrix}$	$7.55396 \begin{smallmatrix} + 0.00000 \\ - 0.00254 \end{smallmatrix}$
W_p	$0.096 \begin{smallmatrix} + 0.000 \\ - 0.001 \end{smallmatrix}$	$0.24384 \begin{smallmatrix} + 0.00000 \\ - 0.00254 \end{smallmatrix}$
H_p	$0.096 \begin{smallmatrix} + 0.000 \\ - 0.001 \end{smallmatrix}$	$0.24384 \begin{smallmatrix} + 0.00000 \\ - 0.00254 \end{smallmatrix}$

Figure 3.7. Attributes of a stainless steel plug prior to plate assembly (PF-1301-3).



Dimension	inches	centimeters
D_{b3}	1-1/4	3.175
D_{b2}	7/8	2.2225
D_{b1}	1/2	1.27
D_{bT}	1-3/4	4.445
H_b	5/64	0.1984375
W_b	3/32	0.238125
B_b	1/32	0.079375
R_b	1/64	0.0396875
r_b	1/64	0.0396875
t_b (#31 gage)	0.0105	0.02667
L_{midline} (estimated)	~1.804	~4.582
Area (calculated)	~0.000736 in ²	~0.00475 cm ²

Figure 3.8. Attributes of an uncompressed carbon steel spring prior to plate assembly (PF-1301-4).

3.2.2 ZPPR Plate Mass and Isotopic Information

Composition data presented here was taken from an Argonne database that contained plate-by-plate detailed information on overall plate mass, Pu/Al core mass, and major isotopic composition masses. Fuel and clad masses and compositions for the Pu-Al plates are given in Tables 3-1 and 3-2. Each Pu-Al fuel core was weighed before and after cladding. The required accuracy of these original measurements was 0.01 grams on a balance having a precision of 0.005 grams and the entire population of 1266 3-inch PANN plates was measured. Similarly, samples from each melt were analyzed when the fuel was cast, and these data were used to derive the aluminum, impurity, and plutonium isotopic mass distributions in Table 3-1. These original measurements form the basis of the “hot constants memo” a summary of information in the ANL electronic plate material library (ADEN library). The last and most recently issued hot constants memo is dated April 2001⁹.

Table 3-1: As Fabricated PANN Plate Information, July 1, 1960

	Mean Mass per Plate (g)	Standard Deviation (g)	Minimum (g)	Maximum (g)
²³⁸ Pu	0	0	0	0
²³⁹ Pu	99.029	0.270	98.139	99.693
²⁴⁰ Pu	4.724	0.100	4.518	4.955
²⁴¹ Pu	0.460	0.065	0.341	0.585
²⁴² Pu	0.005	0.009	0	0.030
²⁴¹ Am	0	0	0	0
Al	1.158	0.0464	1.046	1.217
Impurities (by Difference)	0.007	0.009	0.001	0.036
Total for Core	105.383	0.2497	104.636	105.884
Cladding	24.765	0.046	24.711	54.872
Total for Plate	130.148	0.248	129.476	130.650

(a) Information based on detailed plate database.

Table 3-2. 304-L Stainless Steel Cladding Mass and Composition for the PANN Plates

Clad Mass (g)	Composition, wt. %									
	C	Si	P	S	Cr	Mn	Fe	Ni	Cu	Mo
24.76	0.065	0.477	0.024	0.020	18.455	1.696	69.701	8.965	0.279	0.319

⁹ Klann, R.T., B.D. Austin, S.E. Aumeier, D.N. Olsen. *Inventory of Special Nuclear Materials from the Zero Power Physics Reactor*. Argonne National Laboratory-West. ANL-NT-176. April 2001.

At ANL in 1960, there was a significant effort put into Pu-Al alloy development as part of the Experimental Breeder Reactor (EBR)-II project. An internal ANL memorandum¹⁰ gives the density of plutonium alloy with 1.1 wt.% aluminum as ranging between 15.11 and 15.27 g/cm³, with a mean value of 15.19 g/cm³.

3.3 Experimental Configurations

3.3.1 Plutonium Baseline Experiments

Five TEX experiments were designed to establish baseline configurations covering the thermal, intermediate, and fast fission energy regimes. For all five experiments, the ZPPR plates will be arranged in layers of 24 plates (6 plates by 4 plates), resulting in approximately a 12 in by 12 in footprint. Figure 3.9 shows the maximum dimensions of a layer, based on ZPPR plate documentation.

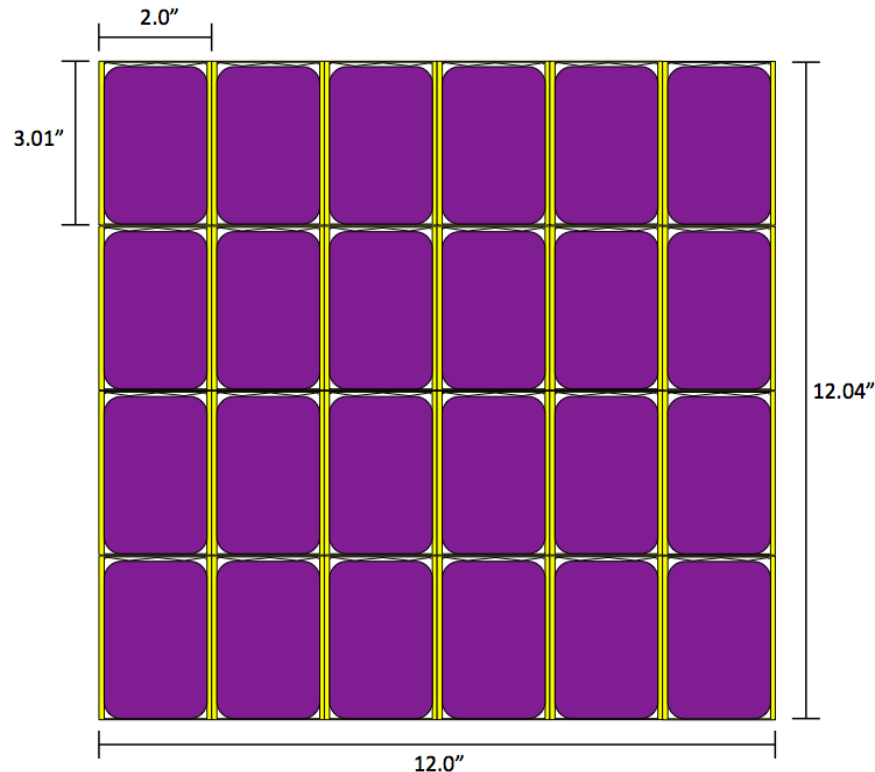


Figure 3.9: Single Layer of 24 Pu/Al ZPPR Plates Arranged in a Square Pattern

Multiple layers will be stacked together with varying thicknesses of interspersed polyethylene placed between the layers to tune the neutron spectrum of the assembly.

¹⁰ Shuck, A.B. Internal Memorandum from A.B. Shuck to F.W. Thalgott. *Specification for PF-1301/3 Pu-Al ZPR-III Elements*. Argonne National Laboratory. Metallurgy Division. July 27, 1960.

The plutonium layers will be arranged on trays to facilitate stacking of the experimental assembly. There will be two kinds of trays used for the plutonium baseline experiments. The first tray, with a 0.01" aluminum bottom, is only used in the fast (unmoderated) case and has an integrated heat dispersal plate that extends beyond the edge of the tray. Aluminum 6061 will be used for stability of the tray. The second tray, with a 1/16" thick high-density polyethylene (CH₂) bottom in addition to a 0.01" aluminum bottom, provides moderation, heat dispersal, and support for the Pu plates. The trays incorporate 1" of radial reflection around the edge of the plutonium layer, provided by a polyethylene frame. The trays are held together with polyethylene rivets or pins that are poly-welded in place in eight locations around the perimeter of the tray. Drawings of the two trays are shown in Figure 3.10 (aluminum-bottomed tray) and Figure 3.11 (polyethylene-bottomed tray).

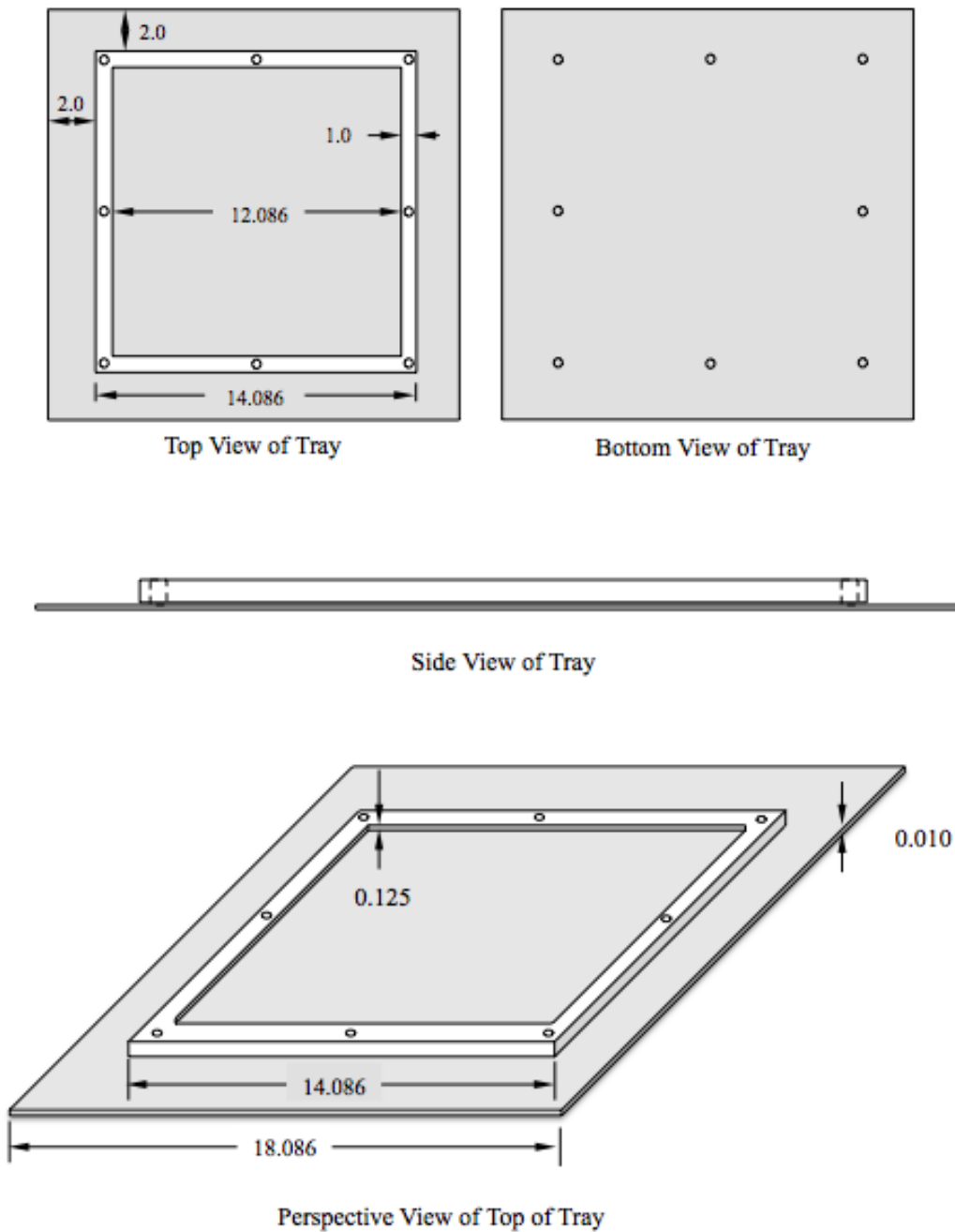


Figure 3.10: Aluminum and Polyethylene Tray for Use in Unmoderated Experiments. The top figures show plan views of the tray (from above and below), the middle figure shows a side-on view of the tray, and the bottom figure is a perspective view showing the well for the ZPPR Pu layer. All dimensions are shown in inches. The eight small circles around the outside of the tray show the polyethylene pin locations.

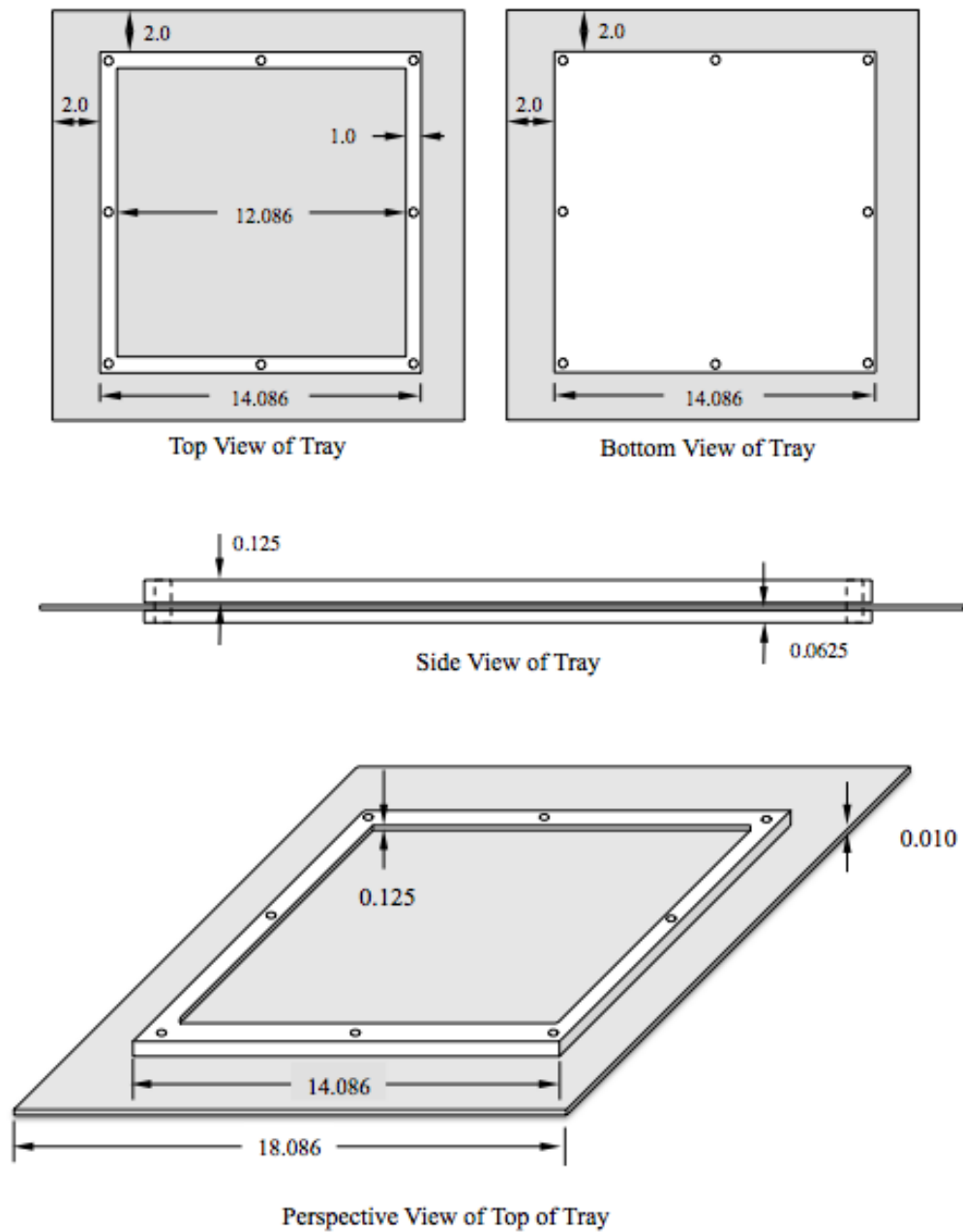


Figure 3.11: Aluminum and Polyethylene Tray for Use in Moderated Experiments. The top figures show plan views of the tray (from above and below), the middle figure shows a side-on view of the tray, and the bottom figure is a perspective view showing the well for the ZPPR Pu layer. All dimensions are shown in inches. The eight small circles around the outside of the tray show the polyethylene pin locations. This tray differs from the tray shown in Figure 3.10 by the 1/16" inch of polyethylene layer below the aluminum heat dispersal plate, which provides additional stability to the plate and moderation for the experiment.

The 1" of close-fitting polyethylene provided by the frame will help decouple the experiment from the effects of room return. Additional 1" thick slabs of polyethylene will be added to the top and bottom of the stack for additional reflection.

Additionally, a 1/16" diameter cylindrical slot will be machined in the bottom of some of the polyethylene trays to accommodate existing thermocouples to collect temperature data on the experimental stacks. These slots are shown in the drawings provided in Appendix B.

Thin aluminum plates (0.01" thick) are incorporated into the tray design and will be in contact below each plutonium layer to transfer heat out of the assembly (see Section 4.2 of this report for a discussion of the thermal analysis of the experiments). The aluminum plate will be 18.05" by 18.05" to extend beyond the edge of the 1" polyethylene reflector by 2" all around.

Five experimental configurations will be part of the baseline TEX Pu ZPPR series. The difference between the experiments will be the thickness of polyethylene moderator that will be placed between each 24 plate plutonium layer. The polyethylene thickness between each layer will be varied from zero to 1 inch, including the 1/16" of polyethylene provided by the moderated trays. Polyethylene will be added to the stack in the form of plastic sheets of varying thicknesses. A 1/16" diameter cylindrical slot will be machined in the bottom of some of the polyethylene-bottomed trays to accommodate existing thermocouples to collect temperature data on the experimental stacks. These slots are shown in the drawings provided in Appendix B.

Cross section views of the five configurations are shown in Figures 3.12 through 3.16. For all pictures, the plutonium fuel meat is shown as purple and the stainless steel cladding is shown as yellow. Polyethylene is shown as blue and aluminum (Planet/Comet platform, platen, and heat dispersal plates) are shown in green. Figure 3.13 gives an additional detailed view with labeled dimensions.

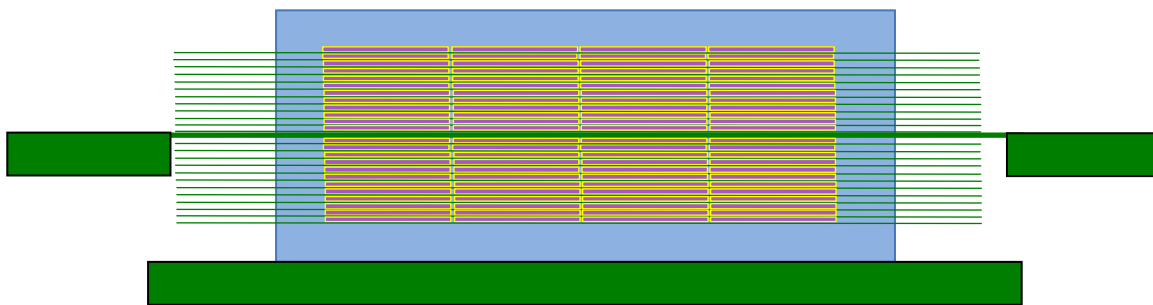


Figure 3.12. Experimental Configuration for Experiment 1: ZPPR Plate Layers with No Interspersed Polyethylene. This experiment consists of 21 layers of Pu and is a fast neutron system.

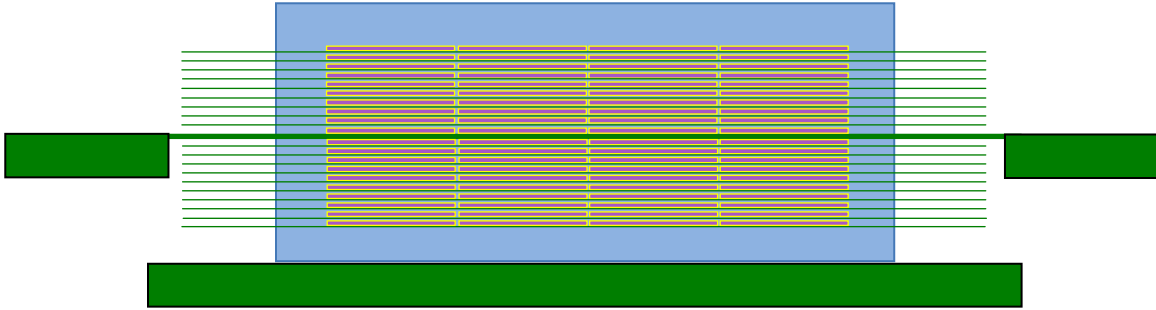


Figure 3.13. Experimental Configuration for Experiment 2: ZPPR Plate Layers with 0.0625 inches Interspersed Polyethylene. This experiment consists of 17 layers of Pu.

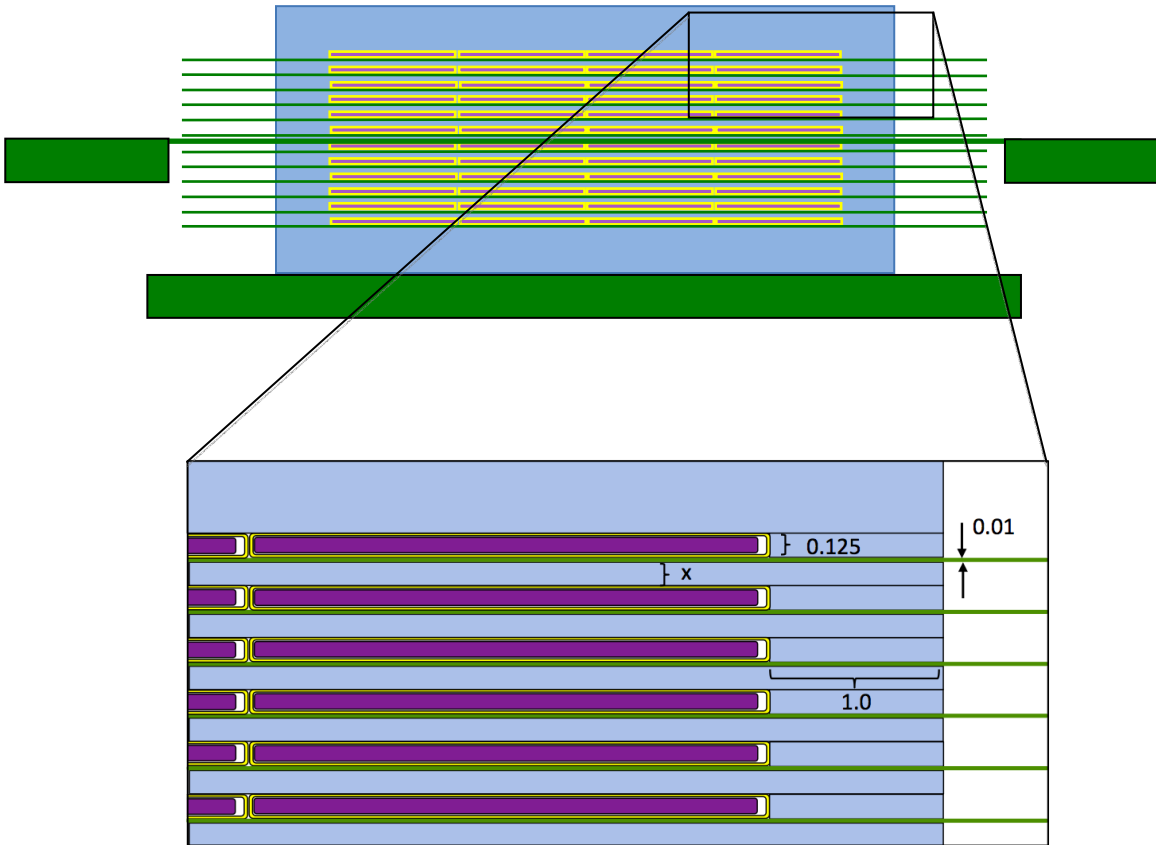


Figure 3.14. Experimental Configuration for Experiment 3: ZPPR Plate Layers with 0.1875 inches Interspersed Polyethylene. This experiment consists of 12 layers of Pu. The “x” in the lower figure is the variable thickness of polyethylene that can be added to the stack.

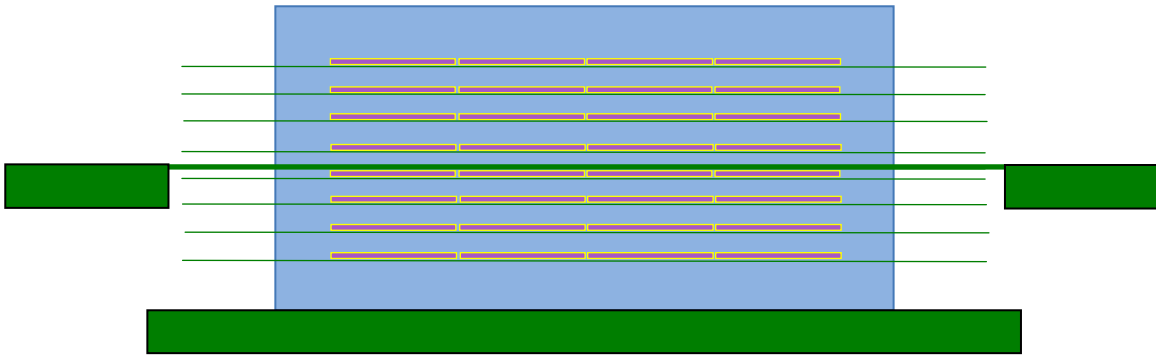


Figure 3.15. Experimental Configuration for Experiment 4: ZPPR Plate Layers with 0.4375" Interspersed Polyethylene. This experiment consists of 8 layers of Pu.

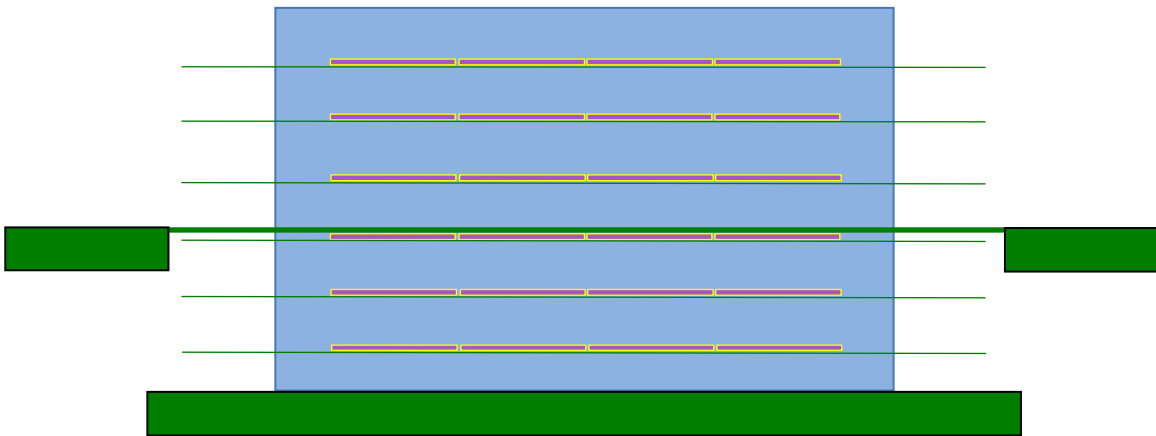


Figure 3.16. Experimental Configuration for Experiment 5: ZPPR Plate Layers with 1" Interspersed Polyethylene. This experiment consists of 6 layers of Pu.

3.3.2 Tantalum Diluent Experiments

Tantalum layers will be added to the five TEX baseline experiments (described above) to provide tests for the tantalum cross sections.

3.3.2.1 Tantalum Plate Description

As part of the ZPPR inventory, ANL had approximately 15000 very pure tantalum plates with nominal outer dimensions of 2" by 3" by 1/16". These plates are made of relatively pure tantalum and are unclad. Data on the tantalum plates from the most recent "hot constants memos" is provided in Table 3-3.

Table 3-3: Tantalum Information from ADEN Database

Size	Average Weight	Ta wt. %	Other wt. %
2"x3"x1/16"	101.95 g	99.968	0.032

Additional information on the tantalum plates was discovered in the Idaho National Laboratory Library Archives. The plates were made by the Union Carbide Corporation and the initial lot of Ta plates were fabricated in 1969. The original drawing could not be located for dimensional tolerances, but a 1969 intra-laboratory correspondence between ANL personnel indicated the acceptable weight range for the plates was between 100 and 104 grams¹¹.

The tantalum plates are currently in storage at the Nevada Nuclear Security Site. Since they are accessible, twenty five plates were chosen at random and measured with electronic calipers and weighed on a electronic balance. The results are presented in Table 3-4.

Table 3-4: Measurement Results for 25 Randomly-Chosen Tantalum Plates

Measured Parameter	Mean	Standard Deviation
Plate Length (in)	2.993	0.0010
Plate Width (in)	1.995	0.0009
Plate Height (in)	0.062	0.0007
Plate Mass (g)	102.122	0.980

A certified report of chemical analysis from the Union Carbide Corporation was found in the ANL archives. The report findings are reproduced in Figure 3.17.

¹¹ Huke, F.B. Internal Memorandum from F.B. Huke to R. Tuma. *Inspection of Tantalum Rod and Plate*. Argonne National Laboratory. July 8, 1969.

UNION CARBIDE CORPORATION
MATERIALS SYSTEMS DIVISION
KOKOMO, INDIANA

CERTIFIED REPORT OF CHEMICAL ANALYSIS AND MECHANICAL TESTS

Argonne National Lab
Acctg Dept.
9700 So. Cass Ave
Argonne, Ill 60440

SPECIFICATION NO. ---- RF-C4A	ALLOY HAYNES Tantalum	CUSTOMER IDENTIFICATION RP-1-49520-B Part 1	OUR IDENTIFICATION Plate 565240
OUR SALES ORDER NO. 70032	CUST. PURCHASE ORDER NO. 644803 Item/Control No.2	QUANTITY SHIPPED 1230 pcs.	DATE SHIPPED 6-25-69

CHEMICAL ANALYSIS

HEAT NO.	Cr	W	Fe	C	Si	Co	Ni	Mn	V	Mo	Cu	Pd	Sn	Cb+Ta
818061	<10	<100	<20	<10	<10	<5	<20	<10	<20	<20	<10	<10	<10	185
	$\frac{Al}{<20}$	$\frac{Ti}{<10}$	$\frac{B}{<5}$	$\frac{Cd}{<10}$	$\frac{Zr}{<50}$	$\frac{Ta}{99.9\%}$	$\frac{Mg}{<5}$	$\frac{O}{21^2}$	$\frac{H}{3^2}$	$\frac{N}{19^2}$	$\frac{Yb}{<10}$	$\frac{E}{<50}$	$\frac{Hf}{<50}$	

Elements in PPM unless otherwise stated.

Figure 3.17. Tantalum Impurity Information from Manufacturer.

3.3.2.2 Tantalum Diluted Critical Configurations

Tantalum layers will be constructed out of 24 Ta ZPPR plates in a similar manner to the Pu/Al ZPPR plate layers (6 plates by 4 plates). For all five experiments, Ta plate layers will be placed on top and in contact with each Pu/Al layer. The Ta plate layers will be rotated 90 degrees to the Pu/Al layers to reduce neutron streaming paths. Figure 3.18 shows the maximum dimensions of a layer, based on the nominal Ta ZPPR plate dimensions.

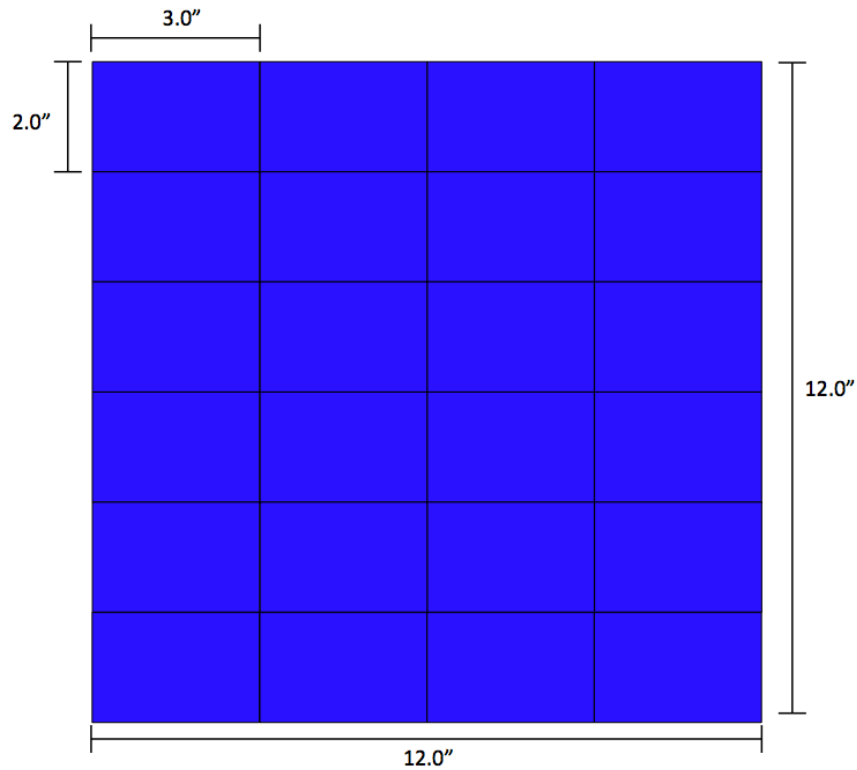


Figure 3.18: Single Layer of 24 Ta ZPPR Plates Arranged in a Square Pattern

As in the TEX Pu baseline experiments, the plutonium layers will be arranged on trays to facilitate stacking of the experimental assembly. Additional trays will be fabricated for the tantalum-diluted experiments that are 1/16" deeper to accommodate the tantalum. For the unmoderated assembly, the 0.01" aluminum bottom tray will be used. The tray bottom is also used as a heat dispersal plate and thus the plutonium will be placed directly on the aluminum bottom and the tantalum layer will be placed on top of the plutonium layer. Aluminum 6061 will be used for stability of the tray. The second tray, with a 1/16" thick high-density polyethylene (CH₂) bottom, provides both moderation and support for the Pu and Ta plates. Again, the Pu will be placed into the tray in contact with the aluminum heat dispersal plate and the tantalum placed on top of the Pu layer. Drawings of the two trays are shown in Figure 3.19 (aluminum-bottomed tray) and Figure 3.20 (polyethylene-bottomed tray).

All configurations will be reflected by 1" of close-fitting polyethylene on all sides to help decouple the experiment from the effects of room return. The tray walls will incorporate the 1" of polyethylene reflection and additional 1" thick slabs of polyethylene will be added to the top and bottom of the stack for reflection.

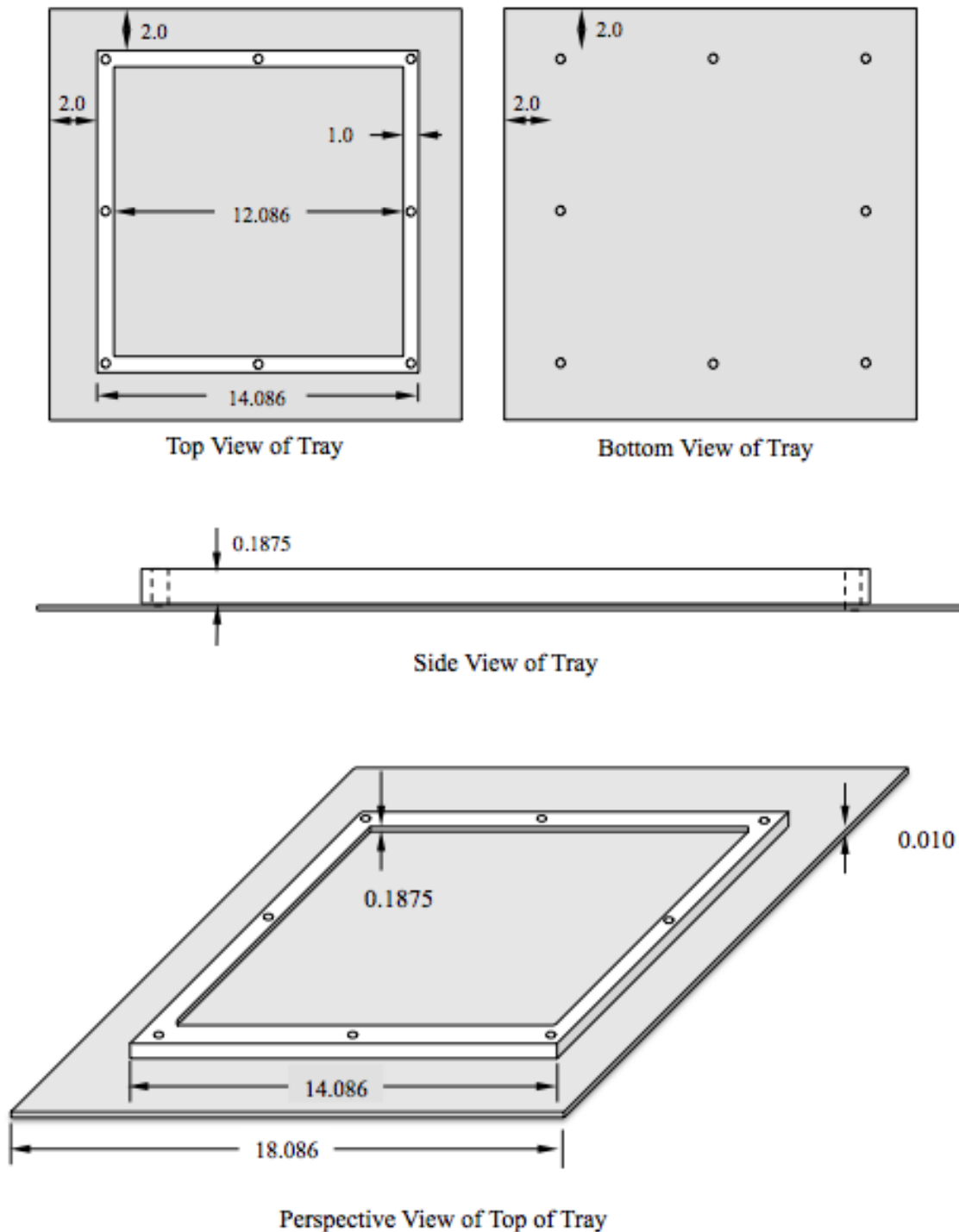


Figure 3.19: Aluminum and Polyethylene Tray for Use in Unmoderated Tantalum Experiments. The top figures show plan views of the tray (from above and below), the middle figure shows a side-on view of the tray, and the bottom figure is a perspective view showing the well for the ZPPR Pu layer. All dimensions are shown in inches. The eight small circles around the outside of the tray show the polyethylene pin locations. The difference between this tray and the tray shown in Figure 3.10 (tray for the baseline line experiments) is a slightly deeper well to accommodate both the Ta and Pu layer.

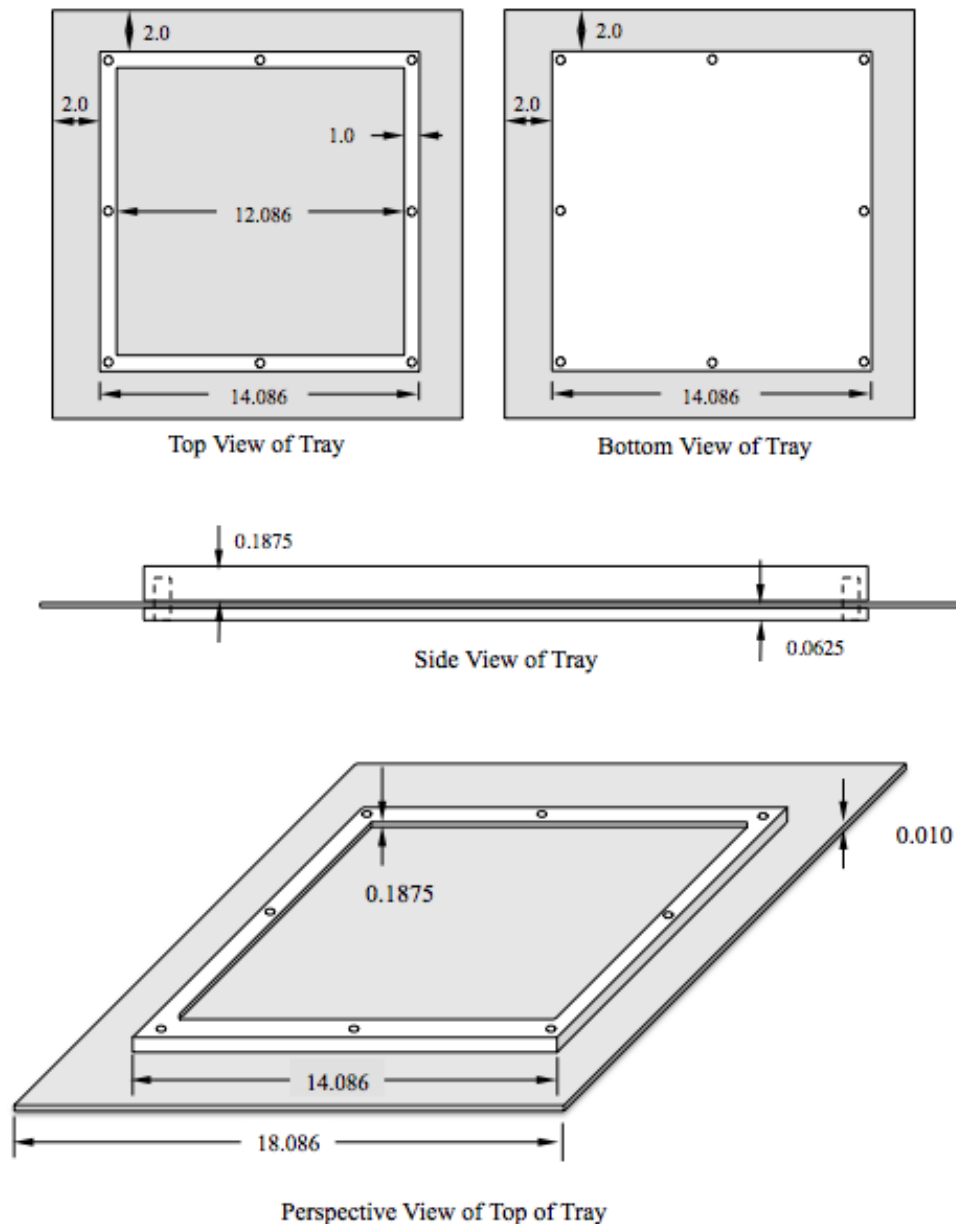


Figure 3.20: Aluminum and Polyethylene Tray for Use in Moderated Tantalum Experiments. The top figures show plan views of the tray (from above and below), the middle figure shows a side-on view of the tray, and the bottom figure is a perspective view showing the well for the ZPPR Pu layer. All dimensions are shown in inches. The eight small circles around the outside of the tray show the polyethylene pin locations. The difference between this tray and the tray shown in Figure 3.11 (tray for the baseline line experiments) is a slightly deeper well to accommodate both the Ta and Pu layer.

Five experimental configurations will be part of the Ta-diluted TEX Pu ZPPR series. The difference between the experiments will be the thickness of polyethylene moderator that will be placed between each Pu/Ta layer. The polyethylene thickness between each layer will be varied from zero to 1 inch. Cross section views of the five configurations

are shown in Figures 3.21 through 3.25. For all pictures, the plutonium fuel meat is shown as purple and the stainless steel cladding is shown as yellow. Polyethylene is shown as blue and aluminum (Planet platform, platen, and heat dispersal plates) are shown in green. Tantalum is shown in blue. The tantalum diluted stacks are taller than the Pu baseline experiments, as the additional of the tantalum increases parasitic absorption of neutrons and the separation distance between the Pu layers, thus increasing the critical mass.

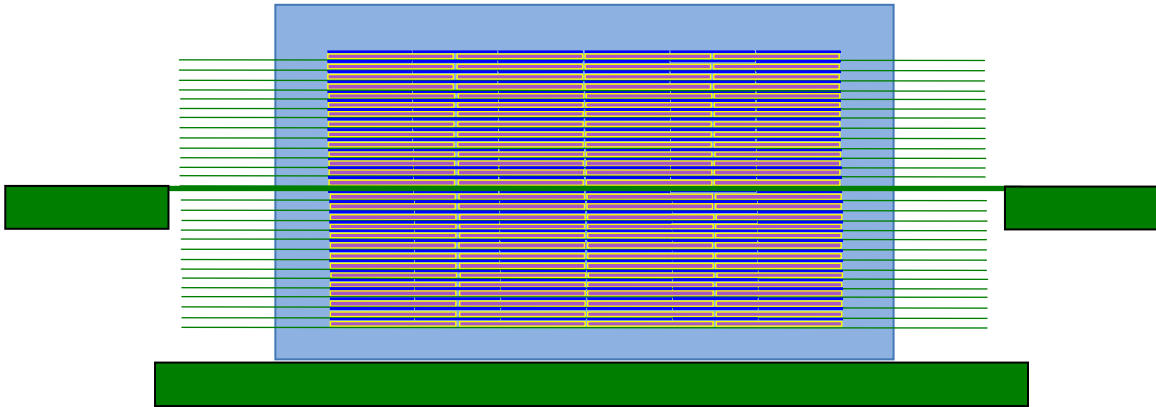


Figure 3.21. Experimental Configuration for Experiment 6: ZPPR Plate Layers with Tantalum and No Interspersed Polyethylene. This experiment consists of 26 layers of Pu and is a fast neutron system, an increase of 5 layers over the baseline case.

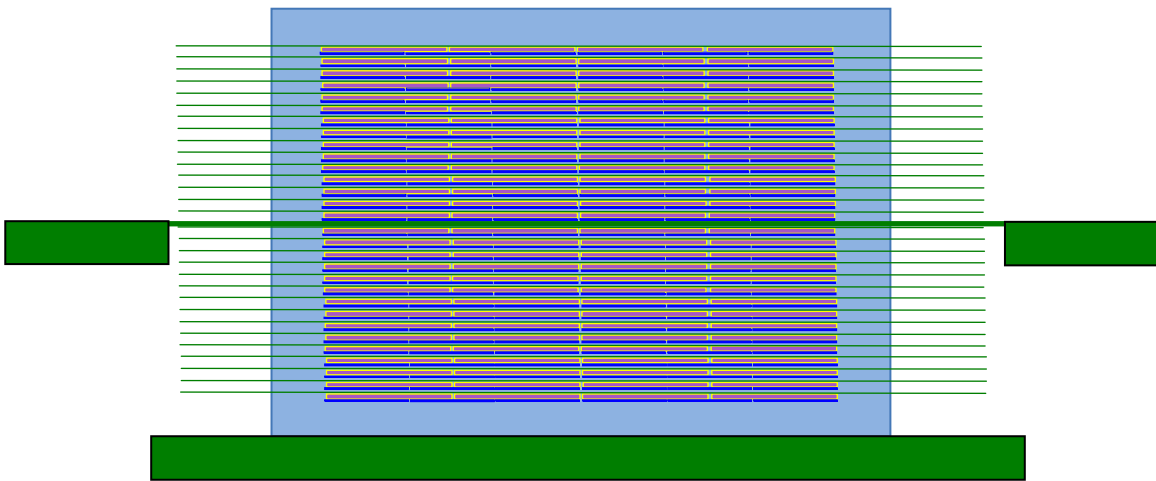


Figure 3.22. Experimental Configuration for Experiment 7: ZPPR Plate Layers with Tantalum and 0.0625 inches Interspersed Polyethylene. This experiment consists of 30 layers of Pu, an increase of 12 layers over the baseline case.

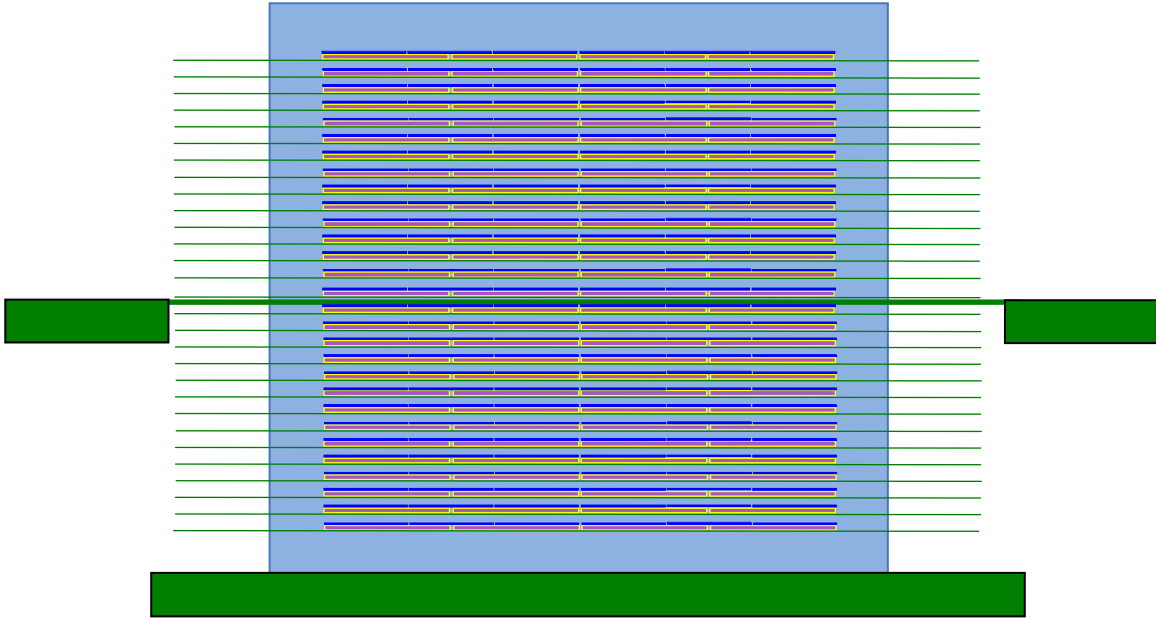


Figure 3.23. Experimental Configuration for Experiment 8: ZPPR Plate Layers with Tantalum and 0.1875 inches Interspersed Polyethylene. This experiment consists of 29 layers of Pu, an increase of 17 layers over the baseline case.

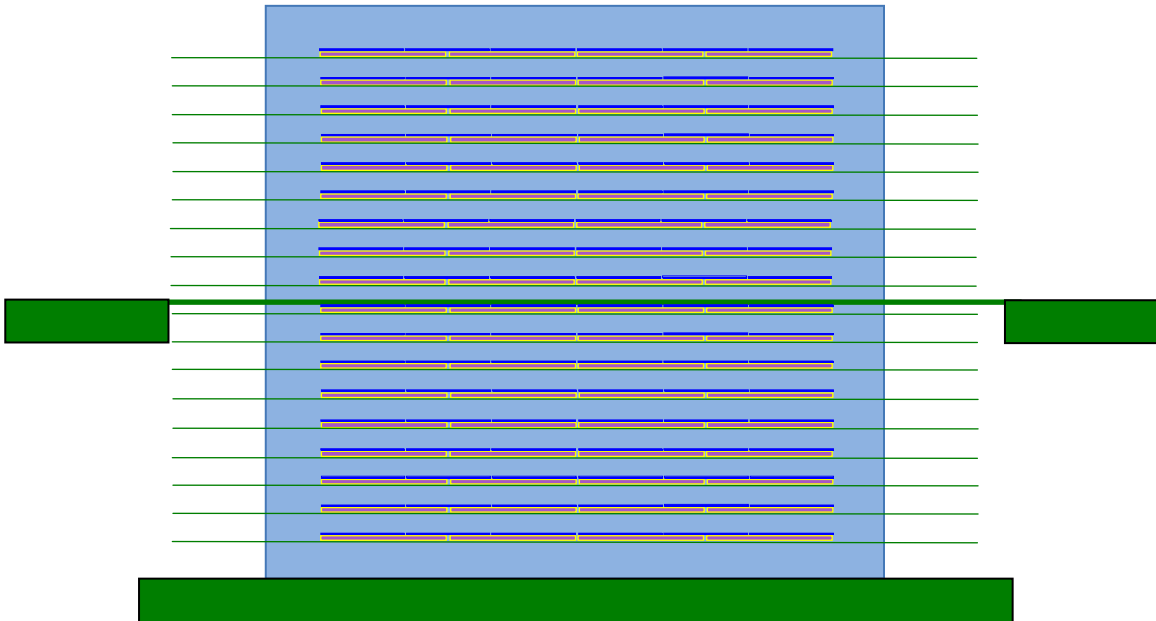


Figure 3.24. Experimental Configuration for Experiment 9: ZPPR Plate Layers with Tantalum and 0.4375" Interspersed Polyethylene. This experiment consists of 18 layers of Pu, an increase of 10 layers over the baseline case.

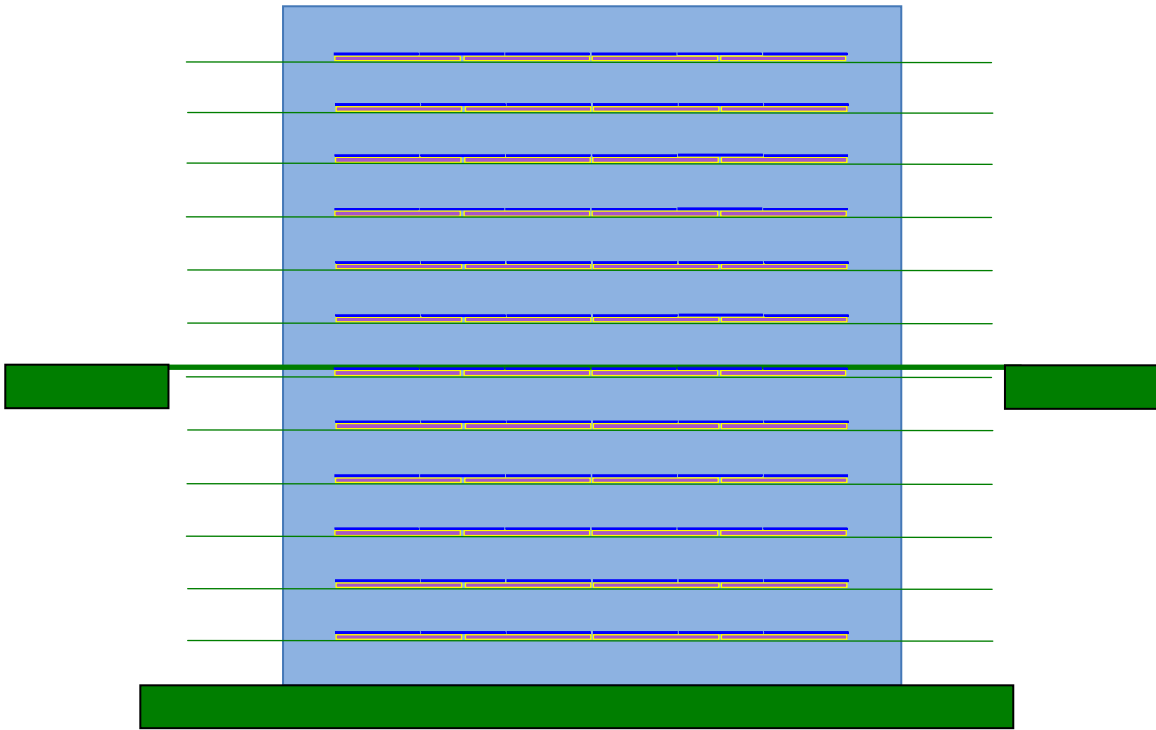


Figure 3.25. Experimental Configuration for Experiment 10: ZPPR Plate Layers with Tantalum and 1” Interspersed Polyethylene. This experiment consists of 12 layers of Pu, an increase of 6 layers over the baseline case.

4.0 Calculational Models of the Experiments

Design of the first phase of the TEX experiments required a number of calculations, addressing criticality, thermal analysis, and weight stress analysis for the aluminum diaphragm. A discussion of the methodologies used for these calculations and their results is provided in the following sections.

4.1 Criticality and Spectrum Calculations

4.1.1 Methodology and Code Used

The Monte Carlo neutron transport code, MCNP5, version 1.60, developed at Los Alamos National Laboratory, was used to calculate critical configurations and the corresponding neutron fission spectrum for the TEX configurations with ZPPR plates. Continuous energy ENDF/B-VII.1 cross sections (.80c) were used in all MCNP5 calculations, save for a few minor constituents where ENDF/B-VII cross sections were unavailable. All materials were modeled using room temperature (293 K) cross sections. The non-default parameters used for the MCNP5 runs are listed in Table 4-1.

Table 4-1: Parameters Used in MCNP5 v 1.60 Calculations

Parameter	Description	Value
gen	Number of generations run	1250
npg	Number of neutrons started per generation	10^4
nsk	Number of generations skipped (not included in k_{eff} calculation)	97

4.1.2 MCNP5 Model of Plutonium/Aluminum ZPPR Plates

A computational model of the Pu ZPPR plates was developed for MCNP5 based on the historical information (original drawings, specifications, alloy research, and actual measurements) presented in Section 3.0.

The ZPPR plates are comprised of three materials: plutonium alloyed with 1.1 wt% aluminum (core), 304L stainless steel (cladding), and carbon steel (spring). Plutonium/aluminum alloy and the 304L stainless steel constituents are given by the “hot constants memo,” a summary of original measurement information contained in the ANL electronic plate material library (ADEN library). The last and most recently issued hot constants memo is dated April 2001¹². However, the plutonium/aluminum isotopic information is as of July 1960. Considering the plates are now over 50 years old, the isotopics (particularly ingrowth of ^{241}Am) need to be adjusted. ORIGEN, part of the SCALE package, was used to decay the plutonium to July 2015 (closer to the potential experiment date). Table 4-2 gives the original and updated Pu/Al alloy isotopics. The updated isotopics were used for the MCNP5 model. Unaccounted for impurities based on the average plate information presented in column 2 of Table 4-2 total 0.007 grams. Impurities and decay products as of July 1, 2015 amounted to a total of 0.247 grams out of a 105.383 gram Pu/Al core. For the MCNP models, the unknown impurities and decay products were modeled as void.

¹² Klann, R.T., B.D. Austin, S.E. Aumeier, D.N. Olsen. *Inventory of Special Nuclear Materials from the Zero Power Physics Reactor*. Argonne National Laboratory-West. ANL-NT-176. April 2001.

Table 4-2: ZPPR Plutonium/Aluminum Alloy Constituents

	As Fabricated July 1, 1960 ^(a)	Calculated Decay to July 1, 2015 ^(b)
²³⁸ Pu Mass (g)	0	0
²³⁹ Pu Mass (g)	99.0289	98.87
²⁴⁰ Pu Mass (g)	4.7244	4.697
²⁴¹ Pu Mass (g)	0.4595	0.0032
²⁴² Pu Mass (g)	0.0049	0.0049
²⁴¹ Am Mass (g)	0	0.4021
Al Mass (g)	1.1584	1.1584
Total (g)	105.376	105.136
Total Reported Pellet Mass	105.383	

(a) Information based on detailed plate database.

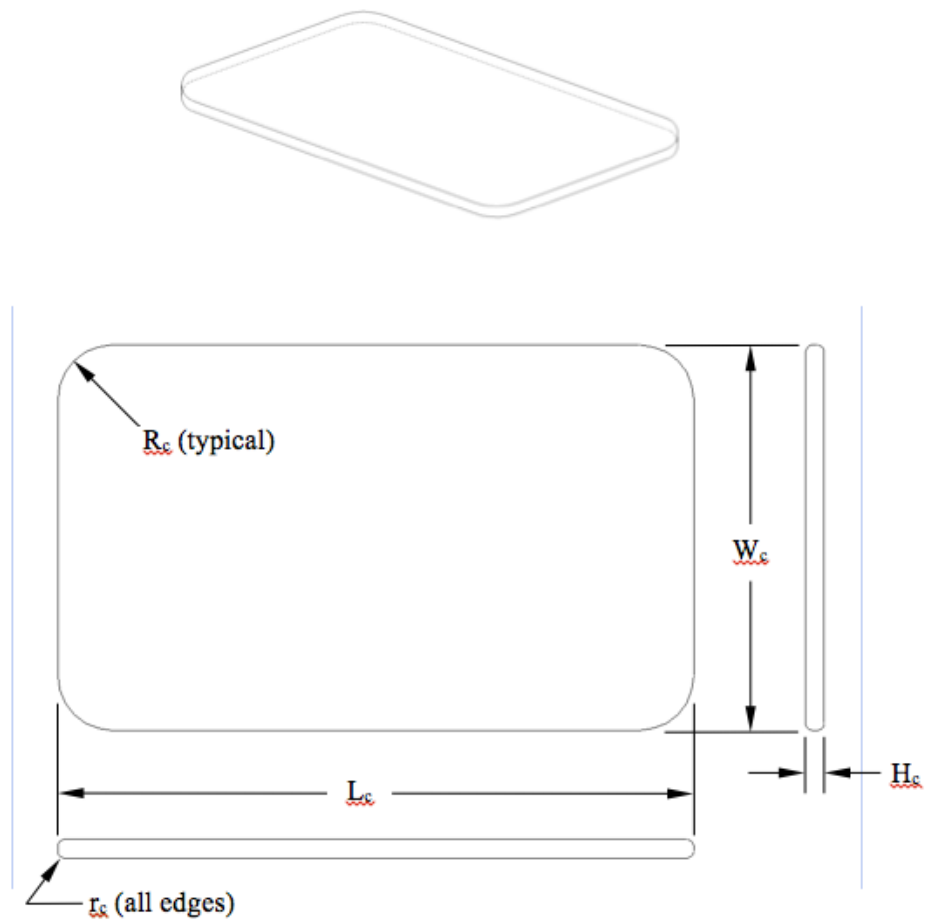
(b) Decay calculated by SCALE 6.1/Origen.

Table 4-3 provides the 304L stainless steel constituents, as presented in the hot constants memos. This composition was used directly for the MCNP5 model.

Table 4-3. 304-L Stainless Steel Cladding Mass and Composition for the PANN Plates

Clad Mass (g)	Composition, wt.%									
	C	Si	P	S	Cr	Mn	Fe	Ni	Cu	Mo
24.76	0.065	0.477	0.024	0.020	18.455	1.696	69.701	8.965	0.279	0.319

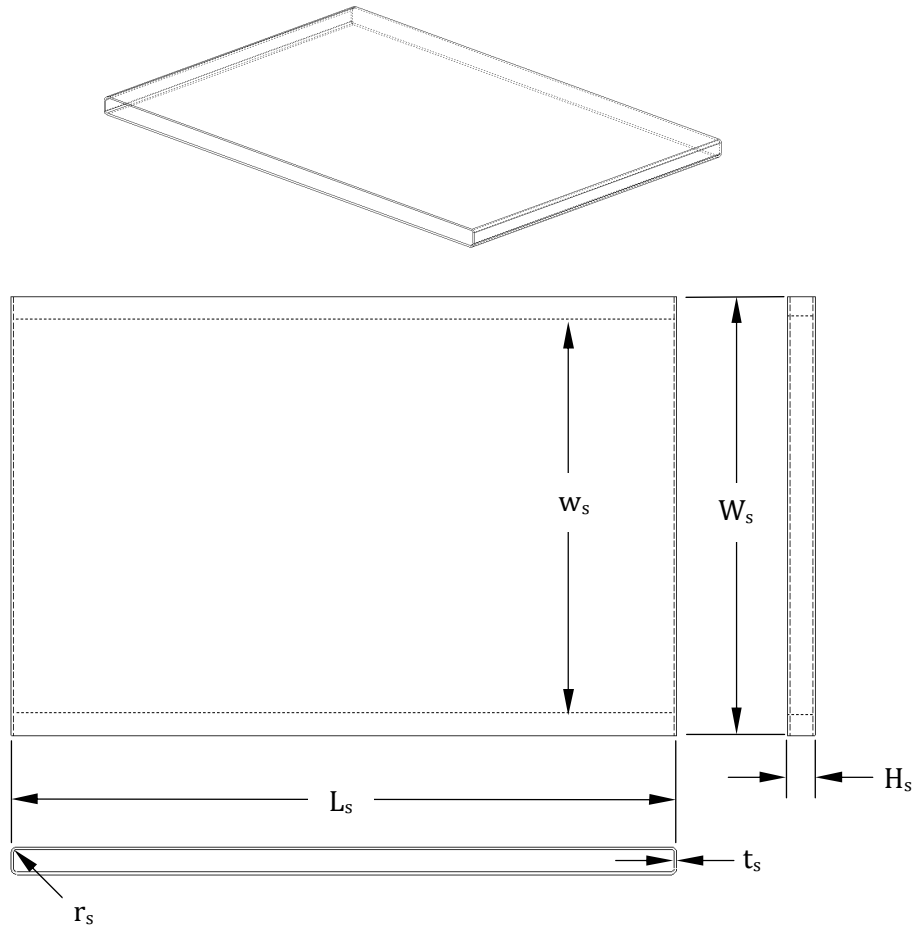
In developing the MCNP5 model, it quickly became clear that the plutonium pellet would necessarily be close to the minimum specifications. This is due to the tight tolerance on the ²³⁹Pu content and the fact that although the original specification was written for 93.5 wt.% ²³⁹Pu content plutonium, the actual plates were made from slightly higher ²³⁹Pu content material (95.02 wt.%). Adhering closely to the minimum size specifications for the Pu core (as detailed in Figure 4.1) and modeling the impurities and decay products as void resulted in a Pu/Al density of 15.10891 g/cm³, in very good agreement with published alloy densities.



Dimension	inches	centimeters
L_c	2.923	7.424
W_c	1.763	4.478
H_c	0.084	0.213
R_c	0.246	0.635
r_c	0.031	0.079

Figure 4.1. MCNP5 Model of the Plutonium-Aluminum Alloy Core.

Figure 4.2 gives dimensional information for the stainless steel cladding sleeve around the Pu/Al core. The cladding dimensions for the MCNP5 model were based on iterative volume calculations using the expected density of 304L stainless steel and the minimum and maximum dimensions from the PANN specifications as strict guidelines.

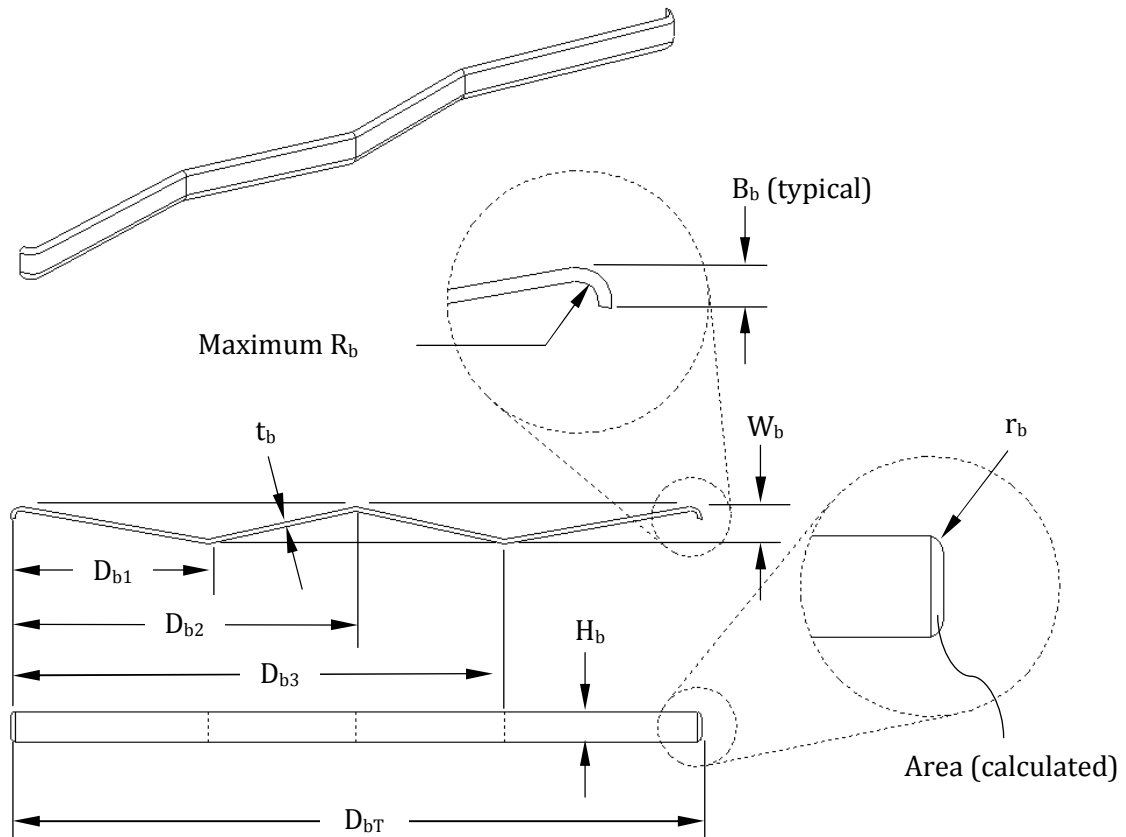


Dimension	inches	centimeters
L_s	3.003	7.629
W_s	1.970	5.004
w_s	1.780	4.521
H_s	0.1205	0.306
t_s	0.011	0.0279
r_s	0.0156	0.0397

Figure 4.2. MCNP5 Model of the stainless steel outer sleeve.

Section 3 describes the uncompressed carbon steel spring as represented on the PANN specification drawing. When assembled into the finished plate, the spring is designed to be compressed and push the Pu/Al core against stainless steel cladding. AutoCAD was used to realistically compress the spring to the correct dimensions between the Pu/Al core and the stainless steel cladding. These compressed dimensions used for the MCNP5 model are detailed in Figure 4.3.

Figure 4.4 shows 2D images taken from the Interactive Plotter (IP) viewer from MCNP5 for the XY, XZ, and YZ planes of the final ZPPR plate. The plutonium is centered within the cladding (same void on both sides) except for the dimension containing the spring, where the Pu/Al core is in contact with both the far cladding wall and the spring.



Dimension	inches	centimeters
D_{b3}	1.268	3.221
D_{b2}	0.886	2.250
D_{b1}	0.504	1.279
D_{bT}	1.772	4.50
H_b	0.0701	0.1782
W_b	0.058	0.1473
B_b	0.031	0.0794
R_b	0.0156	0.03969
r_b	0.0156	0.03969
t_b (#31 gage)	0.0105	0.02667
Area (calculated)	~0.000736 in ²	~0.00475 cm ²

Figure 4.3. MCNP5 Model of compressed carbon steel spring.

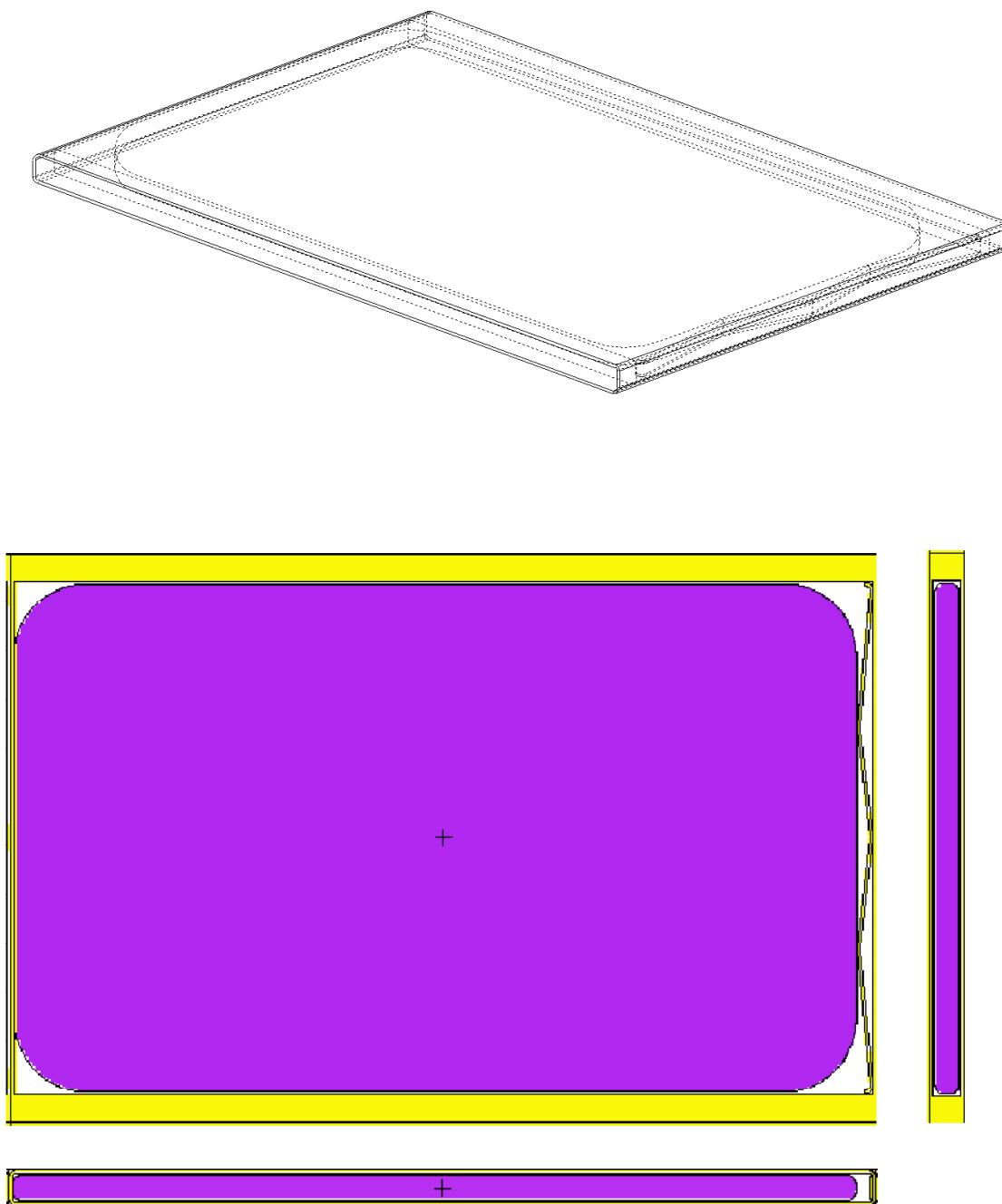


Figure 4.4: Full MCNP5 Model of a Pu/Al ZPPR plate. The pictures presented in this figure are screen captures from the interactive plotter function in MCNP5. The plutonium/aluminum alloy is shown in purple while the steel cladding and spring is shown in yellow. Dimensions are given in previous figures. The plutonium is centered within the cladding in two dimensions; in the third dimension, the dimension with the spring, the Pu/Al core is in contact with the far cladding wall on the opposite side of the spring.

4.1.3 MCNP5 Model of Experimental Configurations

4.1.3.1 Aluminum Support Structure

Based on the drawing presented as Figure 3.1, the aluminum upper support platen was modeled in MCNP as shown in Figure 4.5. The outer dimensions are 45" by 45" (114.3 cm by 114.3 cm) and the outer plate thickness is 1" (2.54 cm). A 19" (48.26 cm) square thin diaphragm is supported in the center of the platen. The diaphragm is 0.125" (0.3175 cm) thick. The entire platen, including the diaphragm, was modeled as Al-6061.

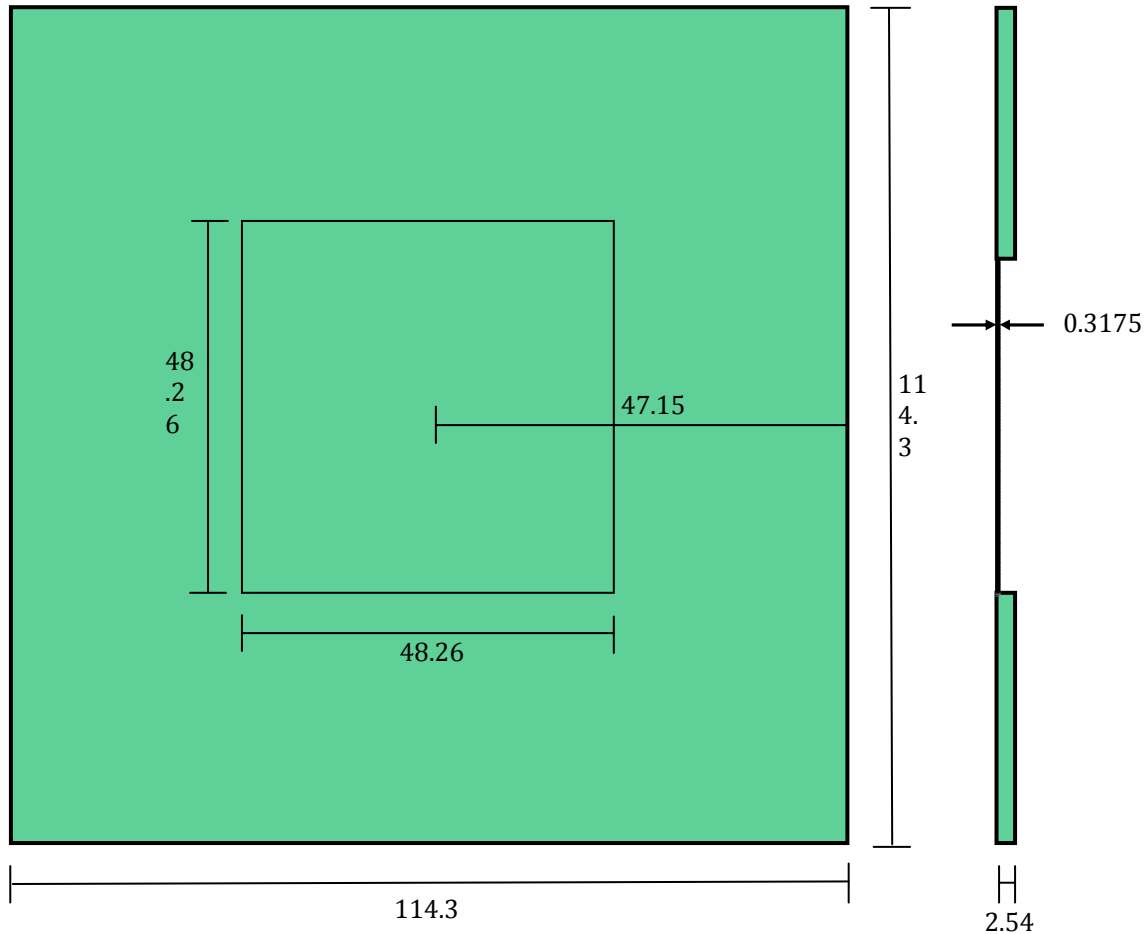


Figure 4.5. Upper Support Platen for TEX Experiments as Modeled in MCNP.

The 1" (2.54 cm) aluminum platform that supports the lower, movable half of the experiment was modeled as shown in Figure 4.6. The platform was modeled at Al-6061.

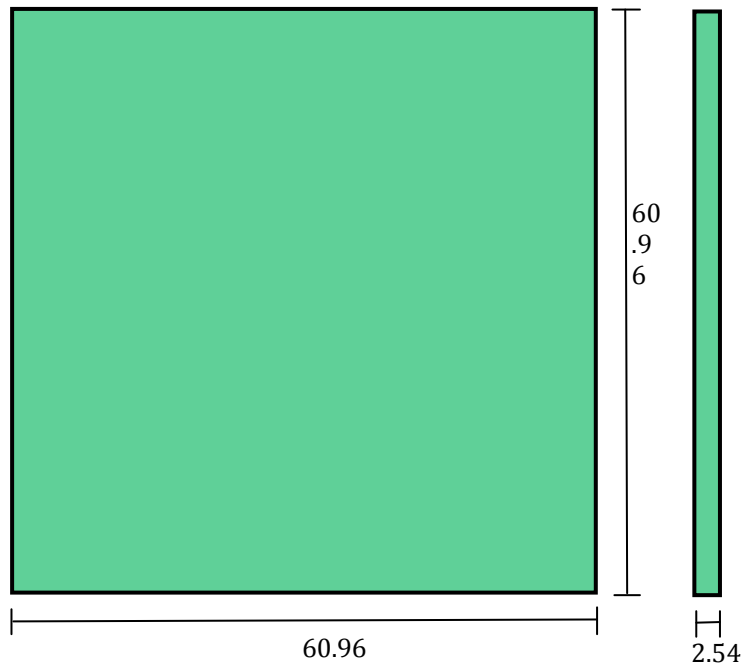


Figure 4.6. Lower Support Platform for TEX Experiments as Modeled in MCNP.

4.1.3.2 Baseline Pu ZPPR Experiment Models

The ZPPR Pu/Al MCNP5 plate model described above was used to model all five baseline experiments (Experiments 1-5). The Pu/Al plates were arranged into 6 plate by 4 plate layers, as shown by the screen capture from the MCNP5 interactive plotter in Figure 4.7. One inch of polyethylene reflection was modeled around the sides of the layers. The plates were modeled as touching and the polyethylene was modeled with no space between the plates and the polyethylene.

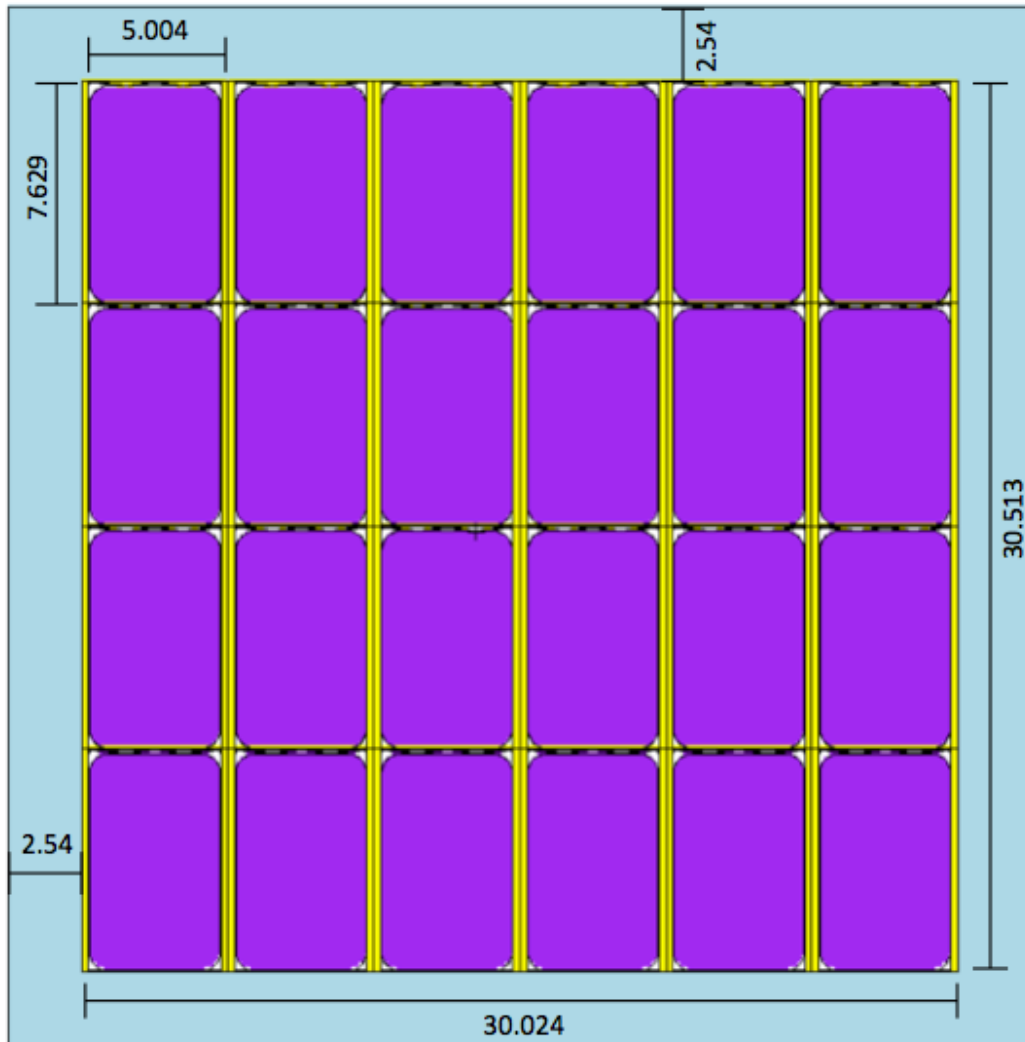


Figure 4.7: MCNP5 Model of a Pu/Al ZPPR Plate Layer with 1" of Polyethylene Reflection. This picture is a screen capture from the interactive plotter function in MCNP5. The plutonium/aluminum alloy is shown in purple, the steel cladding and spring is shown in yellow, and the polyethylene is shown in light blue. Dimensions are given in centimeters.

Figure 4.8 shows MCNP5 screen captures in the YZ direction for Experiment 1, the Pu ZPPR unmoderated baseline case with no polyethylene between each layer. A 0.0254 cm aluminum heat dispersal plate was modeled under each plutonium layer. No air gaps were modeled between each layer.

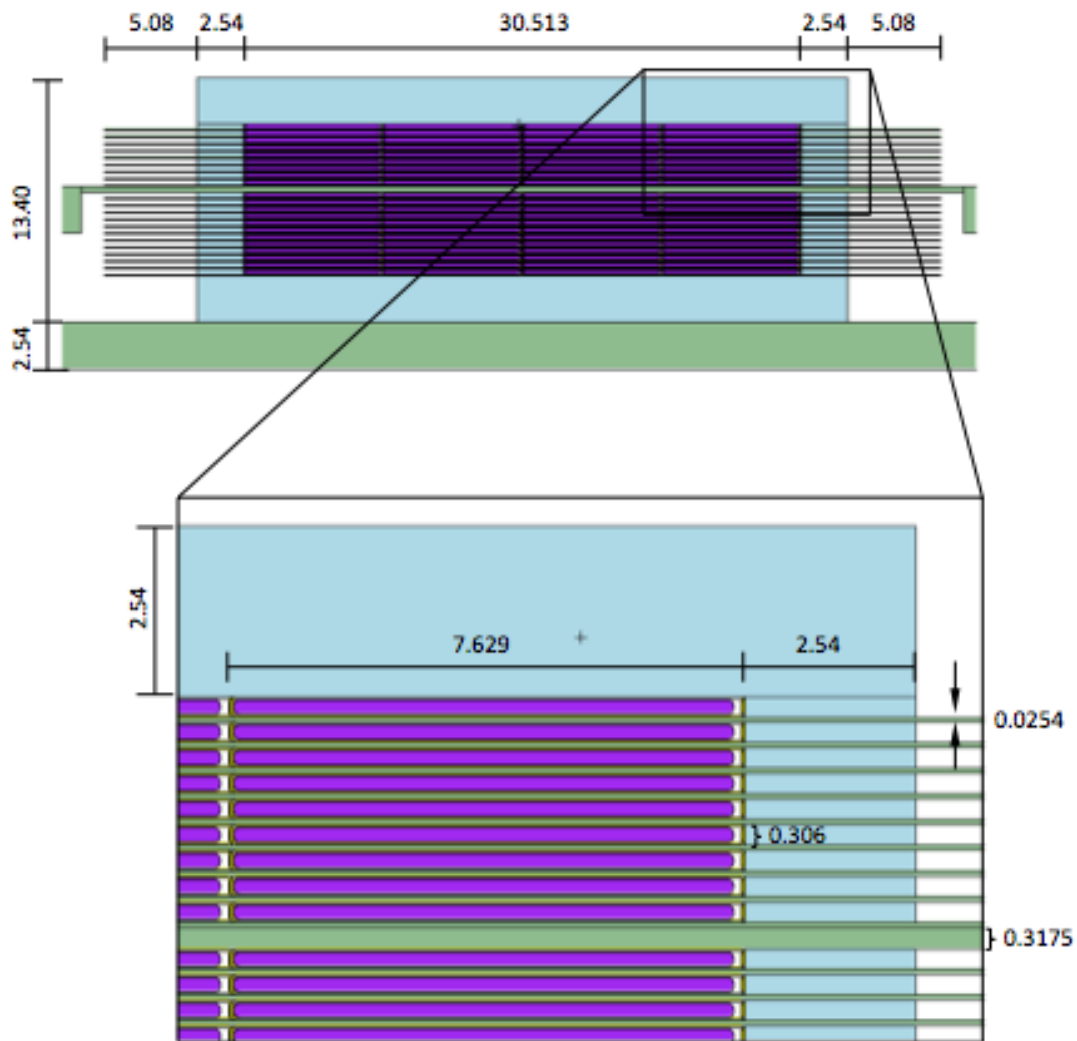


Figure 4.8: MCNP5 Model of Experiment 1, Pu ZPPR Unmoderated Baseline Case (No Polyethylene Between Each Layer). This picture is a screen capture from the interactive plotter function in MCNP5. The plutonium/aluminum alloy is shown in purple, the steel cladding and spring is shown in yellow, and the polyethylene is shown in light blue. Aluminum (heat dispersal plate and support structure) is shown in green. In the top figure, the picture was cut off and does not show the full width of the upper aluminum platen (green) in the interest of showing more detail in the assembly region. Dimensions are given in centimeters.

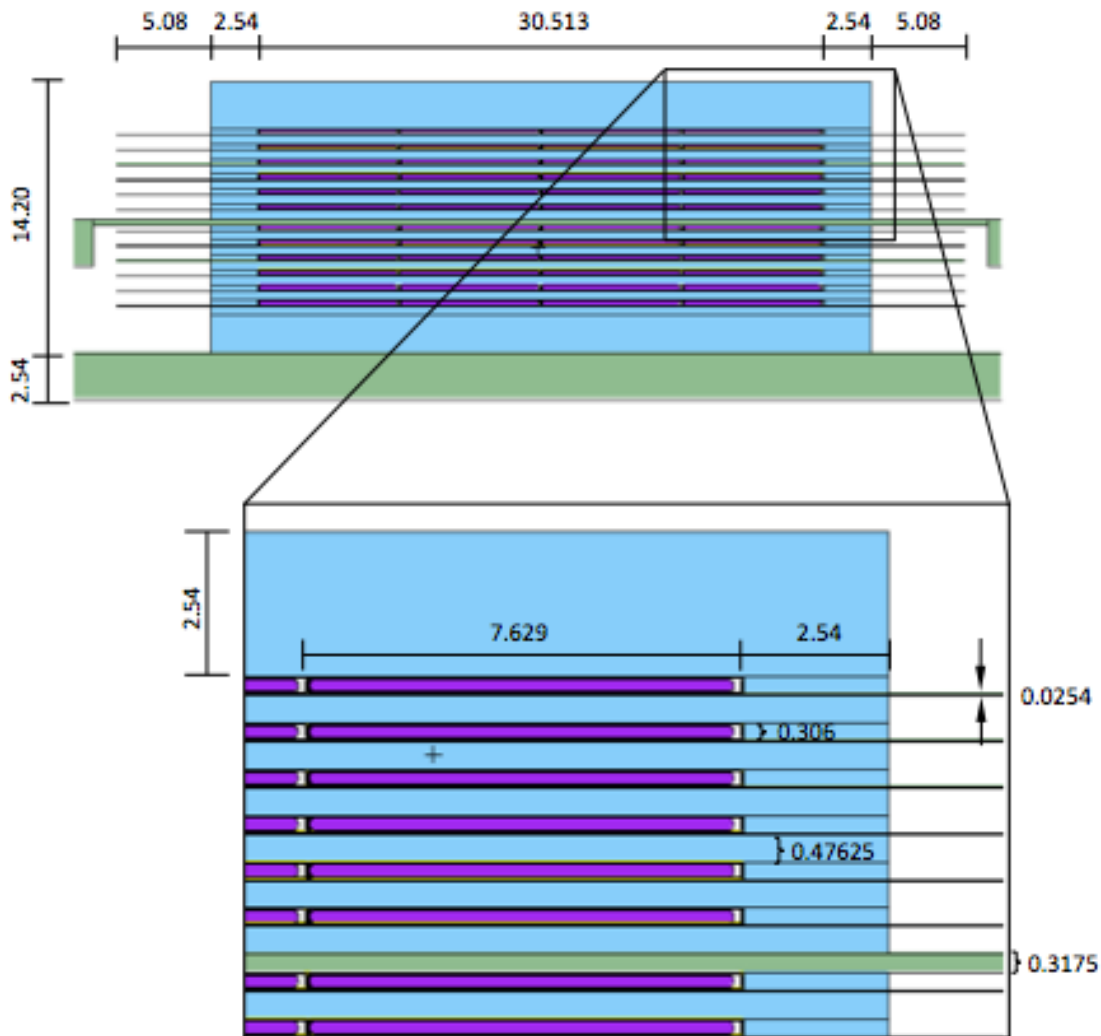


Figure 4.9: MCNP5 Model of Experiment 3, Pu ZPPR Baseline Case with 0.47625 cm (3/16") Polyethylene Between Each Layer. This picture is a screen capture from the interactive plotter function in MCNP5. The plutonium/aluminum alloy is shown in purple, the steel cladding and spring is shown in yellow, and the polyethylene is shown in light blue. Aluminum heat dispersal plates and support structure is shown in green. In the top figure, the picture was cut off and does not show the full width of the upper aluminum platen (green) in the interest of showing more detail in the assembly region. Dimensions are given in centimeters.

4.1.3.2 Tantalum-Diluted Pu ZPPR Experiment Models

The five baseline ZPPR Pu/Al MCNP5 models described in Section 4.1.3.2 (above) were modified to include layers of tantalum diluent plates (Experiments 6-10) adjacent to each plutonium layer. The tantalum plates, like the Pu ZPPR plates, were arranged into 6 plate by 4 plate layers, as shown in Figure 4.10. The tantalum plate layers were modeled orthogonally to the Pu plate layers, i.e, the Pu plates were arranged in a 6 by 4 plate

arrangement and the Ta layers were arranged in a 4 by 6 plate arrangement. The tantalum layers were placed on top of the plutonium layers.

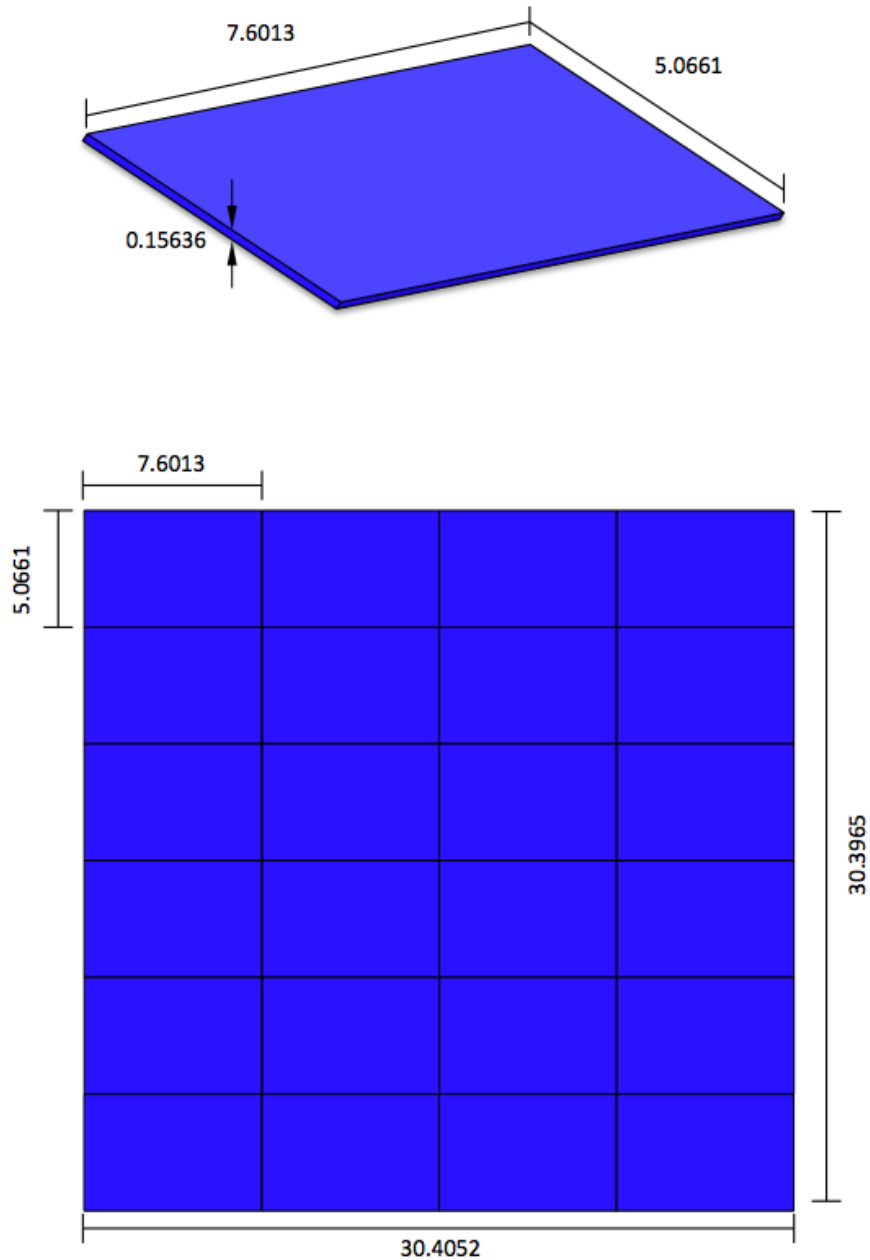


Figure 4.10: MCNP5 Model of Tantalum Plate and Tantalum Plate Layers. Dimensions are given in centimeters.

Everything else about the models remained the same, including the surrounding one inch of polyethylene reflection and the heat dispersal plates. Iterative calculations were

performed to find the number of layers required for a critical assembly. Figure 4.11 shows the MCNP5 geometry for Experiment 6, the unmoderated Pu ZPPR plate stack with tantalum dilution.

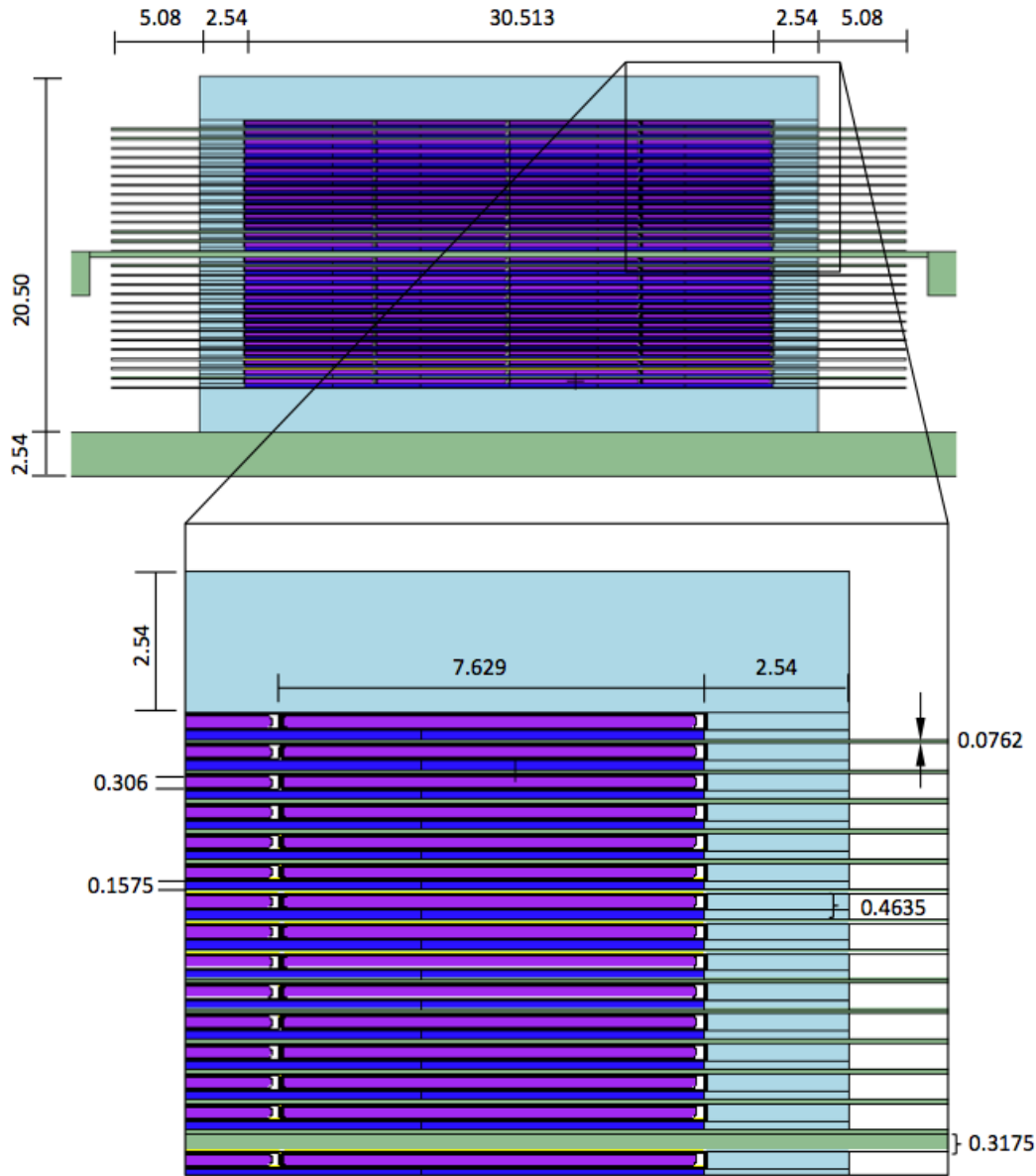


Figure 4.11: MCNP5 Model of Experiment 6, Pu ZPPR Unmoderated Tantalum-Diluted Case (No Polyethylene Between Each Layer). This picture is a screen capture from the interactive plotter function in MCNP5. The plutonium/aluminum alloy is shown in purple, the steel cladding and spring is shown in yellow, the tantalum is shown in dark blue, and the polyethylene is shown in light blue. Aluminum (heat dispersal plate and support structure) is shown in green. In the top figure, the picture was cut off and does not show the full width of the upper aluminum platen (green) in the interest of showing more detail in the assembly region. Dimensions are given in centimeters.

4.1.4 MCNP5 Calculation Results

Iterative MCNP calculations were performed to determine critical configurations for a range of polyethylene thickness between fuel plate layers. As described in Section 4.1.3, two sets of critical configurations were modeled: the first set consists of the baseline ZPPR experiments moderated by polyethylene, while the second set include layers of tantalum plates adjacent to ZPPR fuel plate layers.

4.1.4.1 Baseline Pu ZPPR Experiments Results

The first set of calculations modeled the baseline case of ZPPR Pu/Al plate layers moderated by varying polyethylene thicknesses. The polyethylene thicknesses modeled were 0, 1/16", 3/16", 7/16", and 1". Table 4-4 shows MCNP k_{eff} results for the configurations with various thicknesses of polyethylene between ZPPR plate layers. The number of Pu layers reported in the table is the integer number of approximately 12" by 12" square layers required for criticality (actually made up of 24 individual ZPPR plates), which is why all the cases have some degree of excess reactivity. When conducting an experiment, a delayed critical configuration (closer to k_{eff} of 1) could be achieved either through partial Pu plate layers or spacing between the upper and lower halves of the assembly and aluminum shims. Additional calculations for just critical configurations are presented in Appendices C and D.

Table 4-4: $k_{\text{eff}} \pm \sigma$ for ZPPR Plate Layers without Ta

Case ID	Thickness of PE Plates (inches)	Thickness of PE Plates (cm)	Number of Pu Layers	$k_{\text{eff}} \pm \sigma$
bl_0_21c	0 (no PE)	0 (no PE)	21	1.0298 ± 0.0002
bl_116_17c	1/16	0.15875	17	1.0115 ± 0.0002
bl_316_12c	3/16	0.47625	12	1.0091 ± 0.0003
bl_716_8c	7/16	1.11125	8	1.0240 ± 0.0003
bl_1_6c	1	2.54	6	1.0548 ± 0.0003

Table 4-5 summarizes critical dimensions for the assemblies with varying polyethylene thicknesses. The stack lengths and widths (sixth column) do not include the aluminum heat dispersal plates, which extend an additional 2" (5.08 cm) on all sides of the assembly. Calculations showed that the location of the heat dispersal plate (either on top or below the plutonium layers) caused negligible changes to k_{eff} . The aluminum heat dispersal plates are placed below the plutonium layers to assist in heat transfer.

Table 4-5: Critical Dimensions for Pu ZPPR Plates without Ta Moderated by Polyethylene.

Case ID	Thickness of PE	Critical Mass	Number of Pu	Number of ZPPR	Stack Length x Width	Stack Height
---------	-----------------	---------------	--------------	----------------	----------------------	--------------

	Plates (in)	(kg ²³⁹ Pu)	Layers	Plates	(cm)	(cm)
bl_0_21c	0 (no PE)	49.8	21	504	35.59 x 35.10	12.5
bl_116_17c	1/16	40.3	17	408	35.59 x 35.10	13.5
bl_316_12c	3/16	28.5	12	288	35.59 x 35.10	12.0
bl_716_8c	7/16	19.0	8	192	35.59 x 35.10	15.9
bl_1_6c	1	14.2	6	144	35.59 x 35.10	20.5

For each critical configuration in Table 4-5, the fission fraction as a function of energy was extracted from the MCNP output. Table 4-6 reports the Energy of Average Lethargy of Fission (EALF) and total fraction of fissions occurring in the thermal, intermediate, and fast regimes for each case.

Table 4-6: MCNP Spectra Results for Pu ZPPR Plates without Ta Moderated by Polyethylene.

Case ID	Thickness of PE Plates (in)	EALF (eV)	Thermal Fission Fraction (<0.625 eV)	Intermediate Fission Fraction (0.625 eV-100 KeV)	Fast Fission Fraction (>100 KeV)
bl_0_21c	0 (no PE)	7.28E+04	0.09	0.17	0.74
bl_116_17c	1/16	5.38E+03	0.14	0.38	0.49
bl_316_12c	3/16	2.44E+02	0.27	0.43	0.30
bl_716_8c	7/16	1.57E+01	0.48	0.33	0.19
bl_1_6c	1	2.10	0.67	0.21	0.12

Based on the TEX objective for experiments that span a range of energy regimes, the configurations highlighted in blue in the table above are suggested for actual experiments. The fission fraction per unit lethargy as a function of neutron energy for the five experiments is plotted in Figure 4.12, and the intermediate energy region data are highlighted in Figure 4.13. Figure 4.14 is a Cumulative Distribution Function (CDF) graph that visually displays the fission fraction as a function of neutron energy for the five experiments. The lower curves on the CDF graph are the less moderated systems.

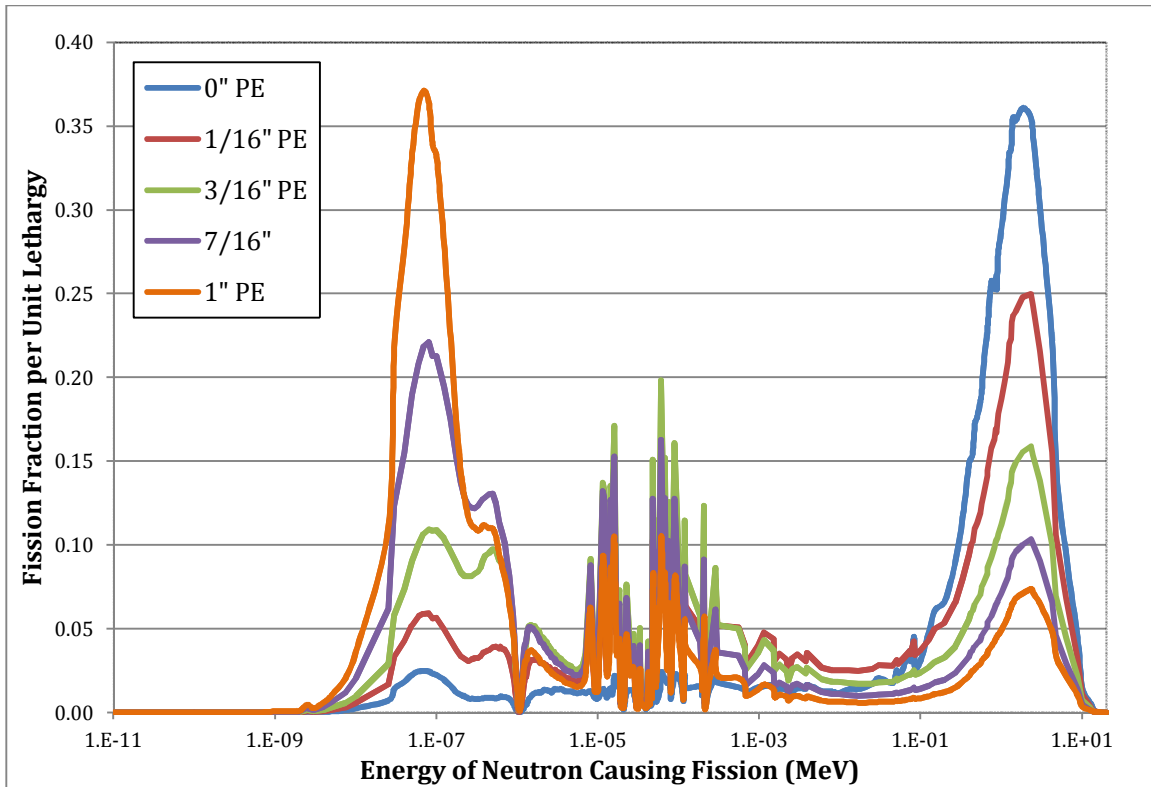


Figure 4.12 Fission Fraction per Unit Lethargy as a Function of Neutron Energy for Pu ZPPR Plates without Ta Moderated by Varying Thicknesses of Polyethylene.

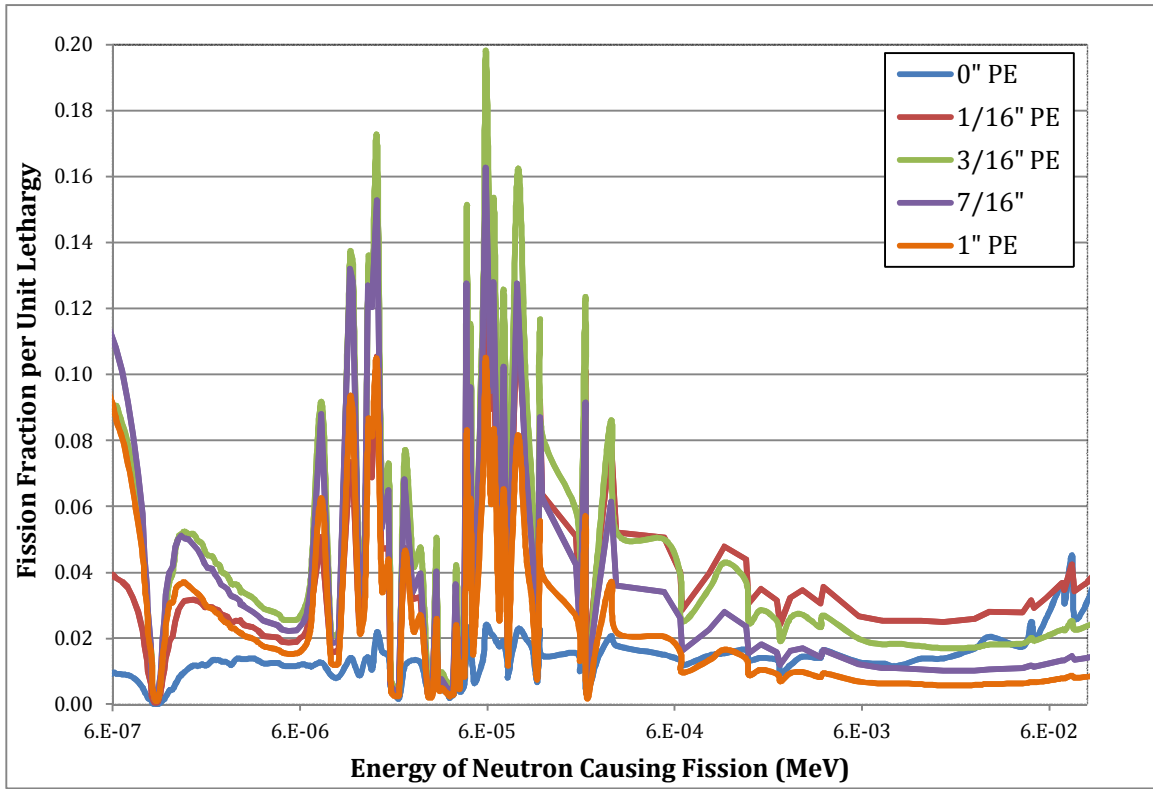


Figure 4.13: Fission Fraction per Unit Lethargy as a Function of Neutron Energy in the Intermediate Energy Region for Pu ZPPR Plates Baseline Experiments Moderated by Varying Thicknesses of Polyethylene.

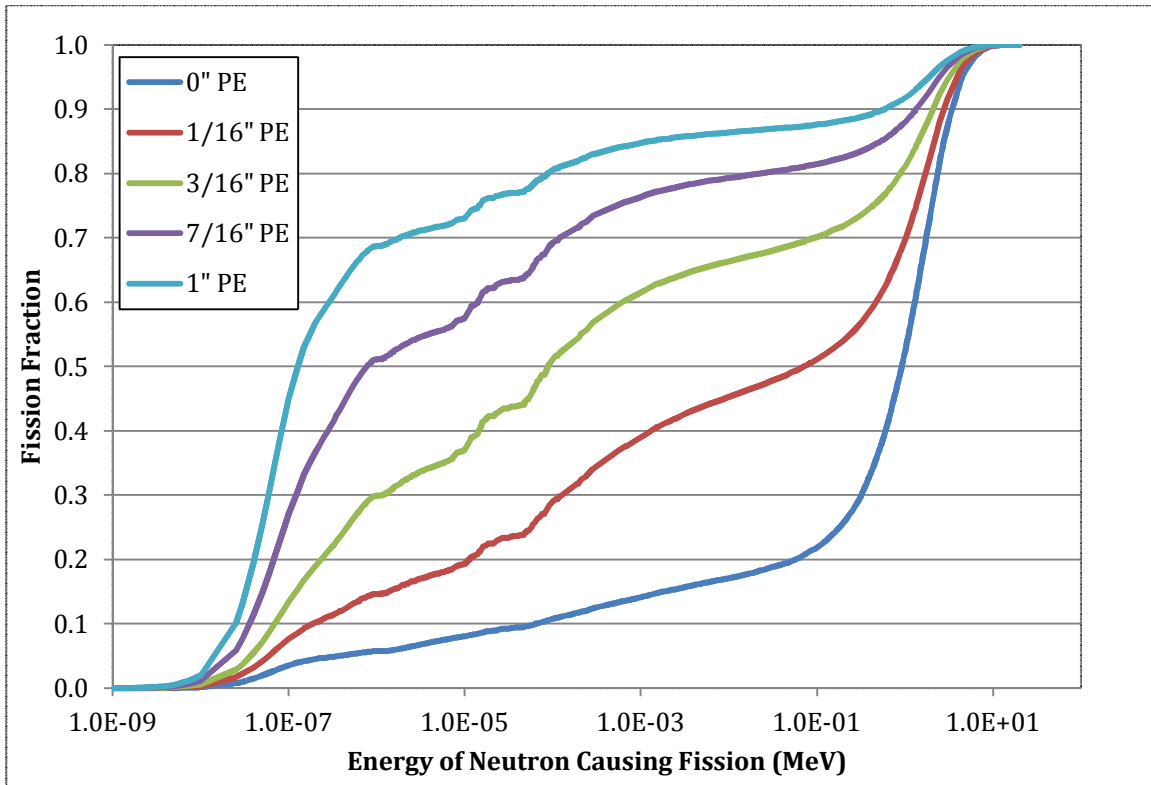


Figure 4.14: Cumulative Distribution Function of Fission Fraction as a Function of Neutron Energy for Pu ZPPR Plates without Ta Moderated by Varying Thicknesses of Polyethylene.

The MCNP results reported in Table 4-6 and Figures 4.12-4.14 demonstrate that polyethylene can be used with the Pu ZPPR plates to tune the neutron spectrum from hard (74% fast fission with no polyethylene moderator) to more intermediate or even thermal. The case with the highest percentage of fissions in the intermediate range used 3/16 in of PE, with 43% of the fissions resulting from intermediate energy neutrons.

Since one of the original TEX goals was to create intermediate spectrum experiments (where 50% or more of the fissions occur from the energy range (0.65 eV to 100 keV), additional calculations were completed that replaced the polyethylene between ZPPR layers with borated polyethylene. These scoping calculation indicated that with 3/16" borated polyethylene, a system where 52% of the fissions occur in the intermediate energy range could be created with the Pu/Al ZPPR plates, if desired for future experiments.

4.1.4.2 Pu ZPPR Experiments Diluted with Ta

The second set of calculations started with the baseline cases of ZPPR Pu/Al plate layers moderated polyethylene and added a layer of tantalum ZPPR plates (1/16" thick) above every Pu layer. The polyethylene thicknesses modeled were 0, 1/16", 3/16", 7/16", and

1", corresponding to 0, 0.15875 cm, 0.47625 cm, 1.1113 cm, and 2.54 cm. Table 4-7 shows MCNP k_{eff} results for the configurations with various thicknesses of polyethylene between ZPPR plate layers. The number of Pu layers reported in the table is the integer number of approximately 12" by 12" square layers required for criticality (actually made up of 24 individual ZPPR plates), which is why all the cases have some degree of excess reactivity. When conducting an experiment, a delayed critical configuration (closer to k_{eff} of 1) could be achieved either through partial Pu plate layers or spacing between the upper and lower halves of the assembly. Additional calculations for just critical configurations are presented in Appendices C and D.

Table 4-7: $k_{\text{eff}} \pm \sigma$ for ZPPR Plate Layers with Ta Layers.

Case ID	Thickness of PE Plates (inches)	Thickness of PE Plates (cm)	Number of Pu Layers	$k_{\text{eff}} \pm \sigma$
ta_0_26cc	0 (no PE)	0	26	1.0048 ± 0.0002
ta_116_30cc	1/16	0.15875	30	1.0050 ± 0.0002
ta_316_29c	3/16	0.47625	29	1.0002 ± 0.0002
ta_716_18c	7/16	1.1113	18	1.0036 ± 0.0003
ta_1_12cc	1	2.54	12	1.0119 ± 0.0002

Table 4-8 summarizes critical dimensions for varying polyethylene thicknesses. With Ta layers, the number of Pu layers increased by 6 to 17 layers, depending on the spectrum of critical configuration.

Table 4-8: Critical Dimensions for Pu ZPPR Plates with Ta Moderated by Polyethylene.

Case ID	Thickness of PE Plates	Critical Mass (kg ^{239}Pu)	Number of Pu Layers	Number of ZPPR Plates	Stack Length x Width (cm)	Stack Height (cm)
ta_0_26cc	0 (no PE)	61.7	26	624	35.59 x 35.10	13.0
ta_116_30cc	1/16	71.2	30	720	35.59 x 35.10	19.6
ta_316_29c	3/16	68.8	29	696	35.59 x 35.10	29.3
ta_716_18c	7/16	42.7	18	432	35.59 x 35.10	33.1
ta_1_12cc	1	28.5	12	288	35.59 x 35.10	36.3

For each critical configuration in Table 4-8, the fission fraction as a function of energy was extracted from the MCNP output. Table 4-9 reports the Energy of Average Lethargy of Fission (EALF) and total fraction of fissions occurring in the thermal, intermediate, and fast regimes for each case. The fission fraction per unit lethargy as a function of neutron energy is plotted in Figure 4.15, and the intermediate energy range data are plotted in Figure 4.16. Figure 4.17 is a Cumulative Distribution Function (CDF) graph that visually displays the fission fraction as a function of neutron energy for the five experiments.

Table 4-9: MCNP Spectra Results for Pu ZPPR Plates with Ta Moderated by Polyethylene.

Case ID	Thickness of PE Plates	EALF (eV)	Thermal Fission Fraction (<0.625 eV)	Intermediate Fission Fraction (0.625 eV-100 KeV)	Fast Fission Fraction (>100 KeV)
ta_0_26cc	0 (no PE)	1.13E+05	0.07	0.14	0.79
ta_116_30cc	1/16	1.19E+04	0.8	0.36	0.56
ta_316_29c	3/16	9.14E+02	0.19	0.45	0.36
ta_716_18c	7/16	3.38E+01	0.43	0.36	0.21
ta_1_12cc	1	2.96	0.64	0.22	0.14

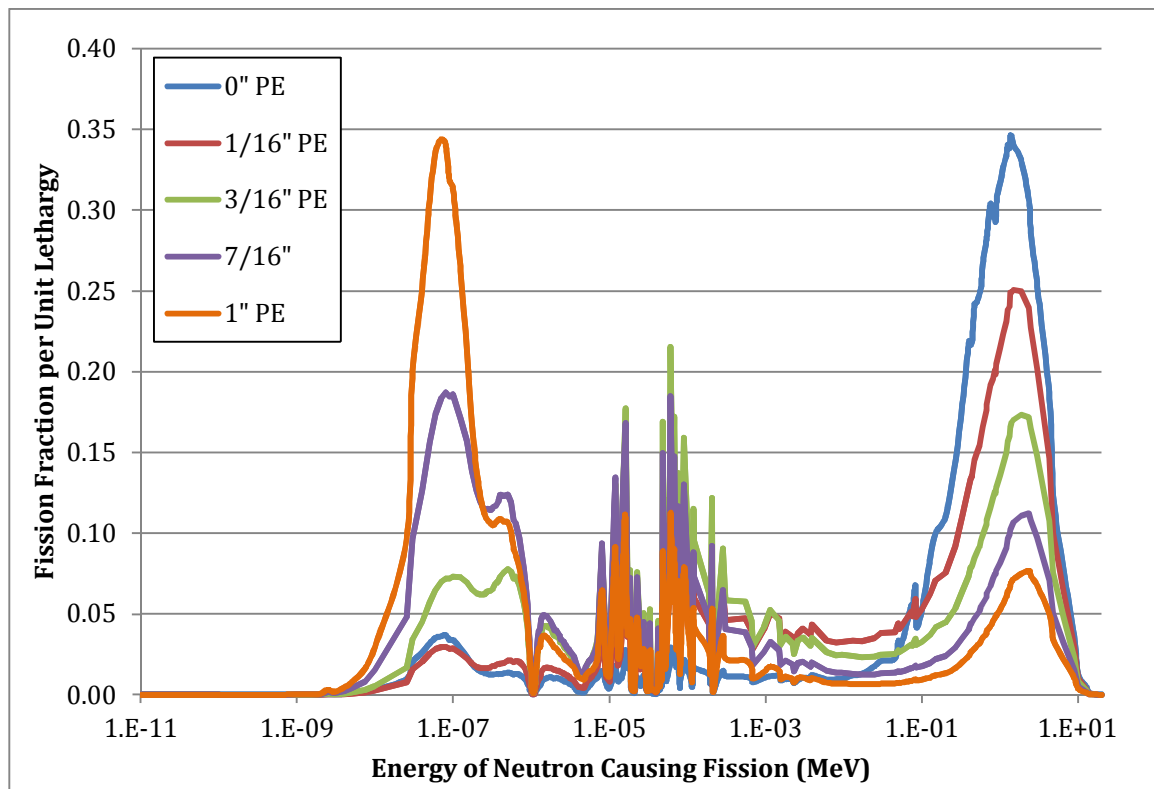


Figure 4.15 Fission Fraction per Unit Lethargy as a Function of Neutron Energy for Pu ZPPR Plates with Ta Moderated by Varying Thicknesses of Polyethylene.

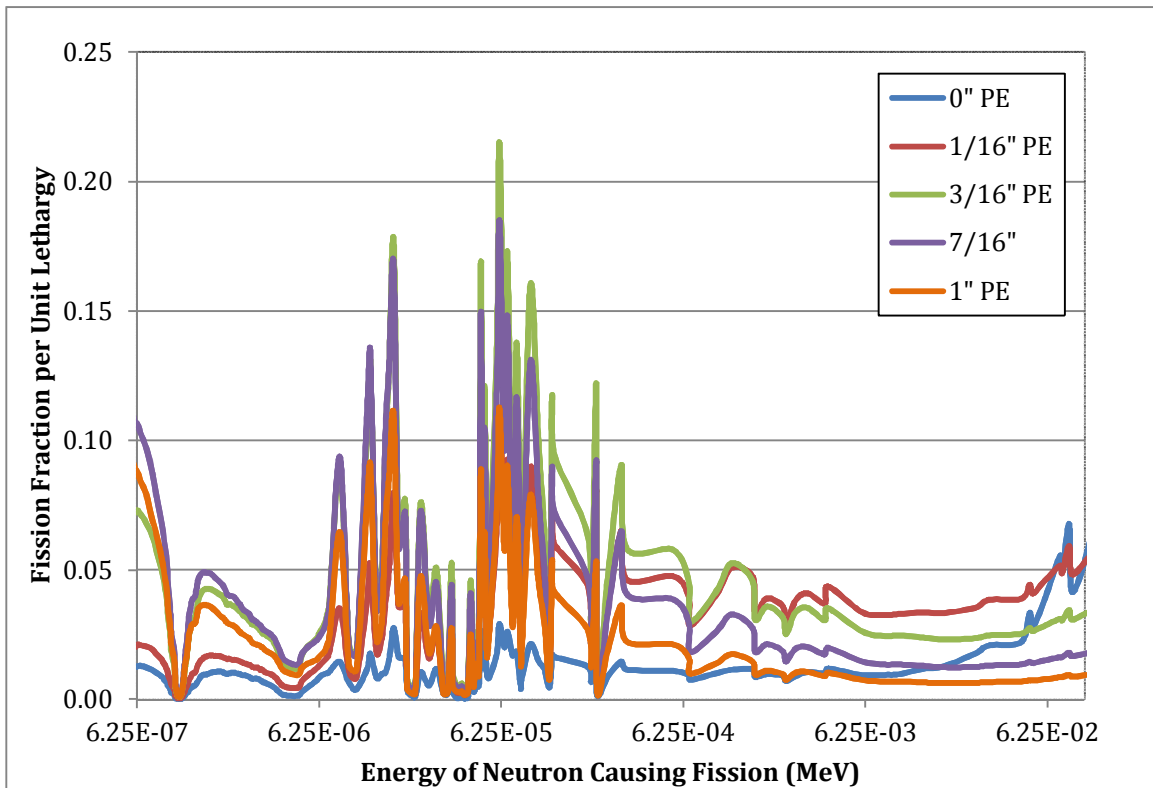


Figure 4.16: Fission Fraction per Unit Lethargy as a Function of Neutron Energy in the Intermediate Energy Region for Pu ZPPR Plates with Ta Moderated by Varying Thicknesses of Polyethylene

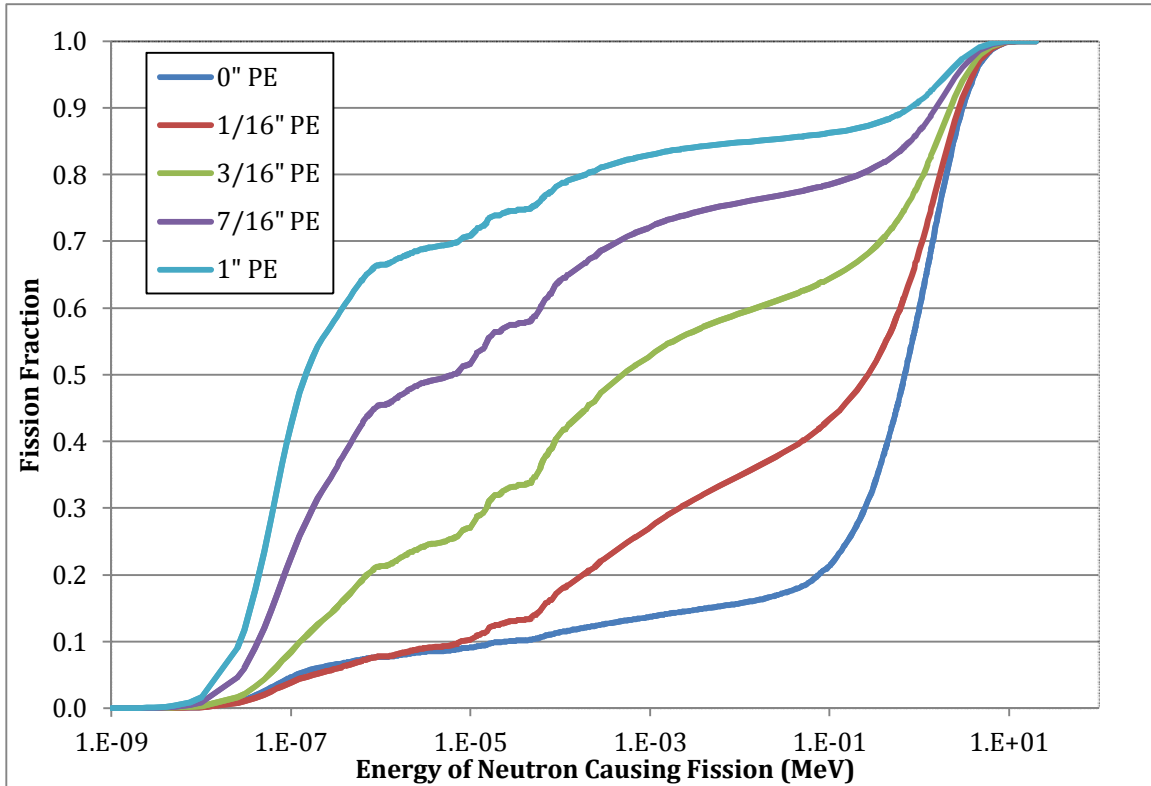


Figure 4.17: Cumulative Distribution Function of Fission Fraction as a Function of Neutron Energy for Pu ZPPR Plates with Ta Moderated by Varying Thicknesses of Polyethylene.

4.2 Uncertainty and Bias Characterization

This section contains results of sensitivity calculations performed to determine the effects of various uncertainties in the reported data on the value of k_{eff} . MCNP5 with continuous-energy cross sections was used. All of the MCNP calculations used continuous-energy cross sections, employing 6,250 generations of neutrons with 200,000 histories per generation. The first 97 generations were excluded from the statistics for each case, producing 1.23 billion active histories in each calculation. The standard deviation in the calculated k_{eff} for the individual MCNP calculation was 0.00002. Experiment 2 was used for all calculations except for the effect of tantalum impurities, which used Experiment 6.

4.2.1 Mass Uncertainties

A description of how the models were varied to determine mass uncertainties is provided in the following sections. The effects of uncertainties in the material mass are summarized in Table 4-10.

4.2.1.1 Pu-239 Mass

The Pu-239 mass in Pu-Al fuel meat (105.136 g) used in the benchmark-model is 98.87 g. As described in Section 3.2.2, Pu-239 content of each plate had the standard deviation of 0.27 g. The Pu-239 mass was increased by 0.27 g, maintaining the other isotope masses the same, and the effect in Δk_{eff} was 0.00008, which is considered to be insignificant.

4.2.1.2 Pu-240 Mass

The Pu-240 mass in Pu-Al fuel meat used in the benchmark-model is 4.697 g. As described in Section 3.2.2, Pu-240 content of each plate had the standard deviation of 0.1 g. The Pu-240 mass was decreased by 0.1 g, maintaining the other isotope masses the same, and the effect in Δk_{eff} was 0.00048.

4.2.1.3 Al Mass

The Al mass in Pu-Al fuel meat used in the benchmark-model is 1.1584, with a given standard deviation of 0.0464 g. The Al mass was decreased by 0.0464 g, maintaining the other isotope masses the same, and the effect in Δk_{eff} was 0.00016.

4.2.1.4 Stainless Steel Sleeve and Plug Masses

In the benchmark model, the mass of the sleeve and plugs used is 24.765 g. As described in Section 3.2.2, the standard deviation of the cladding mass is 0.0464 g. To observe the change in Δk_{eff} , the mass was increased by 0.046 g, and calculated effect was 0.00011 in Δk_{eff} .

4.2.1.5 Carbon Steel Spring Mass

A carbon steel spring is placed in one end of the sleeve to hold the core (fuel) plate against the opposite end of the sleeve. The density used in the benchmark model is 7.82 g/cm^3 . The density of the spring was varied by 0.1 g/cm^3 , and calculated effect was 0.00005 in Δk_{eff} , which is considered insignificant.

4.2.1.6 Polyethylene Plate Mass

The density of polyethylene plates used in the benchmark model is 0.967 g/cm^3 . Densities of the polyethylene plates to be used in the experiments are not yet known. The density of high density polyethylene was increased by 0.005 g/cm^3 , and the effect in Δk_{eff} was 0.00086.

4.2.1.7 Polyethylene Reflector Mass

The density of polyethylene reflector surrounding the ZPPR fuel plates used in the benchmark model is 0.967 g/cm^3 . The density of HDPE was increased by 0.005 g/cm^3 , and the change in Δk_{eff} was 0.00089.

4.2.1.8 Aluminum Mass

ZPPR assembly uses aluminum plates for dissipating heat generated in fuel. Supporting structure is also made of aluminum. The effect of uncertainty in aluminum masses was calculated assuming that the density of aluminum does not vary more than 1% of 2.7 g/cm^3 . Calculated effect for varying the Al density was 0.00026 in Δk_{eff} .

4.2.2 Dimensional Uncertainties

A description of how the models were varied to determine dimensional uncertainties is provided in the following sections. To see the geometry effect only, the component masses were maintained. The effects of uncertainties in the dimensions are summarized in Table 4-10.

4.2.2.1 Polyethylene Moderator Plate Dimensions

The dimensional uncertainty of the polyethylene moderator plates was assessed by varying the width, length, and the thickness. Because the engineering drawings are not yet available, the tolerance for the width and the length was assumed to be ± 0.1 inch while the thickness has a tolerance of ± 0.001 inch. The effect of each of the three dimensional tolerances was calculated and combined quadratically to get $\Delta k_{\text{eff}} = 0.00223$. The resulting standard uncertainty (divide by $\sqrt{3}$) is 0.0013 in Δk_{eff} .

4.2.2.2 Polyethylene Reflector Dimensions

The ZPPR fuel plates are contained in a 1" thick polyethylene reflector. The same tolerances are assumed for the width (0.1"), the length (0.1"), and the thickness (0.001"). In the same way, the effect of each of the three dimensional tolerances was calculated and combined quadratically to get $\Delta k_{\text{eff}} = 0.00216$. The resulting standard uncertainty (divide by $\sqrt{3}$) is 0.0013 in Δk_{eff} .

4.2.2.3 Aluminum Plate Dimensions

A 0.01" thick aluminum plate is placed on top of each ZPPR fuel plate layer to dissipate the heat generated by fuel. For sensitivity calculations, a tolerance of 0.005" is assumed for each of the three directions. These results were combined quadratically and divided by $\sqrt{3}$ to get the standard uncertainty. Calculated effect was 0.0001 in Δk_{eff} . The resulting standard uncertainty (divide by $\sqrt{3}$) is 0.00006 in Δk_{eff} , which is considered to be insignificant.

4.2.2.4 Gaps between Fuel Plates

In each fuel plate layer, twenty four ZPPR fuel plates will be positioned in a single layer making a 6×4 array. Sensitivity calculations were performed assuming a gap thickness of 0.01" between plates, and an axial gap thickness of 0.0005". The gap effect of each of the three dimensional tolerances was calculated and the effects were -0.00015, -0.00012, and -0.0031 in Δk_{eff} . These numbers are combined quadratically, and divided by $\sqrt{3}$ to get -0.0018 in Δk_{eff} .

4.2.3 Determination of Bias

Several calculations were completed to quantify the bias inherent in the models due to the exclusion of some model parameters. A summary of the sources of bias and their values is given in Table 4-11.

4.2.3.1 Impurities in Fuel

According to the measured historical ZPPR plate information in Table 3-1, the maximum mass of fuel impurities is 0.036 g. The detailed information of element composition of the impurities is not known. The effect of impurities in the fuel was assessed assuming that the impurities are composed of 100% carbon, natural uranium, or iron. Four MCNP runs completed, one without impurities, one with 0.036 g carbon impurities, one with 0.036 g uranium impurities, and one with 0.036 g iron impurities, and the change in Δk_{eff} was calculated. The maximum effect was from carbon, which was 0.00024 in Δk_{eff} .

4.2.3.2 Ta Impurities

Impurities of tantalum plates in the ZPPR assembly are reported in Table 3-5. The effect of impurities in the tantalum plate was assessed. Two MCNP runs with and without impurities in the Ta plates were made, and the change in Δk_{eff} was calculated. Calculated effect was -0.00006 in Δk_{eff} , which is considered to be negligible.

4.2.3.3 Temperature

Temperature distribution of the ZPPR fuel plates during experiments is not known yet. The cross section data libraries used for the benchmark model are based on ENDF/B.VII.1 at a temperature of 293 °K. Anticipated fuel temperature is 308 °K. Available neutron cross section data based on 600 °K were applied and adjusted for the temperature change of 15 degrees. The effect was -0.00016 in Δk_{eff} .

4.2.3.4 Room Return

Critical experiments are planned to be performed in the Planet experimental room at NCERC. The ZPPR fuel assembly is quite a distance away from any surrounding walls. The closest wall to the assembly is about 9' away. A detailed model of the experimental room was completed for a separate study¹³ and is fully described in that report. The TEX assembly was modeled as offset in the experimental room and the calculated effect of the room return was 0.00017 in Δk_{eff} .

¹³ Kim, S.S. *12-Rad Zone Anylsis for CAAS Placement at the Device Assembly Facility*. Lawrence Livermore National Laboratory. CSM 1531. September 30, 2008.

Table 4-10. Summary of Uncertainties for TEX Assembly Calculations.

Source of Uncertainty	Parameter Value used	Parameter variation in Calculation	Calculated Effect (Δk_{eff})	Standard Uncertainty of Parameter	Standard Uncertainty in Δk_{eff}
Material Mass					
Pu-239	98.87 g	0.27 g	0.00008	0.27	Negligible
Pu-240	4.697 g	-0.1 g	0.00048	-0.1	0.00048
Al	1.1584 g	-0.0464	0.00016	-0.0464	0.00016
Stainless Steel Sleeve and Plugs	24.765 g	0.046 g	0.00011	0.046	0.00011
Carbon Steel Spring	7.82 g/cm ³	0.1 g/cm ³	0.00005	0.1	Negligible
Polyethylene Plate	0.967 g/cm ³	0.005 g/cm ³	0.00086	0.005	0.00086
Polyethylene Reflector	0.967 g/cm ³	0.005 g/cm ³	0.00089	0.005	0.00089
Aluminum Mass	2.7 g/cm ³	0.027 g/cm ³	0.00026	0.027	0.00026
Geometry Dimensions					
Polyethylene Moderator Plates	13.8" × 14.0" × 1/16"	0.1" (W, L), 0.001" (T)	-0.0022	0.1"/√3, 0.001"/√3	-0.0013
Polyethylene Reflector	1" thick	0.1" (W,L), 0.001" (T)	-0.0022	0.1/√3, 0.001"/√3	-0.0013
Aluminum Plate	0.01" thick	0.005"	0.0001	0.005/√3	Negligible
Gaps between Fuel Plates	1.97" × 3.00" × 0.1205"	0.01" (W, L) 0.0005" (H)	-0.0031	0.01"/√3, 0.0005"/√3	-0.0018
Total Uncertainty	Quadrature Sum: 0.0026				

Table 4-11. Summary of Bias for TEX Assembly Calculations.

Source of Bias	Parameter Value used	Parameter variation in Calculation	Calculated Effect (Δk_{eff})	Standard Uncertainty of Parameter	Standard Bias in Δk_{eff}
Fuel Impurities	No Impurities	With Impurities	0.00024	With Impurities	0.00024
Ta impurities	No Impurities	With Impurities	-0.00006	With Impurities	Negligible
Temperature	293 °K	15 degrees	-0.00016	15 degrees	-0.00016
Room Return	No Room	With Room	0.00017	With Room	0.00017
Total Uncertainty	Sum: 0.00057				

4.2.4 Summary of Uncertainty and Bias Calculations

As shown in Table 4-10, the sources of uncertainty from mass uncertainties pertaining to the ZPPR plate (plutonium, aluminum, steel) are very low, especially for the ^{239}Pu content. This is not a surprising result, as the plates were procured with strict ^{239}Pu requirements as described in Section 2.0. A larger contributor to the delta k_{eff} was uncertainty in the polyethylene mass and dimensions. As the plates have yet to be fabricated, these perturbations were educated guesses and thus can be lessened through procurement specifications and piece-by-piece measurements. A concerted effort can also be made to lessen any gaps between plates in the assembly, which also have a relatively large effect on k_{eff} .

Fuel and tantalum impurities, temperature, and room return were shown introduce a slight positive bias to the calculations. The fuel impurity bias is an overestimate, as it assumes the worst case with the maximum impurity level from all plates and that the impurities are all carbon. The temperature is also likely overestimated, as the aluminum heat dispersal plates will largely mitigate the temperature increases across the assembly.

4.3 Thermal Analysis of ZPPR TEX Configurations

As shown in the preceding sections, the TEX experimental configurations involve substantial quantities of plutonium ZPPR plates. Plutonium is a substantial heat source due to alpha decay and spontaneous fission rates. Therefore, stack temperature is a concern when designing the experimental configurations, both from a safety point of view (polyethylene has a relatively low melting point) and a neutron physics point of view (cross sections are dependent on temperature). To address this issue, a steady-state thermal analysis using finite element methodology was completed to assist in the design of the TEX ZPPR experiments.

4.3.1 Methodology

ANSYS 14.5.0 was used to simulate multiple TEX experimental configurations using the Pu ZPPR plates. ANSYS is a finite element analysis (FEA)-based tool and was used to solve the differential equations that describe the flow of heat through the stack of ZPPR plates. FEA relies on splitting up the complex geometry of the stack into small sections that have a much simpler geometry. This results in the creation of a mesh based on simple geometric elements, such as a cube, tetrahedral, or hexahedra. These experimental configurations differed in the number of layers and the thickness of high density polyethylene moderator between the layers. A 3D solid model of the stack and all its subcomponents was created.

ANSYS models the flow of heat from hot to cold bodies by three different modes, all of which are driven by a temperature gradient. The first mode is conduction and occurs in a stationary medium of either a solid or fluid. Convection accounts for the transfer of heat between a fluid and solid surface that are at different temperatures. The third mode is thermal radiation and is due to the emission and absorption of electromagnetic waves from the surface of bodies.

The first mode conduction is driven by the collision and transfer of energy from higher energy molecules to lower energy molecules. The rate equation for heat conduction is expressed by Fourier's law,

$$q_x'' = -k \frac{dT}{dx} = k \frac{\Delta T}{L}$$

The heat flux q_x'' (W/m²) is the rate of heat transfer in the x direction per unit area perpendicular to the direction of heat transfer. The heat flux is proportional to the temperature gradient, $\frac{dT}{dx}$ where k is the thermal conductivity (W/mK). The values used for the thermal conductivity, k of the various materials in the stack are given in Tables 4-13 and 4-14 below.

Convective heat transfer accounts for the random motion (diffusion) within a fluid, as well as, the bulk motion of a fluid and the associated energy transfer that accompanies these motions. Forced convection occurs when the flow of the fluid is driven by some external source such as a fan or a pump. Natural convection on the other hand, occurs

due to buoyancy forces. For hot surfaces fluid next to the surface heats up and begins to rise due to buoyancy, inducing a flow. Convective heat flux (W/m^2) is described by the following equation also known as Newton's law of cooling,

$$q'' = h(T_s - T_f)$$

Convective heat flux is proportional to the temperature difference between the surface T_s and fluid T_f . h ($\text{W/m}^2\text{K}$) is the convection heat transfer coefficient. All exterior surfaces of the stack use a standard stagnant air convective heat transfer coefficient $h = 5 \text{ W/m}^2\text{K}$. Thermal radiation is the energy emitted from the surface of a material. Radiation does not require a medium to transfer heat like conduction and convection and may occur in a vacuum. The rate of heat transfer from a surface due to radiation is,

$$q''_{rad} = \varepsilon\sigma(T_s^4 - T_{sur}^4)$$

The rate of thermal radiation is proportional to the difference of the body's surface temperature, T_s to the fourth power and the temperature of the surroundings T_{sur} to the fourth power. Therefore the importance of thermal radiation is strongly dependent on the temperature difference between the surface and surroundings. ε is the emissivity of the surface and is a measure of how well a surface radiates relative to a black body where a value of 1 indicates a radiation efficiency equivalent to a black body. σ is the Boltzman constant ($\sigma = 5.67 \times 10^{-8} \text{ W/m}^2\text{K}^4$). Thermal radiation boundary conditions were applied to all exterior surfaces, the values of ε used for each material are given in Table 4-13.

Heat transfer between two bodies in contact with one another depends on the surface roughness of the two surfaces, the hardness of each material, the contact pressure, as well as, the gas residing in the gaps between the two bodies. The effect of all these things is captured by modeling a contact resistance between the two surfaces. For a unit area of the interface the contact resistance is,

$$R''_{t,c} = \frac{T_A - T_B}{q''_x}$$

4.3.2 ANSYS Model of ZPPR Stacks

Figure 4.18 shows the solid model for a single plate and its cladding. Each plate is composed of plutonium (5 wt% ^{240}Pu)/aluminum (1%) alloy surplus Zero Power Physics Reactor (ZPPR) fuel. The plate is clad in stainless steel with outer cladding dimensions of 1/8" (0.3175 cm) by 2" (5.08 cm) by 3" (7.62 cm). A steel spring is contained within the cladding and pushes one end of the ZPPR plate against the stainless steel cladding. The stainless steel cladding was filled with a 50/50 mixture of helium and argon by volume percent up to a final pressure of half an atmosphere. Within the model this gas mixture was replaced by air at atmospheric pressure. This substitution was made because over the years some air may have diffused into the cladding. Air is a poorer conductor of

heat than a 50/50 mixture of argon and helium so this change will result in more conservative results.

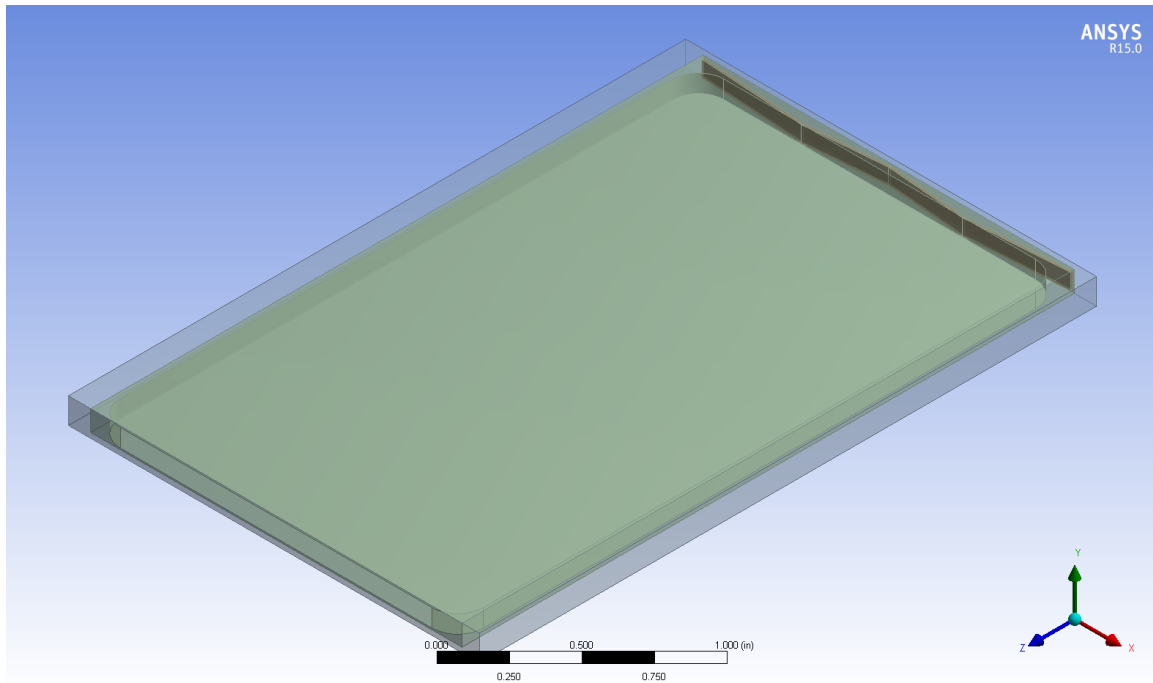


Figure 4.18. Geometry as implemented in ANSYS for single plate. The spring is to the upper right of the figure.

Twenty-four plates are arranged on plates of high density polyethylene (HDPE). The layers are stacked on top of one another and the thickness in-between the layers varies for the different experiments, from zero thickness (only an aluminum sheet is used in-between the layers) to one inch thick HDPE layers. There is a one inch layer of HDPE around all exterior sides of the stack of ZPPR plates. One quarter of a single layer of ZPPR plates is shown in Figure 4.19. Quarter symmetry was used for the ANSYS based thermal analysis with a zero gradient/adiabatic boundary condition was used on the two interior faces.

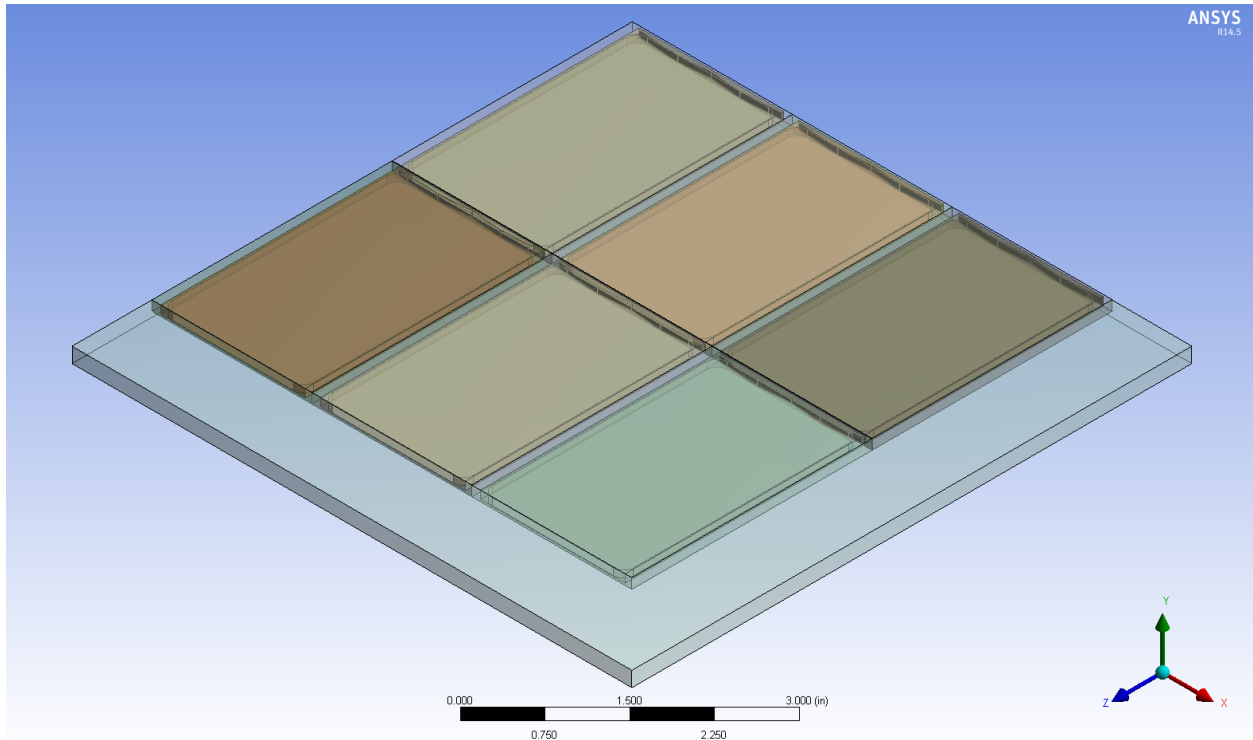


Figure 4.19. Solid model of single layer of plates and HDPE plate with quarter symmetry as implemented in ANSYS. The springs are all oriented to the upper right of each plate. The HDPE plate is 1/16 in thick, with a 1 in rim around the exterior sides.

4.3.2.1 Heat Source

Under non-multiplying conditions, the plutonium plates will produce heat from mainly alpha decay and a small contribution from spontaneous fission. The heat source per plutonium plate was calculated using specific power values (mW/g) from Los Alamos document LA-UR-07-5226¹⁴. The total heat source per plate was calculated to be 269.9 mW. On a per volume basis each ZPPR plate generates 39299.5 W/m³.

Table 4-12: ZPPR Plate Heat Generation by Isotope

Isotope	Mass per ZPPR Plate (g)	Specific Power (mW/g) ¹⁴	Heat Source (mW)
²³⁹ Pu	98.87	1.9288	190.700456
²⁴⁰ Pu	4.697	7.0824	33.2660328
²⁴¹ Pu	0.0032	3.412	0.0109184
²⁴² Pu	0.0049	0.1159	0.00056791
²⁴¹ Am	0.4021	114.2	45.91982
Total	103.9772		269.8977951

¹⁴ Bracken, D.S. and C.R. Rudy. "Chapter 10: Principles and Applications of Calorimetric Assay." *Passive Nondestructive Assay of Nuclear Materials*. 2007 Addendum. LA-UR-07-5226. 2007.

4.3.2.2 Setting and Constants Used for ANSYS Models

A 3D mesh was generated from the 3D solid model of the stack. Figure 4.20 shows a meshed stack of 17 layers of ZPPR plates with quarter symmetry, the solid model of this geometry is shown in Figure 6. All models of the experiments utilize quarter symmetry with zero gradient boundary conditions on interior surfaces. Because the stack is symmetric across these planes the solution is equivalent to solving the entire stack, but results in a greatly reduced mesh and therefore requires less computational resources to solve.

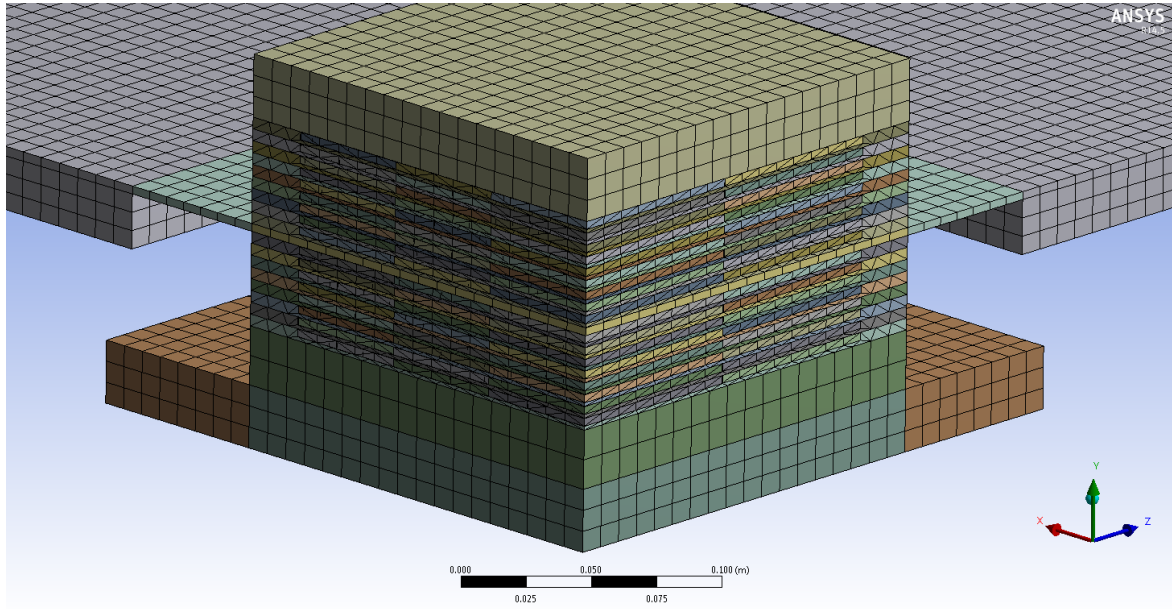


Figure 4.20. 17 layer stack with 1/16 in thick HDPE moderator plates meshed in ANSYS.

Within ANSYS a pinball region is defined in which a ball is placed between two adjacent bodies. All elements within the same ball are assumed to be in thermal contact with one another with a given contact resistance. Elements outside of this pinball are assumed to be perfectly insulated from one another. A ball radius of 1×10^{-4} m was used and a contact resistance assuming that air was the interfacial fluid was used and is listed in Table 4-13.

Table 4-13. Thermal Properties of Materials Used in Simulations.

Part	Material	Property	Value	Source
Sleeve	304 Stainless Steel	Thermal conductivity, k	16.3 (W/m K)	15
Spring	1060 Steel	Thermal conductivity, k	49.8 (W/m K)	16
Plate/ Frames	High density polyethylene	Thermal conductivity, k	0.4 (W/m K)	17
Plate/ Frame	High density polyethylene	Emissivity (at 300 K), ϵ	0.8	18
Support	6061 Aluminum	Thermal conductivity, k	180.0 (W/m K)	15
Support	6061 Aluminum	Emissivity (at 300 K), ϵ	0.04	19- Table A.8
Gas	Air	Thermal Resistance, R''	3.64×10^3 (W/m ² K)	20, 19-Table 3.1
Gas	He	Thermal Resistance, R''	9.52×10^3 (W/m ² K)	20, 19-Table 3.1

Table 4-14: Thermal Conductivity (k) of Materials as a Function of Temperature

Air ¹⁹ (Table A.4)		Plutonium Alloy Core ²¹	
Temperature (C)	k (W/m K)	Temperature (C)	k (W/m K)
26.85	0.0263	26.85	0.0263
76.85	0.0300	76.85	0.0300
126.85	0.0338	126.85	0.0338
176.85	0.0373	176.85	0.0373
226.85	0.0407	226.85	0.0407

¹⁵ Dalder, E., *Engineering Design Safety Standards Chapter F: Physical, Mechanical, and Electrical Properties of Common Materials*. Lawrence Livermore National Laboratory, UCRL-TM-217236, 2005.

¹⁶ AISI 1060 Carbon Steel, <http://www.azom.com/article.aspx?ArticleID=6542>

¹⁷ Polystone G natural technical data sheet, Rochling Engineering Plastics KG.

¹⁸ <http://people.csail.mit.edu/jaffer/FreeSnell/polyethylene.html#Background%20Emissivity>

¹⁹ Incropera, Frank P. and DeWitt, David P., *Introduction to heat transfer*, 3rd Edition. John Wiley & Sons, 1996.

²⁰ Fried, E., "Thermal Conduction Contribution to Heat Transfer at Contacts," in R. P. Tye, Ed., *Thermal Conductivity*, Vol. 2, Academic Press, London, 1969.

²¹ Foote, Frank G., *Annual Report for 1960 Metallurgy Division*, Argonne National Laboratory, AEC Research and Development Report ANL-6330, 1960.

4.3.3 Thermal Analysis Results

4.3.3.1 Initial Results- No Aluminum

Initial calculations were completed that simply modeled a stack of Pu ZPPR plate layers and polyethylene moderation, with no aluminum support structure or heat dispersal plates. The first calculation was completed on the expected “worst case” for heating: Experiment 2, which has 17 layers of plutonium plates and 1/16” interspersed polyethylene. Figure 4.21 shows a simulation of 17 layers of ZPPR plates without the support structures. Each layer of the 24 ZPPR plates is placed on a 1/16 in thick HDPE sheet that is 14 in by 14 in. The peak temperature of 92.2 C occurs in the center of the stack of ZPPR layers. This experimental setup is predicted to surpass the maximum long term service temperature of 80 C for the high density polyethylene [3].

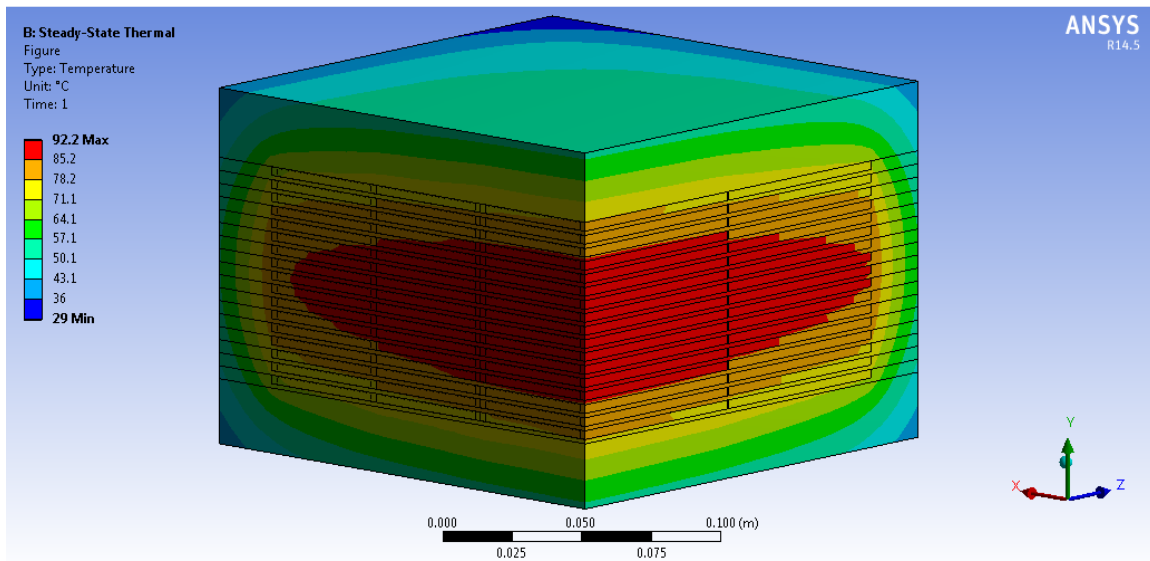


Figure 4.21. Steady-state temperature contours on interior corner with 17 layers of ZPPR plates with 1/16 inches of interspersed polyethylene. Simulation does not include aluminum support structures. The stack of plates are surrounded by one inch of polyethylene. The peak temperature is 92.2 C and occurs at the center of the stack.

4.3.3.2 Results with Aluminum Plates and Support Structure

Based on the initial high temperature results, a design for the aluminum heat dispersal plates was developed. Experiments 1-5 were simulated using the thermal analysis described in Section 4.3.1. A summary of the maximum temperatures found in the thermal analysis for each of the experimental configurations can be found in Table 4-15. Each layer of 24 ZPPR plates is surrounded by 1 in of HDPE on the sides and the very top and bottom layers have a 1 in HDPE layer above or below, respectively. The analysis looked at a 0.03” aluminum fin bottom that extends 2” beyond the 1” HDPE reflector to remove heat from the assembly. Experiments 2-5 use polyethylene moderator plates of varying bottom thickness and have a 0.01” aluminum heat dispersal plate, also called a

“fin”, on top of every Pu layer. The stack is split in two by a 19” x 19” aluminum diaphragm with a thickness of 0.125 in. The support for the diaphragm is 1 in thick aluminum and is 45” x 45”. The stack rests on a 1” thick aluminum plate that is 20” by 20”. The ambient (room) temperature was set to 22 C for all simulations, based on discussions with NCERC personnel.

Table 4-15. Maximum Temperature for Each Experiment with and without Fins

Experiment Modeled	HDPE Thickness (in)	Pu Layers	T _{max} Without Fins (C)	T _{max} With Fins (C)
1	0	21	32.6	
2	1/16	17	52.6	36.3
3	3/16	12	44.9	34.6
4	7/16	8	39.1	32.7
5	1	6	36.6	31.8

4.3.3.3 Experiment 1 Model

The first setup presented is one in which there are 21 layers of ZPPR plates. Each layer of 24 ZPPR plates is placed on a 0.03 in thick aluminum sheet that is 18 in by 18 in. There are 11 layers of the ZPPR plates above the diaphragm and 10 layers below. Figure 4.22 shows the inner corner of the quarter symmetry geometry as implemented in ANSYS. The various components that make up the stack are colored based on material.

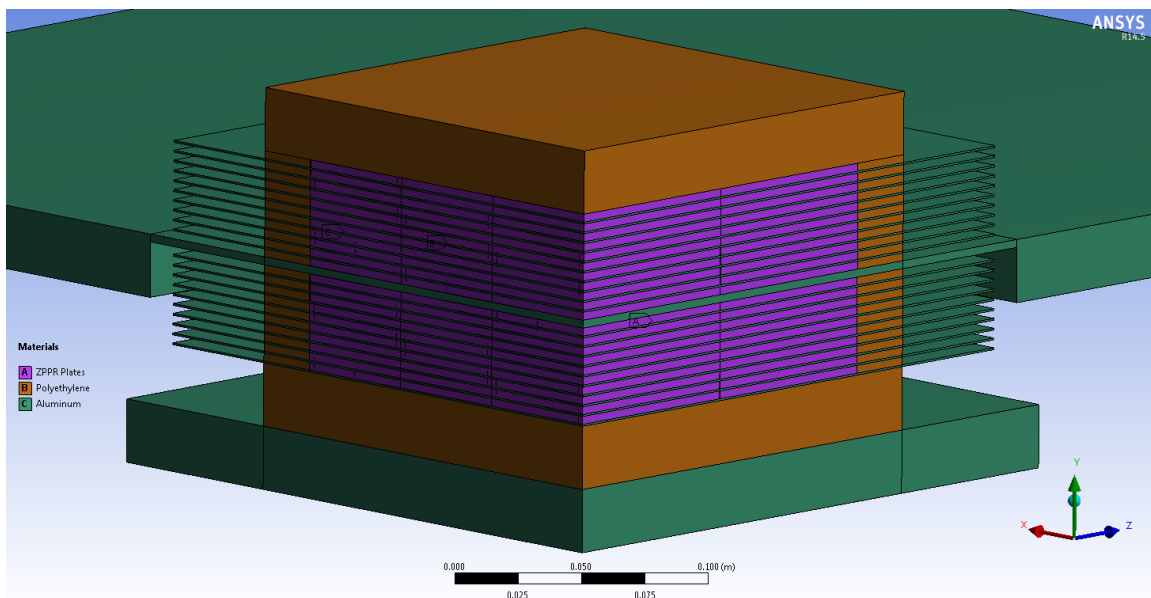


Figure 4.22. ANSYS Model of Experiment 1. Interior corner of solid model with 21 layers of ZPPR plates with no interspersed polyethylene and 0.03 inch aluminum fin. Stack of plates are surrounded by one inch of polyethylene. There are 11 layers above the 0.125 inch thick aluminum diaphragm and 10 below.

Based on the steady state thermal analysis, the peak temperature of 32.4 C occurs in the center of the upper stack of ZPPR layers. Aluminum is a very good conductor and since

the bottom layer is sandwiched between two large aluminum plates it stays cooler. The aluminum that each ZPPR layer sits on acts as a fin and transfers most of the heat from the ZPPR plates to the surroundings through conduction and convection, leaving most of the stack just above the ambient room temperature of 22 C. A colorized image of the temperature variations over the stack is shown in Figure 4.23.

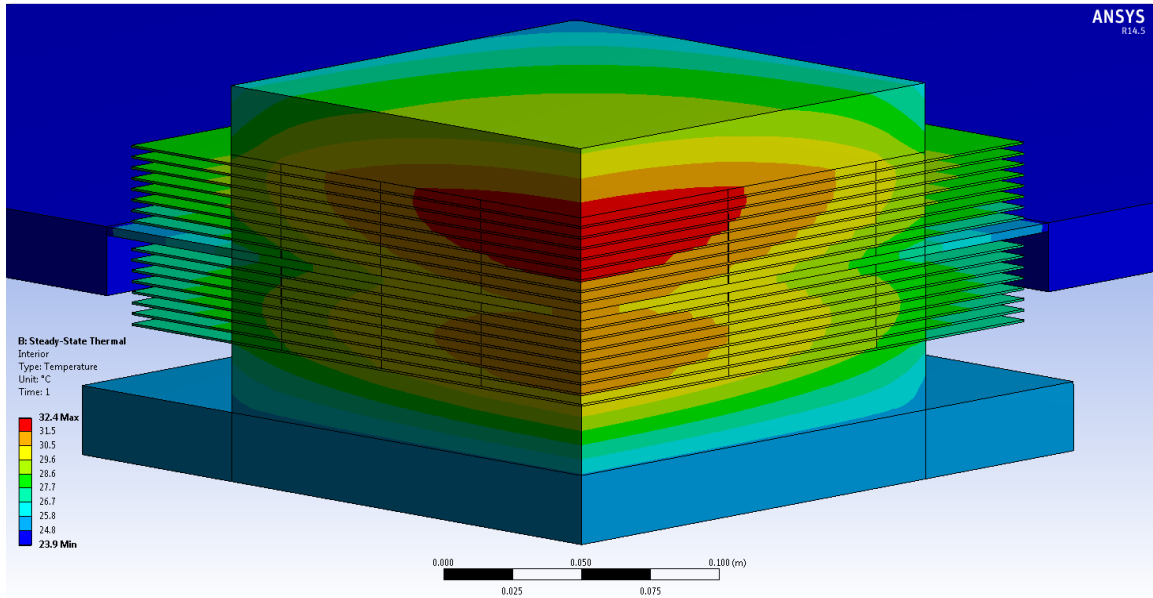


Figure 4.23. Temperature Map of Experiment 1. Steady-state temperature contours on interior corner of 21 layers of ZPPR plates with no interspersed polyethylene and 0.03 inch aluminum fin. The peak temperature is 32.4 C and occurs at the center of the upper stack.

4.3.3.2 Experiment 2 Model- With and Without Fins

Experiments 2-5 were modeled both with and without fins to quantify the fins' effects on the peak temperature of the experimental stacks. Experiment 2 has 17 layers of ZPPR plates and each layer is placed on a 1/16 in thick HDPE sheet that is 14 in by 14 in. There are nine layers of the ZPPR plates above the diaphragm and eight layers below. The geometry is shown in Figure 4.24 in which the different materials that make up the stack are denoted by different colors.

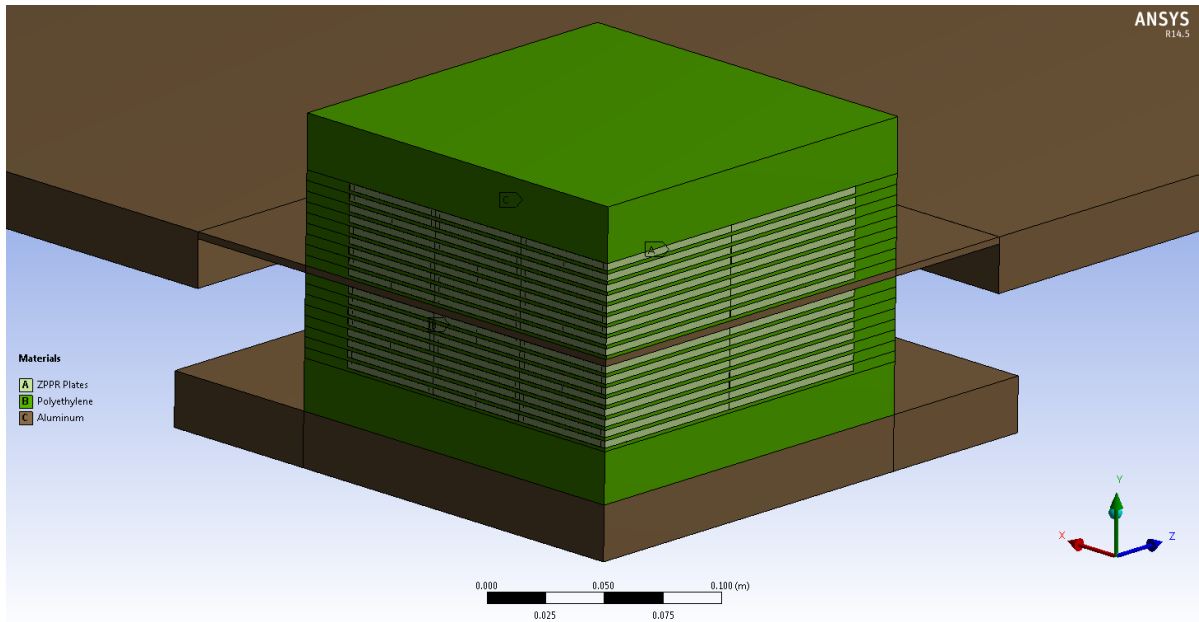


Figure 4.24. ANSYS Geometry for Experiment 2, without Fins. Interior corner of solid model with 17 layers of ZPPR plates with 1/16 inches of interspersed polyethylene. The stack of plates are surrounded by one inch of polyethylene. There are 9 layers above the 0.125 inch thick aluminum diaphragm and 8 below.

The results of the steady state thermal analysis for this experimental setup are shown in Figure 4.25. The peak temperature of 52.6 C occurs in the center of the upper stack of ZPPR layers. Again the upper stack is a few degrees warmer than the bottom of the stack since it has a less efficient path to conduct its heat away, especially with the interspersed HDPE. HDPE is not nearly as good at conducting heat as aluminum, which can be seen by comparing the thermal conductivity k of the two materials in Table 4-13.

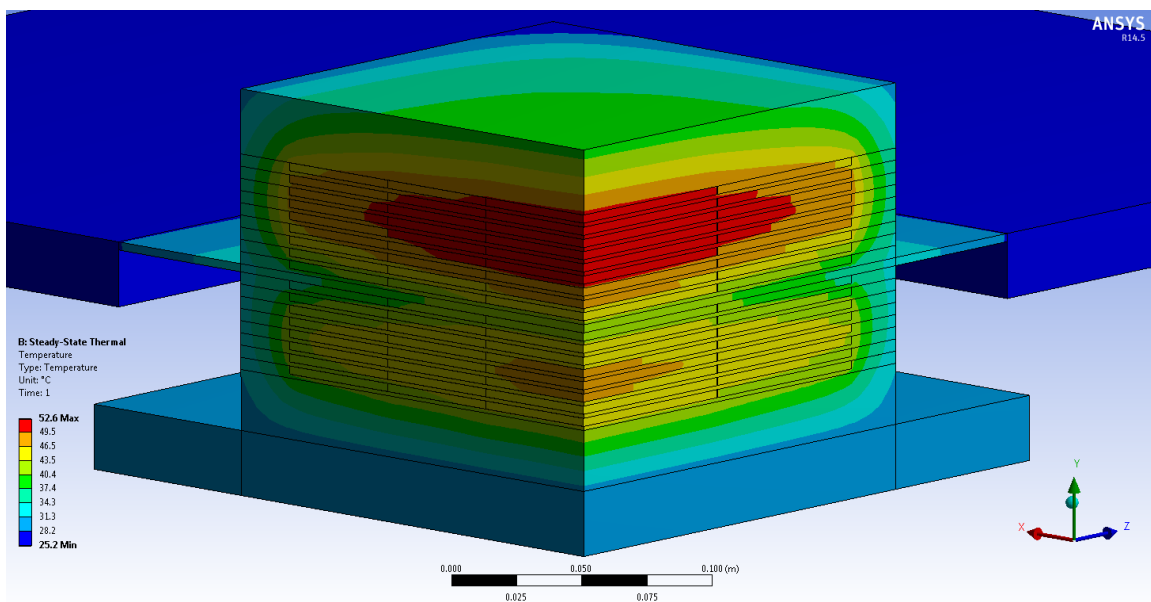


Figure 4.25. Steady State Temperature Contours for Experiment 2, without Fins. The peak temperature is 52.6 C and occurs at the center of the upper stack.

Figure 4.26 shows a similar setup to that shown in Figure 4.25 except that aluminum heat dispersal plates (fins) are placed in contact with each layer of ZPPR plates. The aluminum fins are 18 in by 18 in and 0.01 in thick. The aluminum fins greatly increase heat transfer and decrease the temperatures throughout the stack. Temperature contours for this case are shown in Figure 4.27. The peak temperature for this setup is almost 20 degrees cooler than the case without fins and is 36.3 C.

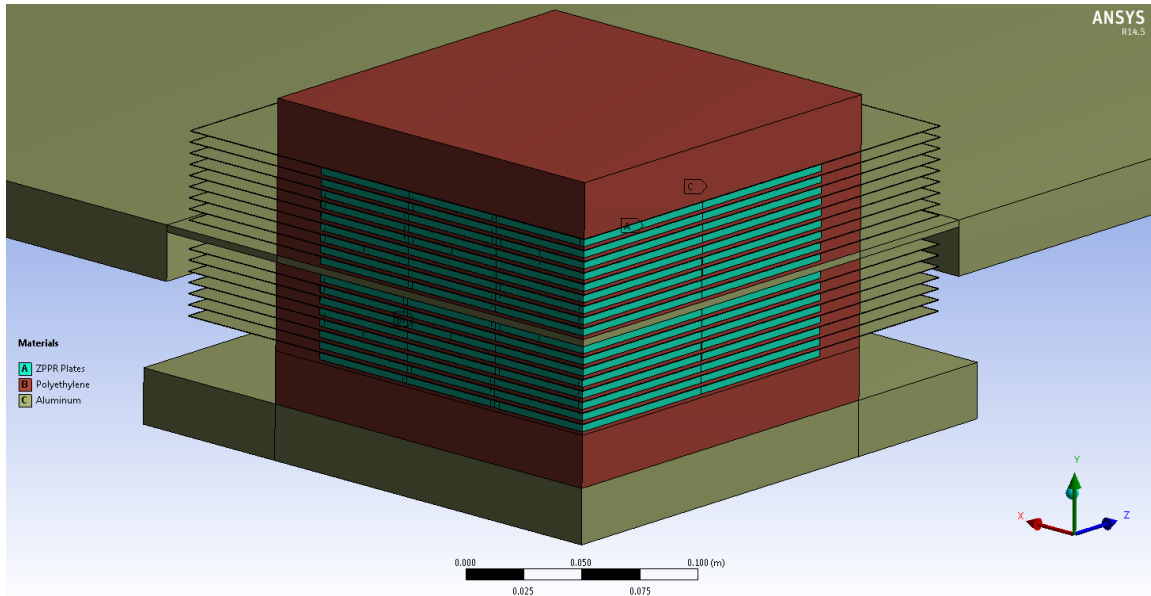


Figure 4.26. ANSYS Geometry for Experiment 2, with Fins. Interior corner of solid model of 17 layers of ZPPR plates with 1/16 inches of interspersed polyethylene and 0.01 inch aluminum fins. Stack of plates are surrounded by one inch of polyethylene. There are 9 layers above the 0.125 inch thick aluminum diaphragm and 8 below.

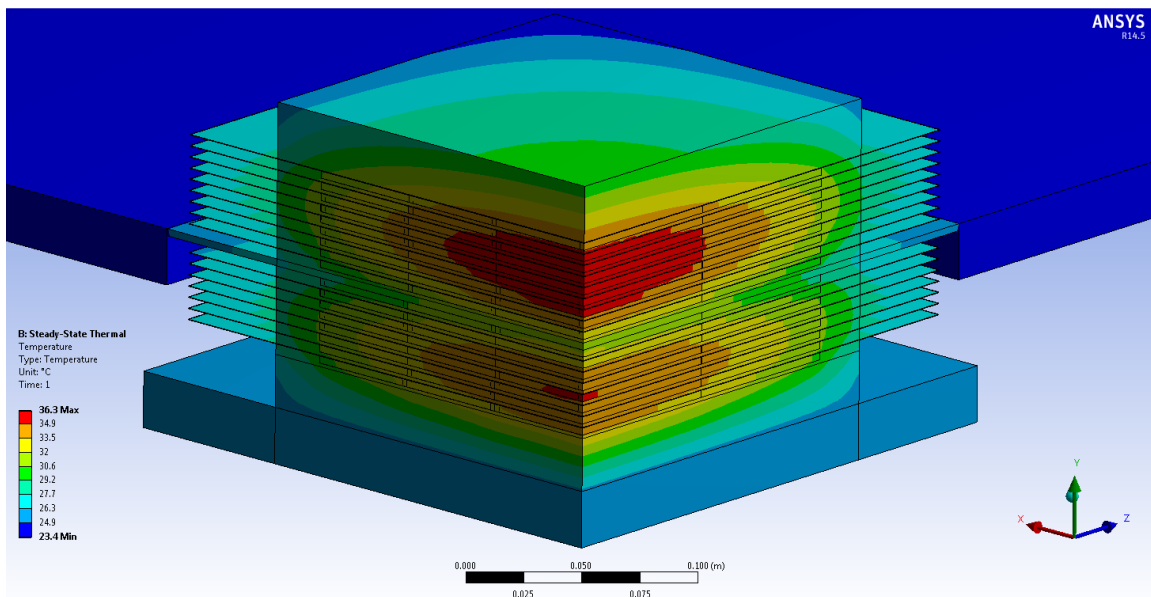


Figure 4.27. Steady State Temperature Contours for Experiment 2, with Fins. The peak temperature is 36.3 C and occurs at the center of the upper stack.

4.3.3.3 Experiment 3 Model- With and Without Fins

Experiment 3 was modeled with 12 layers of ZPPR plates and each Pu layer is placed on a 3/16" thick HDPE sheet that is 14" by 14". There are six layers of the ZPPR plates above the diaphragm and six layers below. The steady state thermal analysis is shown in Figure 4.28. The peak temperature is 44.9 C.

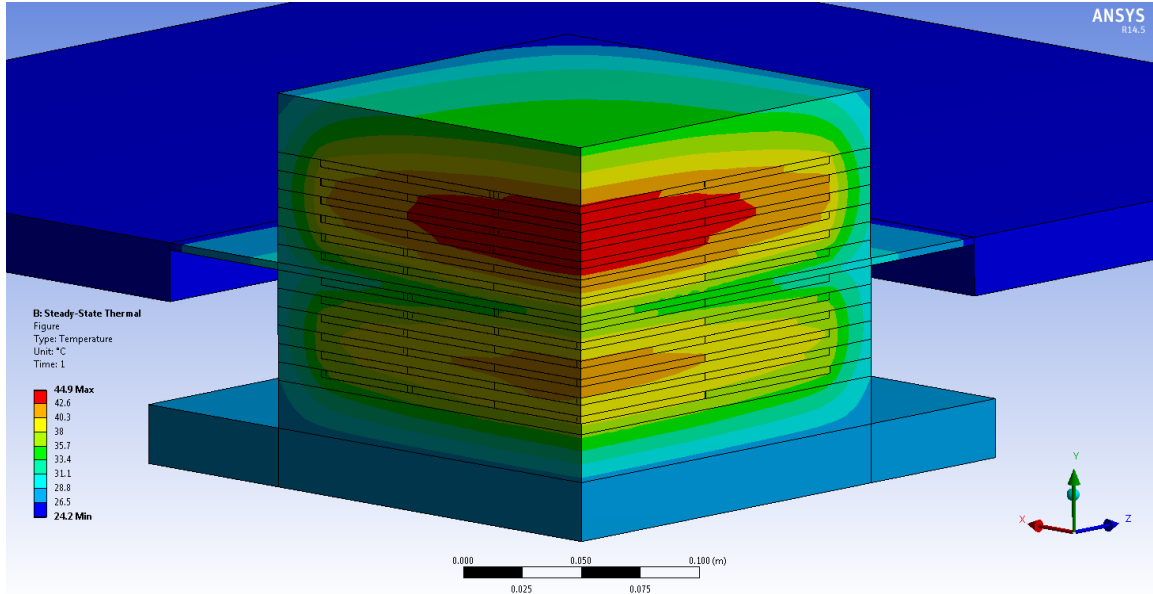


Figure 4.28. Steady State Temperature Contours for Experiment 3, without Fins. Steady-state temperature contours on interior corner of 12 layers of ZPPR plates with 3/16 inches of interspersed polyethylene. Stack of plates are surrounded by one inch of polyethylene. There are 6 layers above the 0.125 inch thick aluminum diaphragm and 6 below. The peak temperature is 44.9 C and occurs at the center of the upper stack.

Figure 4.29 shows a similar setup to that shown in Figure 4.28 except that aluminum heat dispersal plates (fins) are placed in contact with each layer of ZPPR plates. The aluminum fins are 18" by 18" and 0.01" thick. The aluminum fins greatly increase heat transfer and decrease the temperatures throughout the stack. The peak temperature for this setup is again cooler than the case without fins and is 34.6 C.

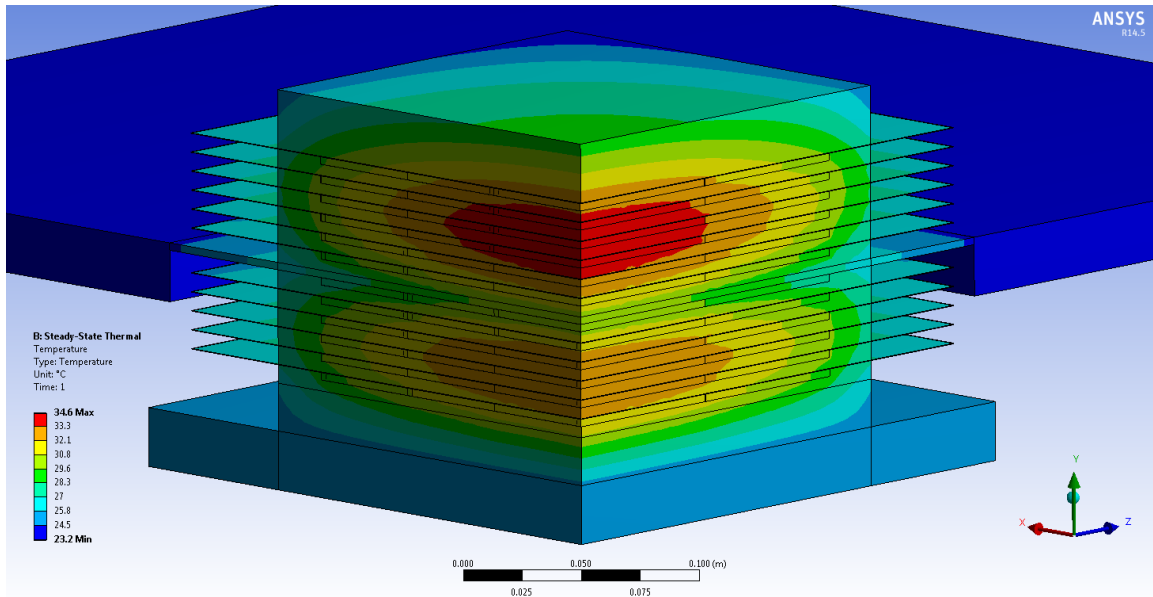


Figure 4.29. Steady State Temperature Contours for Experiment 3, with Fins. The peak temperature is 34.6 C and occurs at the center of the upper stack.

4.3.3.4 Experiment 4 Model- With and Without Fins

Experiment 4 has eight layers of ZPPR plates with each layer on a 7/16 in thick HDPE sheet that is 14” by 14”. There are four layers of the ZPPR plates above the diaphragm and four layers below. The steady state thermal analysis is shown in Figure 4.30. The peak temperature is 39.1 C and occurs in the upper half of the stack.

Figure 4.31 shows a similar setup to that shown in Figure 4.30 except that sheets of aluminum are placed in contact with each layer of ZPPR plates. The aluminum fins are 18” by 18” and 0.01” thick. The aluminum fins greatly increase heat transfer and decrease the temperatures throughout the stack. The peak temperature for this setup is again cooler than the case without fins and is 32.7 C.

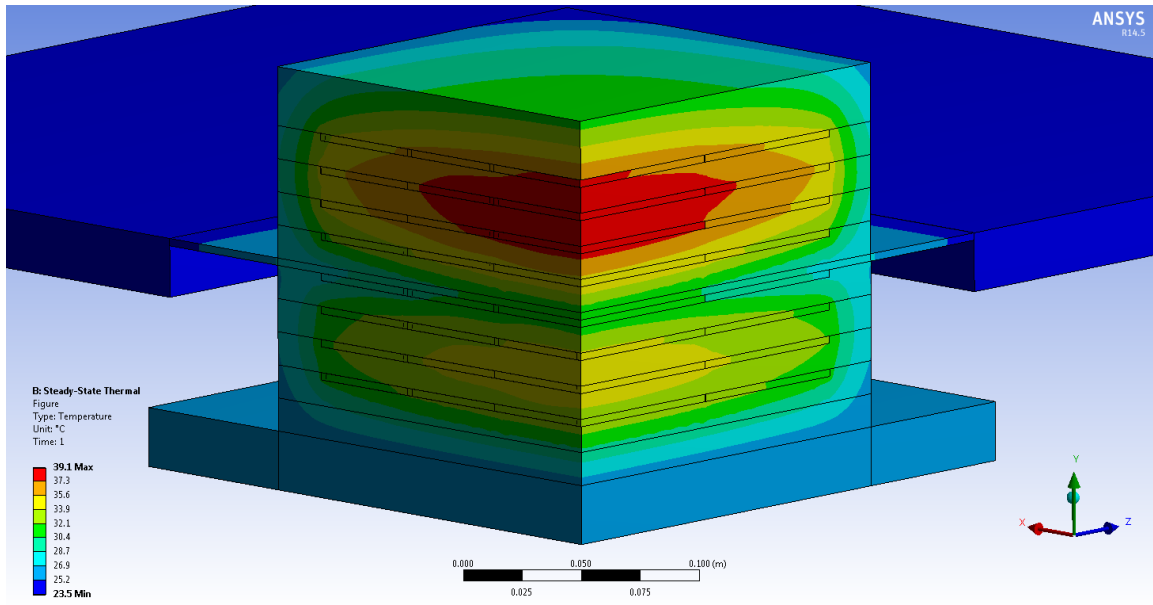


Figure 4.30. Steady State Temperature Contours for Experiment 4, without Fins. Steady-state temperature contours on interior corner of 8 layers of ZPPR plates with 7/16 inches of interspersed polyethylene. Stack of plates are surrounded by one inch of polyethylene. There are 4 layers above the 0.125 inch thick aluminum diaphragm and 4 below. The peak temperature is 39.1 C and occurs at the center of the upper stack.

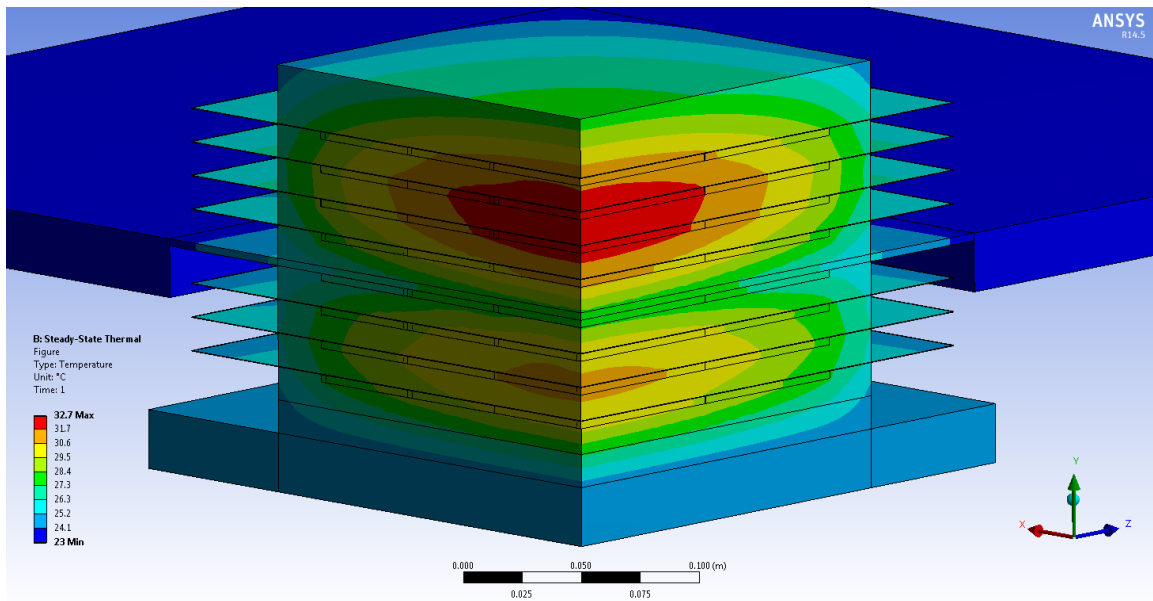


Figure 4.31. Steady State Temperature Contours for Experiment 4, with Fins. The peak temperature is 32.7 C and occurs at the center of the upper stack.

4.3.3.5 Experiment 5 Model- With and Without Fins

The final experiment setup (Experiment 5) has six layers of ZPPR plates with each layer on a 1" thick HDPE sheet that is 14" by 14". There are three layers of the ZPPR plates above the diaphragm and three layers below. The steady state thermal analysis is shown in Figure 4.32. The peak temperature is 36.6 C and occurs in the upper half of the stack. Figure 4.33 shows a similar setup to that shown in Figure 4.32 except that sheets of aluminum are placed in contact with each layer of ZPPR plates. The aluminum fins are 18" by 18" and 0.01" thick. The aluminum fins greatly increase heat transfer and decrease the temperatures throughout the stack. The peak temperature for this setup is again cooler than the case without fins and is 32.7 C.

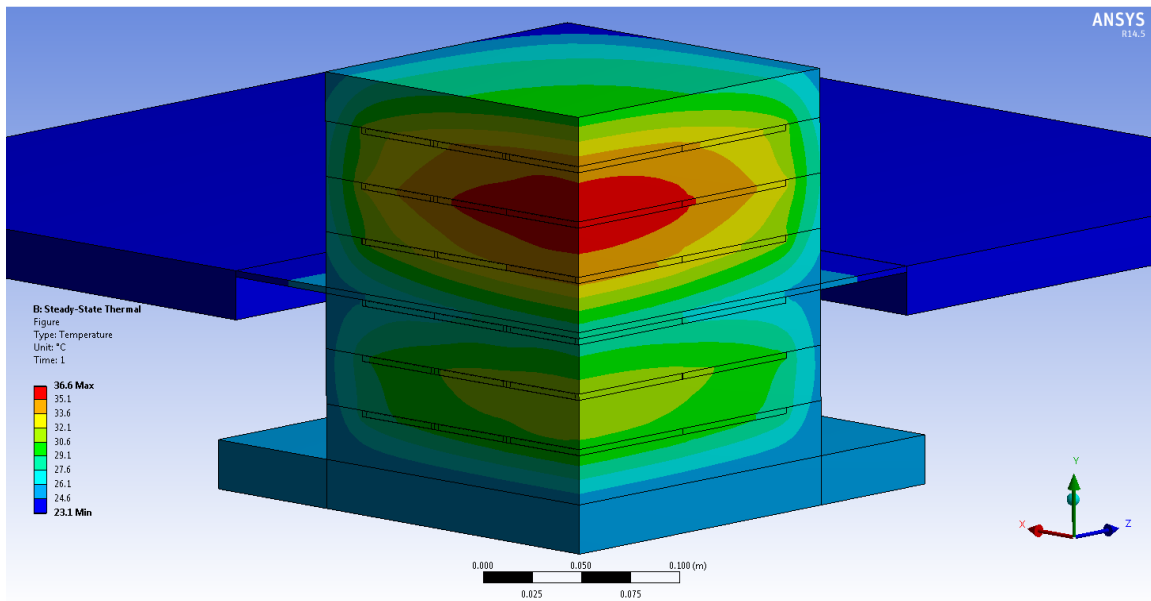


Figure 4-32. Steady State Temperature Contours for Experiment 5, without Fins. Steady-state temperature contours on interior corner of 6 layers of ZPPR plates with 1 inch of interspersed polyethylene. Stack of plates are surrounded by one inch of polyethylene. There are 3 layers above the 0.125 inch thick aluminum diaphragm and 3 below. The peak temperature is 36.6 C and occurs at the center of the upper stack.

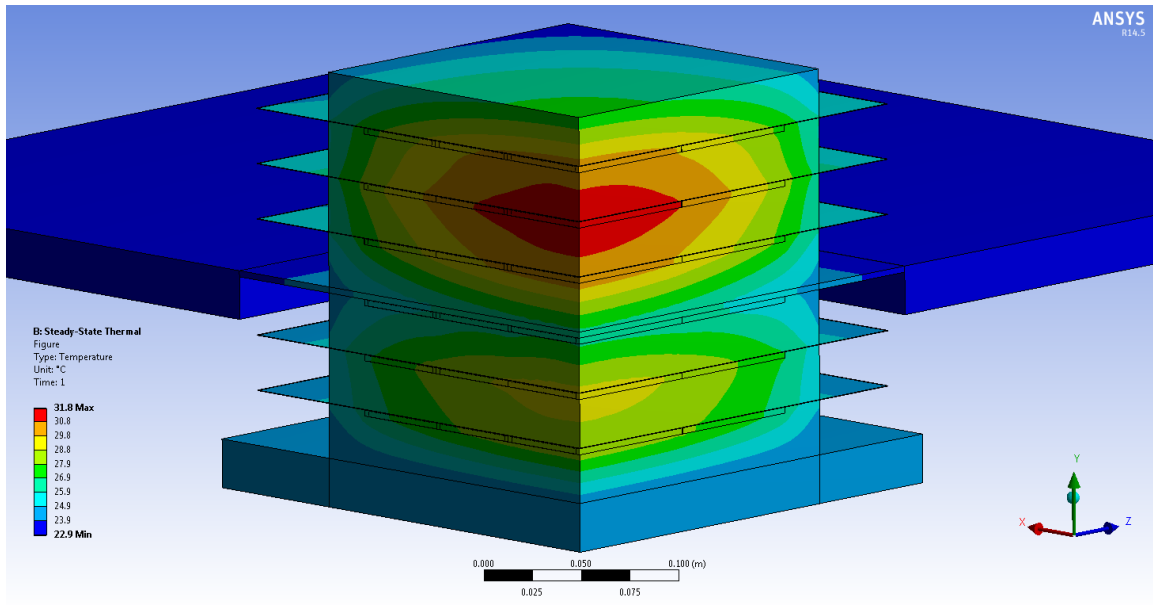


Figure 4.33. Steady State Temperature Contours for Experiment 5, with Fins. The peak temperature is 31.8 C and occurs at the center of the upper stack.

4.3.3.6 Mesh Independence of the Solution

Each experimental condition was solved on a coarse mesh and then a fine mesh to verify that the solution was not dependent on the mesh size chosen. Table 4-16 shows the results for each simulation with the two mesh settings and lists the peak temperature found for each. The number of elements for each simulation is listed, as well as, the mesh relevance setting used in ANSYS. The largest discrepancy between the solutions with different mesh resolutions was 0.7 C, but most simulations were within 0.2 C.

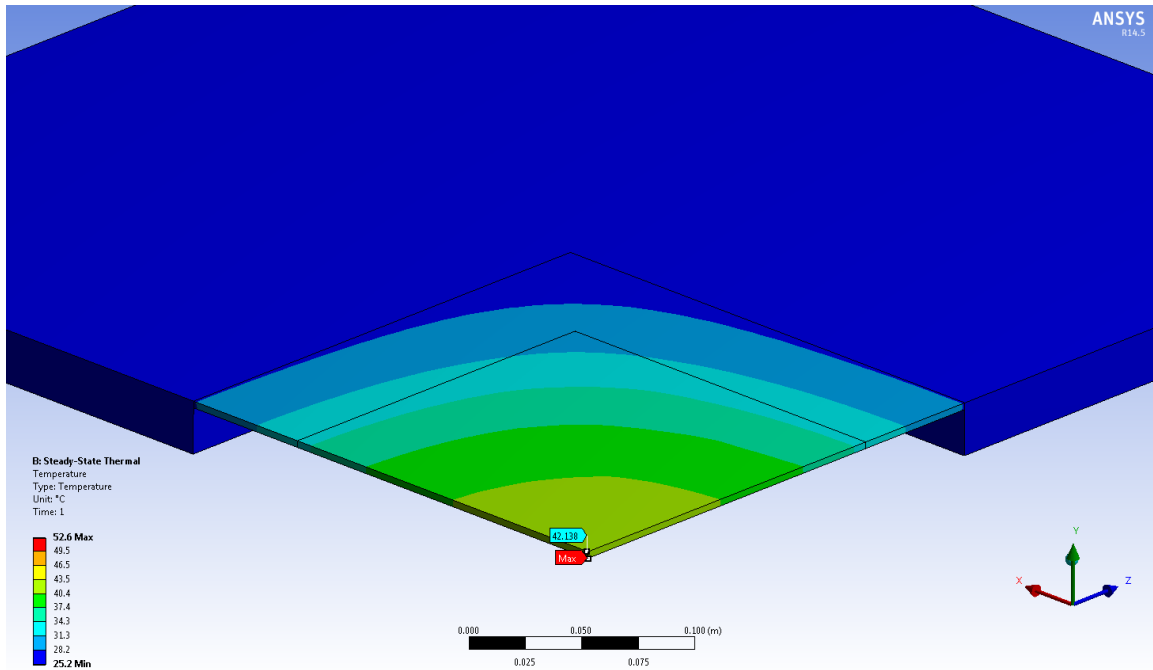
Table 4-16. Mesh Independence of Simulation Results

Pu Layers	Poly Thickness [in]	Fins?	Mesh Size	Number of elements	Peak Temperature [C]
21	0	Yes	Medium 0	126504	32.5
21	0	Yes	Fine 50	266662	32.6
17	1/16	No	Medium 0	110317	51.9
17	1/16	No	Fine 50	245809	52.6
17	1/16	Yes	Medium 0	113964	36.2
17	1/16	Yes	Fine 50	254817	36.3
12	3/16	No	Medium 0	78099	44.6
12	3/16	No	Fine 50	179041	44.9
12	3/16	Yes	Medium 0	78187	34.6
12	3/16	Yes	Fine 50	183667	34.6
8	7/16	No	Medium 0	53195	38.9
8	7/16	No	Fine 50	131969	39.1
8	7/16	Yes	Medium 0	52863	32.7
8	7/16	Yes	Fine 50	137031	32.7
6	1	No	Medium 0	40344	36.6
6	1	No	Fine 50	123396	36.6
6	1	Yes	Medium 0	39619	31.8
6	1	Yes	Fine 50	124106	31.8
17*	1/16	No	Coarse 0	139957	91.6
17*	1/16	No	Coarse 75	242986	92.2

*These simulations exclude support structures.

4.3.3.7 Diaphragm Temperature Gradient

Diaphragm warpage could be a concern with a temperature gradient associated with a high-temperature experiment. As shown in Table 4-15, Experiment 2 (17 layers of Pu ZPPR plates interspersed with 1/16" poly) was found to be the hottest experiment modeled, with a peak temperature in the stack of 52.6 °C. However, ANSYS predicts the aluminum diaphragm will stay significantly cooler in Experiment 2, as shown by the heat contour map presented in Figure 4.34. The maximum temperature for the diaphragm is predicted to be 42.138 °C, occurring at the center, resulting in a temperature gradient of only 17 degrees. Therefore, diaphragm warpage should not be a concern for these experiments.



4.3.4 Thermal Analysis Conclusions

Initial calculations indicated a risk of the experimental temperatures exceeding maximum long-term service temperature (80 C) for high density polyethylene. When additional experimental details were added to the models, such as the aluminum platen and platform supporting the stacks, temperatures were decreased to a maximum of 52.6 C for Experiment 2, with 17 layers of Pu and 1/16" thick polyethylene. For cases separated by the aluminum diaphragm, the peak temperature within the stack always occurred in the upper half of the stack because the bottom half of the stack was sandwiched by two large aluminum plates, which provided an efficient path for heat to escape. For the same reason the peak temperature was always lower for the setup with aluminum fins in-between each layer of ZPPR plates. As the number of ZPPR layers decreased so did the temperatures throughout the stack. The mesh size was shown to have minimal effect on the calculated temperatures.

Therefore, the aluminum heat dispersal plates are likely not required to keep the temperature below the polyethylene impact temperature of 80 C. However, the fins help normalize the temperature over the five experiments and will allow for easier cross-comparison of cross section results by minimizing the temperature variable. Also, the fins might be necessary with larger Pu loadings required by diluting the stack with other diluent materials.

4.4 Structural Load Analysis for Aluminum Platen and Diaphragm

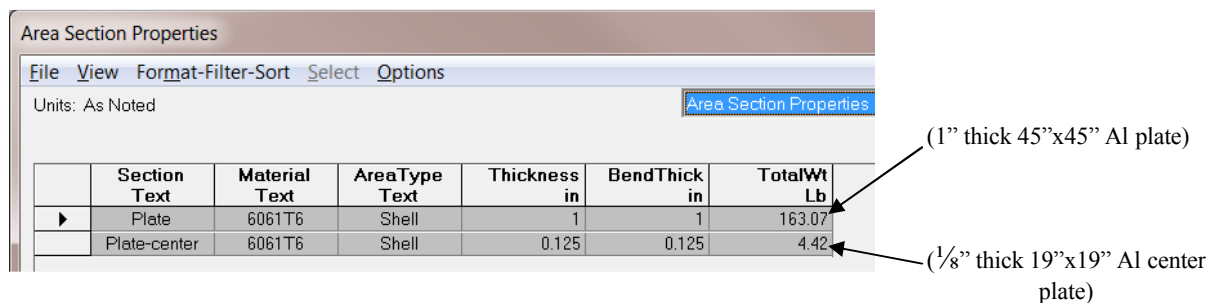
A structural analysis of the aluminum diaphragm and platen was completed to ensure the aluminum could adequately support the weight of the experiment. NCERC requires all diaphragms to have a safety factor of 4 for the supported weight. Based on the critical configurations calculated in Section 4.1, a conservative bounding mass for half of the experiment was chosen as 125 kg. For the highest mass experiment (Experiment 7 with 30 layers of Pu and tantalum), half the experiment stack is approximately 87 kg, including 15 layers of Pu, tantalum, polyethylene, and aluminum sheets. Therefore, the load analysis looked at a 45" by 45" plate supported at each corner for a 500 kg dead weight (including a safety factor of 4) for the TEX experiments.

4.4.1 Load Analysis Methodology

A general purpose finite element software, SAP2000, was used to evaluate the diaphragm design of the TEX experiment. SAP2000 is a general purpose finite element software that performs static or dynamic, linear or nonlinear analysis of structural systems. These features, and many more, make SAP2000 the state-of-the-art in structural analysis program. SAP2000 is one of the software available in the LLNL Engineering Toolkit. SAP2000 is developed by Computers & Structures Inc.

4.4.2 SAP2000 FEA model

Based on the drawing presented as Figure 3.1, the aluminum upper support platen was modeled as shell members in SAP2000. The outer dimensions are 45" by 45" (114.3 cm by 114.3 cm) and the outer plate thickness is 1" (2.54 cm). A 19" (48.26 cm) square thin diaphragm is supported in the center of the platen. The diaphragm is 0.125" (0.3175 cm) thick. The entire platen, including the diaphragm, was modeled as Al-6061. A screen capture from SAP2000 is shown in Figure 4.35 below, giving the modeled properties.



	Section Text	Material Text	AreaType Text	Thickness in	BendThick in	TotalWt Lb
▶	Plate	6061T6	Shell	1	1	163.07
	Plate-center	6061T6	Shell	0.125	0.125	4.42

Figure 4.35. Properties of TEX Platen Modeled in SAP2000.

Two different deadweight loads were applied, the expected 100 kg load and a 500 kg load (incorporating a 5X safety factor). The applied was modeled at the center of the aluminum plate over an area of 12.5"x12.5", as shown in Figure 4.36.

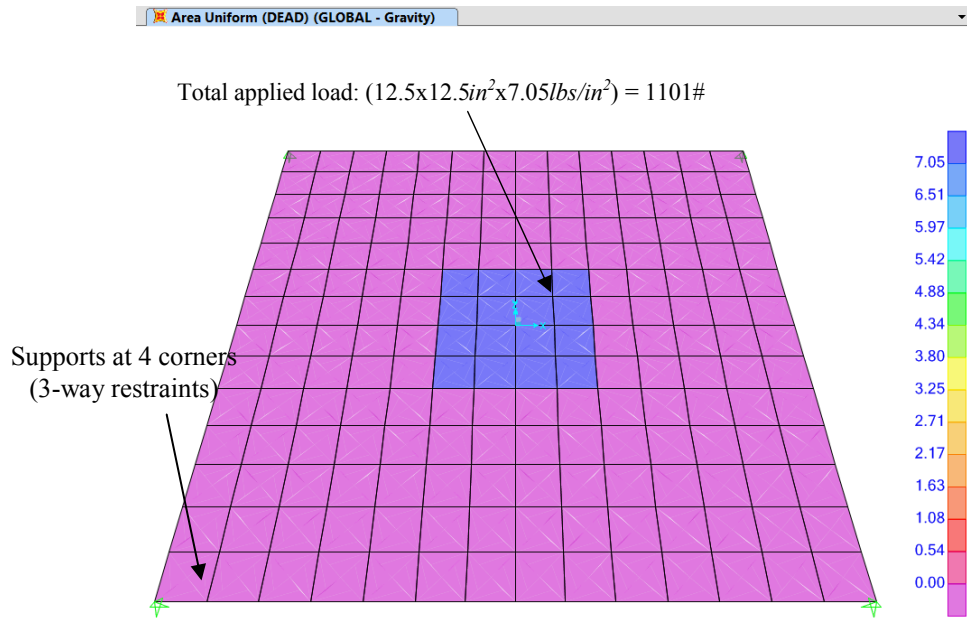
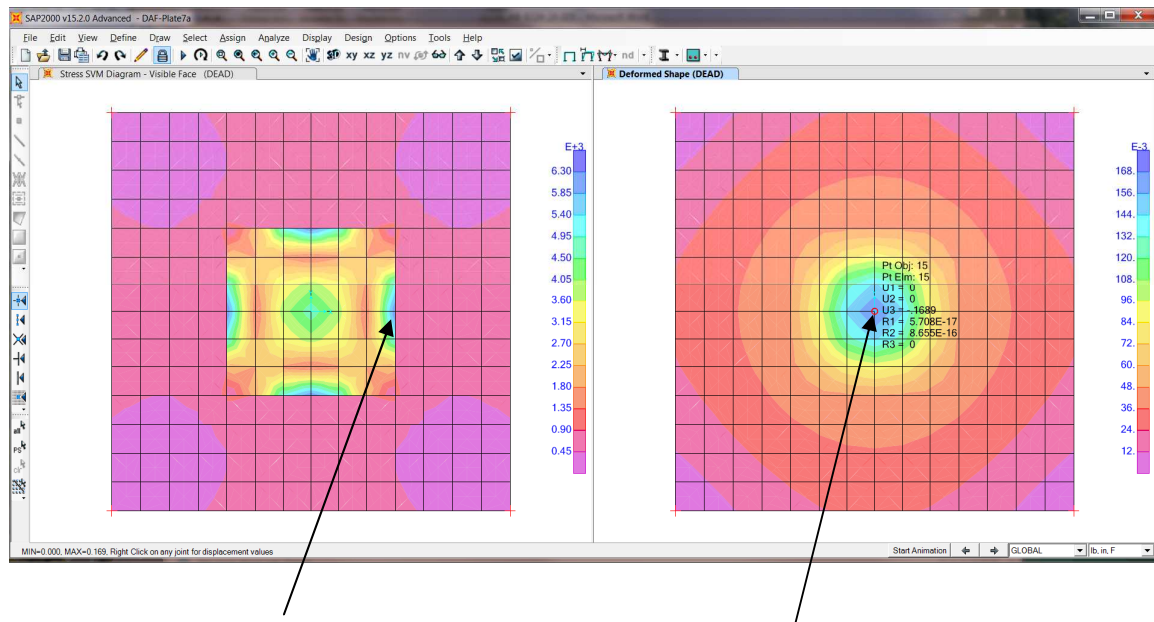


Figure 4.36. SAP2000 Model of Al Platen Showing Applied Load.

4.4.3 Load Analysis Results and Conclusions

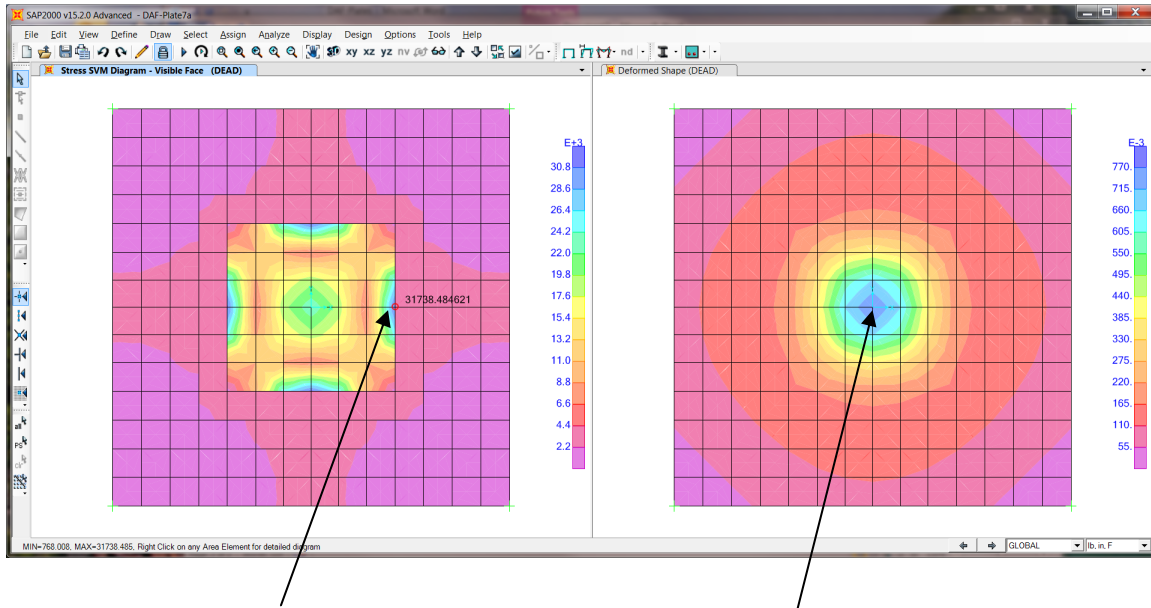
The SAP2000 Results are shown in Figure 4.37 (100 kg) and Figure 4.38 (500 kg). The images on the right show color-coded stress (in psi) put on the diaphragm from the dead load. For the 500 kg safety calculation, the maximum stress experienced by the plate was 31,738 psi, well below the yield stress of 35,000 psi for Al-6061. The image on the right of the figures shows the deflection map of the 0.125" Al-6061 diaphragm, which has its maximal deflection at the center of 0.78" for the 500 kg load and the maximum deflection of the 100 kg load of 0.17".



Maximum stress = 6730 *psi*

Maximum deflection = 0.17"

Figure 4.37. SAP2000 Results Showing Stress Map (left figure) and Displacement Map (right figure) of the TEX Al-6061 Platen in Response to a 100 kg Deadweight Load.



Maximum stress = 31,738 *psi*

Maximum deflection = 0.78"

Figure 4.38. SAP2000 Results Showing Stress Map (left figure) and Displacement Map (right figure) of the TEX Al-6061 Platen in Response to a 500 kg Deadweight Load.

As shown by the SAP2000 results, the platen design is robust enough to withstand five times the anticipated mass of the TEX experiments. The expected stresses and deflections are much lower, with the maximum deflection being approximately 0.17". The platen was designed with additional margin over the current expected TEX experimental masses to account for additional diluent materials the NCSP might want to test in the future.

5.0 Cost Estimates for Fabrication

The highest-cost components of the described TEX experiments are the fissile material (Pu ZPPR plates) and the tantalum diluent plates. Both of these types of plates already exist and belong to the NCSP.

The remaining parts to be fabricated are four sets of trays, polyethylene reflector and moderator sheets, and the aluminum upper platen and lower platform for use with the Planet critical assembly machine. Table 5-1 lists estimated material and fabrication costs associated with these parts.

Table 5-1: Estimated Costs for Fabricated Parts

Tray TEX-Al-1/8, Aluminum-Bottomed Trays with 1/8" Deep Polyethylene Sides 25 Trays	
3 4'x8' Sheets of 0.01" Al-6061	\$750.00
2 4'x8' Sheets of 1/8" HDPE	\$400.00
Fabrication Costs	\$2000.00
Tray TEX-PE-1/8, Polyethylene-Bottomed Trays with 1/8" Deep Polyethylene Sides 25 Trays	
2 4'x8' Sheets of 1/16" HDPE	\$200.00
3 4'x8' Sheets of 0.01" Al-6061	\$750.00
2 4'x8' Sheets of 1/8" HDPE	\$400.00
Fabrication Costs	\$2000.00
Tray TEX-Al-3/16, Aluminum-Bottomed Trays with 3/16" Deep Polyethylene Sides 30 Trays	
4 4'x8' Sheets of 0.01" Al-6061	\$1000.00
2 4'x8' Sheets of 3/16" HDPE	\$400.00
Fabrication Costs	\$2000.00
Tray TEX-PE-3/16, Polyethylene-Bottomed Trays with 3/16" Deep Polyethylene Sides 35 Trays	
2 4'x8' Sheets of 1/16" HDPE	\$200.00
5 4'x8' Sheets of 0.01" Al-6061	\$1250.00
2 4'x8' Sheets of 3/16" HDPE	\$400.00
Fabrication Costs	\$2500.00
TEX-PS-1/8, Interstitial Poly Plates 1/8" Thick 36 Plates	
2 4'x8' Sheets of 1/8" HDPE	\$400.00
Fabrication Costs	\$500.00
TEX-PS-3/8, Interstitial Poly Plates 3/8" Thick 36 Plates	
2 4'x8' Sheets of 3/8" HDPE	\$650.00
Fabrication Costs	\$500.00
TEX-PS-15/16, Interstitial Poly Plates 15/16" Thick 18 Plates	

1 4'x8' Sheet of 15/16" HDPE	\$450.00
Fabrication Costs	\$500.00
TEX-PS-1, Interstitial Poly Plates 1" Thick 18 Plates	
1 4'x8' Sheet of 1" HDPE	\$450.00
Fabrication Costs	\$500.00
TEX-Al-Platen, 1" Aluminum Platen with 0.125" Inner Diaphragm	
45"x45"x1" Al-6061	\$2000.00
0.125" Al Diaphragm	\$100.00
Fabrication Costs	\$1500.00
Total Material Costs	\$9800.00
Total Fabrication Costs	\$12,000.00
Total Costs for Materials	\$21,800.00

LLNL recommends inspections of the parts once fabricated and constituent and impurity analysis (likely through mass spectroscopy) in order to reduce benchmark uncertainties. LLNL has conservatively estimated those costs to be \$20,000, based on current costs and estimates of laboratory time.

A detailed inspection of all items (or at least a representative sample) is also recommended, including dimensional measurements and contour measurements, particularly of the fissile parts. LLNL estimates these costs to be \$5000 for the non-fissile parts, and \$20,000 for the fissile parts.

6.0 Conclusions and Recommended Schedule for CED-3

The following sections describe considerations for scheduling activities associated with CED-3A (Project Introduction) and CED-3B (Experiment Execution).

6.1 Scheduling Considerations

6.1.1 NCSP Possession of ZPPR Plates

The INL is in the process of transferring the ZPPR inventory to NCERC. As of early FY2015, approximately 25 kg of the Pu ZPPR plates will be available at NCERC. 25 kg is enough material to complete two of the ten proposed experiments (Experiments 4 and 5, baseline undiluted cases with 7/16" and 1" of polyethylene moderator plates). Enough plates to complete all experiments are scheduled to be shipped to NCERC by the first quarter of FY2016.

6.1.2 Fabrication of Moderators, Reflectors, and Fixturing

The most expensive parts of the TEX experiments, namely the Pu/Al ZPPR plates and the tantalum diluent plates, already exist. As described in Section 5.0, reflectors, moderators aluminum heat dispersal plates, and aluminum fixturing for Planet will need to be fabricated. LLNL estimates that these items could be fabricated in Q1 of FY15. There are no long-lead items that need to be fabricated.

6.1.3 Subcritical Measurements to Confirm Temperature Calculations

Section 4.3 of this report provided ANSYS calculations demonstrating that plutonium temperature gradients were mitigated due to the Planet aluminum support structure and the aluminum heat dispersal plates. However, LLNL believes it is prudent to test the efficacy of these features before starting a full critical experiment and suggests completing a thermal (subcritical) experimental measurement to confirm the ANSYS calculations during Q2 of FY15.

6.1.4 Documented Safety Analysis MAR Limit for Planet

Please see Addendum 1 for a discussion of the MAR limits for Planet.

6.1.5 Characterization of ZPPR Plates

A large amount of information was found regarding the construction of the ZPPR plates in the INL archives. The one missing piece of information is the impurity content of the plutonium. The unknown composition of the impurities in the fissile material leads to uncertainty in the benchmark evaluation, although the impurity content is believed to be small (600 ppm). Since these Pu/Al plates are relatively pure and the NCSP has a large amount, they will likely be used for many future experiments at NCERC. LLNL has identified another DOE program that has interest in characterizing the Pu/Al ZPPR plates because it appears to be a unique material. Additionally, LLNL is currently standing up a glovebox at DAF that would be capable of sampling the Pu ZPPR plates. Sampling the plates and analyzing the samples for impurities is not required before the start of the experiments and could be pursued in parallel.

6.2 CED-3 Schedule

FY 2015- Quarter 1 and Quarter 2

- **Project Introduction.** LLNL will work with NSTec and LANL personnel to prepare all facility documentation and reactor safety and experimental plans.

- **Procurements and Fabrication.** LLNL will procure materials and fabricate the associated experimental parts as detailed in Section 5.0.
- **Subcritical Temperature Measurements.** LLNL will work with NSTec and LANL personnel to carry out subcritical stack temperature measurements to benchmark the ANSYS thermal calculations presented in Section 4.2. These measurements could be conducted on either the NCERC or Nuclear Explosive Operations (NEO) side of the DAF and would require changes to existing work packages. While LLNL would like to do these subcritical temperature measurements, they are not required for the critical experiment.
- **Characterization of ZPPR Plates.** LLNL will pursue characterization of the Pu ZPPR plates and investigate cost sharing with other LLNL groups representing other DOE programs. The LLNL glovebox needed to sample the plates at DAF is currently scheduled to begin operations in FY2015. Sampling the plates and analyzing the samples for impurities is not required before the start of the experiments and will be pursued in parallel.

FY 2015- Quarter 3 & 4

- **Experiment Execution.** Currently, enough Pu ZPPR plates are present at NCERC to complete Experiments 4 and 5, the baseline undiluted cases with 7/16" and 1" of polyethylene moderator plates. LLNL will work with NCERC personnel to schedule and conduct these two experiments.

FY 2016

- **Experiment Execution.** Once enough Pu ZPPR plates are received at NCERC (currently scheduled for Q1 of FY16), LLNL will work with NCERC personnel to schedule and conduct the rest of the eight TEX experiments.

6.3 CED-4 Schedule

- **Laboratory Reports.** A laboratory report summarizing each critical configuration will be completed one month after the completion of each experiment. These laboratory reports will record the experimental details needed for the ICSBEP benchmark.
- **ICSBEP Evaluations.** ICSBEP evaluations for Experiments 4 and 5 will be completed in FY16, Q3 for review by the ICSBEP review group in May of 2016. ICSBEP evaluations for the remaining experiments will be completed in FY17, Q3.

Appendix A: Sample MCNP5 Calculations

TEX Pu Baseline Experiment 1

c ZPPR PANN plate model by Allan Krass

c Array model and stack model by Soon Kim

c Edited by Catherine Percher

c

C the outer dimensions of the PANN ZPR plate in this model come to

C Length = 3.003348 inches (7.62850392 cm)

C Width = 1.970 inches (5.0038 cm)

C Height = 0.1205 inches (0.30607 cm)

C ----- Pu Alloy Core -----

C density = 105.136 grams/6.958542864 cc (analytic vol rounded to 9 decimals)

1 1 -15.108910307 &

```
( 108 -109 111 -114 105 -106): & $ full ht main +/- y body
( 107 -108 112 -113 105 -106): & $ full ht main -x body
( 109 -110 112 -113 105 -106): & $ full ht main +x body
(-117 -108 113 105 -106): & $ full height -x,+y corner
(-119 109 113 105 -106): & $ full height +x,+y corner
(-121 -108 -112 105 -106): & $ full height -x,-y corner
(-123 109 -112 105 -106): & $ full height +x,-y corner
( 101 -107 112 -113 115 -116): & $ flat edge -x face
(-125 -107 112 -113 -115): & $ rounded lo edge -x face
(-126 -107 112 -113 116): & $ rounded hi edge -x face
(-102 110 112 -113 115 -116): & $ flat edge +x face
(-127 110 112 -113 -115): & $ rounded lo edge +x face
(-128 110 112 -113 116): & $ rounded hi edge +x face
(-104 114 108 -109 115 -116): & $ flat edge +y face
(-129 114 108 -109 -115): & $ rounded lo edge +y face
(-130 114 108 -109 116): & $ rounded hi edge +y face
( 103 -111 108 -109 115 -116): & $ flat edge -y face
(-131 -111 108 -109 -115): & $ rounded lo edge -y face
(-132 -111 108 -109 116): & $ rounded hi edge -y face
( 117 -118 -108 113 115 -116): & $ -x,+y corner face
( 119 -120 109 113 115 -116): & $ +x,+y corner face
( 121 -122 -108 -112 115 -116): & $ -x,-y corner face
( 123 -124 109 -112 115 -116): & $ +x,-y corner face
(-133 117 -108 113 -115): & $ rnd lo edge -x,+y corner
(-134 117 -108 113 116): & $ rnd hi edge -x,+y corner
(-135 119 109 113 -115): & $ rnd lo edge +x,+y corner
(-136 119 109 113 116): & $ rnd hi edge +x,+y corner
(-137 121 -108 -112 -115): & $ rnd lo edge -x,-y corner
(-138 121 -108 -112 116): & $ rnd hi edge -x,-y corner
(-139 123 109 -112 -115): & $ rnd lo edge +x,-y corner
(-140 123 109 -112 116): & $ rnd hi edge +x,-y corner
```

u=1 imp:n=1

C ----- SS304 Sleeve and Plugs -----

C density = 24.765 grams/3.134781858 cc (analytic vol rounded to 9 decimals)

2 2 -7.90007124 &

```
(201 -204 207 -208 211 -212): & $ flat +z face
(201 -204 207 -208 215 -216): & $ flat -z face
(201 -204 213 -214 209 -210): & $ flat +y face
(201 -204 213 -214 205 -206): & $ flat -y face
(201 -204 208 214 217 -218): & $ rounded +y,+z edge
(201 -204 208 -213 219 -220): & $ rounded +y,-z edge
```



```

(201 -204 -207 214 221 -222): & $ rounded -y,+z edge
(201 -204 -207 -213 223 -224): & $ rounded -y,-z edge
(201 -202 208 214 -217): & $ rnd +y,+z edge -x plug
(201 -202 208 -213 -219): & $ rnd +y,-z edge -x plug
(201 -202 208 -209 213 -214): & $ +y end -x plug
(201 -202 207 -208 212 -215): & $ main body -x plug
(201 -202 -207 206 213 -214): & $ -y end -x plug
(201 -202 -207 214 -221): & $ rnd -y,+z edge -x plug
(201 -202 -207 -213 -223): & $ rnd -y,-z edge -x plug
(203 -204 208 214 -217): & $ rnd +y,+z edge +x plug
(203 -204 208 -213 -219): & $ rnd +y,-z edge +x plug
(203 -204 208 -209 213 -214): & $ +y end +x plug
(203 -204 207 -208 212 -215): & $ main body +x plug
(203 -204 -207 206 213 -214): & $ -y end +x plug
(203 -204 -207 214 -221): & $ rnd -y,+z edge +x plug
(203 -204 -207 -213 -223) & $ rnd -y,-z edge +x plug
u=1 imp:n=1
C ----- Carbon Steel Spring -----
3 3 -7.82 (301 -302 -303 304 -305 -306): & $ -y arm, inner segment
(301 -302 303 -307 -308 -309): & $ +y arm, inner segment
(301 -302 -304 -310 -311 312): & $ -y arm, outer segment
(301 -302 307 -313 -314 315): & $ +y arm, outer segment
(301 -302 310 316 317 -318): & $ curled end, -y
(301 -302 313 319 320 -321) & $ curled end, +y
u=1 imp:n=1
4 0 #1 #2 #3 u=1 imp:n=1
c 1st layer
5 0 201 -204 205 -210 211 -216 u=2 imp:n=1 $void
6 0 #5 u=2 imp:n=1
7 0 201 -204 205 -210 211 -216 lat=1 u=3 imp:n=1
fill=-3:4 -2:3 0:0
2 2 2 2 2 2 2
2 1 1 1 1 1 1 2
2 1 1 1 1 1 1 2
2 1 1 1 1 1 1 2
2 1 1 1 1 1 1 2
2 2 2 2 2 2 2
8 0 #7 u=3 imp:n=1
9 0 -1 fill=3 u=7 imp:n=1
10 5 -0.967 1 u=7 imp:n=1
11 0 -44 fill=7 imp:n=1
c poly
14 6 -2.7 -4 imp:n=1 $al
15 6 -2.7 -5 imp:n=1 $al bottom
16 5 -0.967 -10 imp:n=1 $poly, bottom 1"
19 like 11 but trcl=(0 0 0.33147) imp:n=1 $fuel 2
20 like 14 but trcl=(0 0 0.33147) imp:n=1 $Al 2
21 like 11 but trcl=(0 0 0.66294) imp:n=1 $fuel 3
22 like 14 but trcl=(0 0 0.66294) imp:n=1 $Al 3
23 like 11 but trcl=(0 0 0.99441) imp:n=1 $fuel 4
24 like 14 but trcl=(0 0 0.99441) imp:n=1 $Al 4
25 like 11 but trcl=(0 0 1.32588) imp:n=1 $fuel 5
26 like 14 but trcl=(0 0 1.32588) imp:n=1 $Al 5
27 like 11 but trcl=(0 0 1.65735) imp:n=1 $fuel 6
28 like 14 but trcl=(0 0 1.65735) imp:n=1 $Al 6
29 like 11 but trcl=(0 0 1.98882) imp:n=1 $fuel 7

```

```

30 like 14 but trcl=(0 0 1.98882) imp:n=1 $Al 7
31 like 11 but trcl=(0 0 2.32029) imp:n=1 $fuel 8
32 like 14 but trcl=(0 0 2.32029) imp:n=1 $Al 8
33 like 11 but trcl=(0 0 2.65176) imp:n=1 $fuel 9
34 like 14 but trcl=(0 0 2.65176) imp:n=1 $Al 9
35 like 11 but trcl=(0 0 2.98323) imp:n=1 $fuel 10
36 like 14 but trcl=(0 0 2.98323) imp:n=1 $Al 10
37 like 11 but trcl=(0 0 3.3147) imp:n=1 $fuel 11
38 like 14 but trcl=(0 0 3.3147) imp:n=1 $Al 11
39 6 -2.7 -6 imp:n=1 $middle center
40 6 -2.7 -7 8 imp:n=1 $middle center
41 like 11 but trcl=(0 0 3.96367) imp:n=1 $fuel 12
42 like 14 but trcl=(0 0 3.96367) imp:n=1 $Al 12
43 like 11 but trcl=(0 0 4.29514) imp:n=1 $fuel 13
44 like 14 but trcl=(0 0 4.29514) imp:n=1 $Al 13
45 like 11 but trcl=(0 0 4.62661) imp:n=1 $fuel 14
46 like 14 but trcl=(0 0 4.62661) imp:n=1 $Al 14
47 like 11 but trcl=(0 0 4.95808) imp:n=1 $fuel 15
48 like 14 but trcl=(0 0 4.95808) imp:n=1 $Al 15
49 like 11 but trcl=(0 0 5.28955) imp:n=1 $fuel 16
50 like 14 but trcl=(0 0 5.28955) imp:n=1 $Al 16
51 like 11 but trcl=(0 0 5.62102) imp:n=1 $fuel 17
52 like 14 but trcl=(0 0 5.62102) imp:n=1 $Al 17
53 like 11 but trcl=(0 0 5.95249) imp:n=1 $fuel 18
54 like 14 but trcl=(0 0 5.95249) imp:n=1 $Al 18
55 like 11 but trcl=(0 0 6.28396) imp:n=1 $fuel 19
56 like 14 but trcl=(0 0 6.28396) imp:n=1 $Al 19
57 like 11 but trcl=(0 0 6.61543) imp:n=1 $fuel 20
58 like 14 but trcl=(0 0 6.61543) imp:n=1 $Al 20
59 like 11 but trcl=(0 0 6.9469) imp:n=1 $fuel 21
60 like 14 but trcl=(0 0 6.9469) imp:n=1 $Al 21
911 5 -0.967 -9 imp:n=1 $top poly
997 0 -3 #11 #14 #15 #16 #19 #20 #21 #22 #23
    #24 #25 #26 #27 #28 #29 #30 #31 #32 #33
    #34 #35 #36 #37 #38 #39 #40 #41 #42 #43 #44
    #45 #46 #47 #48 #49 #50 #51 #52 #53 #54 #55
    #56 #57 #58 #59 #60
    #911
    imp:n=1
998 0 3 imp:n=0

c
1 rpp -17.5133 12.5095 -19.0712598 11.44276 -0.153035 0.153035 $fuel
44 rpp -20.0533 15.0495 -21.61126 13.98276 -0.153035 0.153035 $tray tot=0.33147
3 rpp -60 55 -61 54 -6 23
4 rpp -25.1333 20.1295 -26.69126 19.06276 -0.178435 -0.153035 $al
5 rpp -32.9819 27.9781 -34.2943 26.66575 -5.258435 -2.718435 $bottom Al
6 rpp -26.6319 21.6281 -27.9443 20.31575 3.467735 3.785235 $middle center
7 rpp -59.6519 54.6481 -60.9643 53.33575 1.245235 3.785235 $middle
8 rpp -26.6319 21.6281 -27.9443 20.31575 1.245235 3.785235 $middle inside
9 rpp -20.0533 15.0495 -21.61126 13.98276 7.099935 9.639935 $top poly 1"
10 rpp -20.0533 15.0495 -21.61126 13.98276 -2.718435 -0.178435 $bot poly 15/16"
C ----- carbon steel spring surfaces (minimum compression) -----
C
301 3 pz -0.0890775
302 3 pz 0.0890775

```

```

303 3 px 0.0
C -----
304 3 px -0.9707

305 3 p 0.0 -0.0269 0.0 -0.9707 -0.1470 -1.0 -0.9707 -0.1470 1.0
306 3 p 0.0 0.0 0.0 -0.9707 -0.1200 -1.0 -0.9707 -0.1200 1.0
C -----
307 3 px 0.9707
308 3 p 0.0 -0.0269 0.0 0.9707 -0.1470 -1.0 0.9707 -0.1470 1.0
309 3 p 0.0 0.0 0.0 0.9707 -0.1200 -1.0 0.9707 -0.1200 1.0
C -----
310 3 p -2.1839 -0.0664 0.0 -2.1773 -0.0003 -1.0 -2.1773 -0.0003 1.0
311 3 p -2.1799 -0.0269 0.0 -0.9707 -0.1470 -1.0 -0.9707 -0.1470 1.0
312 3 p -2.1773 -0.0003 0.0 -0.9707 -0.1200 -1.0 -0.9707 -0.1200 1.0
C -----
313 3 p 2.1839 -0.0664 0.0 2.1773 -0.0003 -1.0 2.1773 -0.0003 1.0
314 3 p 2.1799 -0.0269 0.0 0.9707 -0.1470 -1.0 0.9707 -0.1470 1.0
315 3 p 2.1773 -0.0003 0.0 0.9707 -0.1200 -1.0 0.9707 -0.1200 1.0
C -----
316 3 p -2.1839 -0.0664 0.0 -2.2478 -0.0840 -1.0 -2.2478 -0.0840 1.0
317 3 c/z -2.1839 -0.0664 0.0396875
318 3 c/z -2.1839 -0.0664 0.0663575
C -----
319 3 p 2.1839 -0.0664 0.0 2.2478 -0.0840 -1.0 2.2478 -0.0840 1.0
320 3 c/z 2.1839 -0.0664 0.0396875
321 3 c/z 2.1839 -0.0664 0.0663575
C -----
C ----- ss304 sleeve surfaces (adjusted dimensions) -----
C the analytic volume of these surfaces in cell 2 calculate to 3.134781858 cc
C -----
201 px -2.5019
202 px -2.2606
203 px 2.2606
204 px 2.5019
C -----
205 py -3.81425196
206 py -3.78587
207 py -3.7461825
208 py 3.7461825
209 py 3.78587
210 py 3.81425196
C -----
211 pz -0.153035
212 pz -0.12465304
213 pz -0.08496554
214 pz 0.08496554
215 pz 0.12465304
216 pz 0.153035
C -----
217 c/x 3.7461825 0.08496554 0.0396875
218 c/x 3.7461825 0.08496554 0.06806946
C -----
219 c/x 3.7461825 -0.08496554 0.0396875
220 c/x 3.7461825 -0.08496554 0.06806946
C -----
221 c/x -3.7461825 0.08496554 0.0396875

```

```

222 c/x -3.7461825 0.08496554 0.06806946
C -----
223 c/x -3.7461825 -0.08496554 0.0396875
224 c/x -3.7461825 -0.08496554 0.06806946
C
C ----- major core body surfaces (max dimensions, min radii) -----
C the analytic volume of these surfaces in cell 1 calculate to 6.958542864 cc
C
101 1 px -2.23901
102 1 px 2.23901
103 1 py -3.71221
104 1 py 3.71221
105 1 pz -0.10668
106 1 pz 0.10668
C ----- minor core body surfaces -----
107 1 px -2.159635
108 1 px -1.60401
109 1 px 1.60401
110 1 px 2.159635
C -----
111 1 py -3.632835
112 1 py -3.07721
113 1 py 3.07721
114 1 py 3.632835
C -----
115 1 pz -0.027305
116 1 pz 0.027305
C -----
117 1 c/z -1.60401 3.07721 0.555625
118 1 c/z -1.60401 3.07721 0.635
119 1 c/z 1.60401 3.07721 0.555625
120 1 c/z 1.60401 3.07721 0.635
121 1 c/z -1.60401 -3.07721 0.555625
122 1 c/z -1.60401 -3.07721 0.635
123 1 c/z 1.60401 -3.07721 0.555625
124 1 c/z 1.60401 -3.07721 0.635
C -----
125 1 c/y -2.159635 -0.027305 0.079375
126 1 c/y -2.159635 0.027305 0.079375
127 1 c/y 2.159635 -0.027305 0.079375
128 1 c/y 2.159635 0.027305 0.079375
C -----
129 1 c/x 3.632835 -0.027305 0.079375
130 1 c/x 3.632835 0.027305 0.079375
131 1 c/x -3.632835 -0.027305 0.079375
132 1 c/x -3.632835 0.027305 0.079375
C -----
133 1 tz -1.60401 3.07721 -0.027305 0.555625 0.079375 0.079375
134 1 tz -1.60401 3.07721 0.027305 0.555625 0.079375 0.079375
135 1 tz 1.60401 3.07721 -0.027305 0.555625 0.079375 0.079375
136 1 tz 1.60401 3.07721 0.027305 0.555625 0.079375 0.079375
137 1 tz -1.60401 -3.07721 -0.027305 0.555625 0.079375 0.079375
138 1 tz -1.60401 -3.07721 0.027305 0.555625 0.079375 0.079375
139 1 tz 1.60401 -3.07721 -0.027305 0.555625 0.079375 0.079375
140 1 tz 1.60401 -3.07721 0.027305 0.555625 0.079375 0.079375
C

```

```

C ---- pu alloy per Catherine 7/7/14 -----
C ----- 105.136 grams of alloy (sum)
m1 94239 -98.87 &
    94240 -4.697 &
    94241 -0.0032 &
    94242 -0.0049 &
    95241 -0.4021 &
    13027 -1.1584
C ---- ss304 per Huntsman 1 July 1983 -----
C ----- 24.765 grams of ss304 (sum)
m2 26000 -17.262 & $ added 1.002 to get proper sum
    24000 -4.57 &
    28000 -2.22 &
    25055 -0.42 &
    14000 -0.118 &
    42000 -0.079 &
    29000 -0.069 &
    6000 -0.016 &
    15031 -0.006 &
    16000 -0.005
C ---- carbon steel @ 7.82 g/cc -----
m3 26000 -0.994 &
    6000 -0.006
c ---- poly 0.967 g/cc ----
m5 1001 2
    6000 1
mt5 poly
m6 13027 -1.0
C -----
mode n
kcode 10000 1.0 97 1250
ksrc 0 0 0
tr1 0.0 -0.073659 0.0
tr3 0.000001 3.7856 0.0
*tr5 0 0 0 90 0 90 180 90 90 90 90 0
tr6 1.3 -1.3 0
C -----
c Neutron Groups
e0 1.00E-11 1.00E-10 5.00E-10 7.50E-10 1.00E-09 1.20E-09
    1.50E-09 2.00E-09 2.50E-09 3.00E-09 4.00E-09 5.00E-09 7.50E-09
    1.00E-08 2.53E-08 3.00E-08 4.00E-08 5.00E-08 6.00E-08
    7.00E-08 8.00E-08 9.00E-08 1.00E-07 1.25E-07 1.50E-07 1.75E-07
    2.00E-07 2.25E-07 2.50E-07 2.75E-07 3.00E-07 3.25E-07
    3.50E-07 3.75E-07 4.00E-07 4.50E-07 5.00E-07 5.50E-07 6.00E-07
    6.25E-07 6.50E-07 7.00E-07 7.50E-07 8.00E-07 8.50E-07
    9.00E-07 9.25E-07 9.50E-07 9.57E-07 1.00E-06 1.01E-06 1.02E-06
    1.03E-06 1.04E-06 1.05E-06 1.06E-06 1.07E-06 1.08E-06
    1.09E-06 1.10E-06 1.11E-06 1.12E-06 1.13E-06 1.14E-06 1.15E-06
    1.18E-06 1.20E-06 1.23E-06 1.25E-06 1.30E-06 1.35E-06
    1.40E-06 1.45E-06 1.50E-06 1.59E-06 1.68E-06 1.77E-06 1.86E-06
    1.94E-06 2.00E-06 2.12E-06 2.21E-06 2.30E-06 2.38E-06
    2.47E-06 2.57E-06 2.67E-06 2.77E-06 2.87E-06 2.97E-06 3.00E-06
    3.05E-06 3.15E-06 3.50E-06 3.73E-06 4.00E-06 4.75E-06
    5.00E-06 5.40E-06 6.00E-06 6.25E-06 6.50E-06 6.75E-06 7.00E-06
    7.15E-06 8.10E-06 9.10E-06 1.00E-05 1.15E-05 1.19E-05

```

```

1.29E-05 1.38E-05 1.44E-05 1.51E-05 1.60E-05 1.70E-05 1.85E-05
1.90E-05 2.00E-05 2.10E-05 2.25E-05 2.50E-05 2.75E-05
3.00E-05 3.13E-05 3.18E-05 3.33E-05 3.38E-05 3.46E-05 3.55E-05
3.70E-05 3.80E-05 3.91E-05 3.96E-05 4.10E-05 4.24E-05
4.40E-05 4.52E-05 4.70E-05 4.83E-05 4.92E-05 5.06E-05 5.20E-05
5.34E-05 5.90E-05 6.10E-05 6.50E-05 6.75E-05 7.20E-05
7.60E-05 8.00E-05 8.02E-05 9.00E-05 1.00E-04 1.08E-04 1.15E-04
1.19E-04 1.22E-04 1.86E-04 1.95E-04 2.08E-04 2.10E-04
2.40E-04 2.85E-04 3.05E-04 5.50E-04 6.70E-04 6.83E-04 9.50E-04
1.15E-03 1.50E-03 1.55E-03 1.80E-03 2.20E-03 2.29E-03
2.58E-03 3.00E-03 3.74E-03 3.90E-03 6.00E-03 8.03E-03 9.50E-03
1.30E-02 1.70E-02 2.50E-02 3.00E-02 4.50E-02 5.00E-02
5.20E-02 6.00E-02 7.34E-02 7.54E-02 8.24E-02 8.50E-02 1.00E-01
1.28E-01 1.50E-01 2.00E-01 2.70E-01 3.30E-01 4.00E-01
4.20E-01 4.40E-01 4.70E-01 5.00E-01 5.50E-01 5.73E-01 6.00E-01
6.70E-01 6.79E-01 7.50E-01 8.20E-01 8.61E-01 8.75E-01
9.00E-01 9.20E-01 1.01E+00 1.10E+00 1.20E+00 1.25E+00 1.32E+00
1.36E+00 1.40E+00 1.50E+00 1.85E+00 2.35E+00 2.48E+00
3.00E+00 4.30E+00 4.80E+00 6.43E+00 8.87E+00 1.00E+01 1.28E+01
1.38E+01 1.46E+01 1.57E+01 1.73E+01 2.00E+01
f4:N (1<7<9<(19 21 23 25 27 29 31 33 35 37 41 43 45 47 49 51 53 55 57 59))
fm4 1 1 -6
sd4 6.958542864
print

```

TEX Pu Baseline Experiment 3

c ZPPR PANN plate model by Allan Krass

c Array model and stack model by Soon Kim

c Edited by Catherine Percher

c

C the outer dimensions of the PANN ZPR plate in this model come to

C Length = 3.003348 inches (7.62850392 cm)

C Width = 1.970 inches (5.0038 cm)

C Height = 0.1205 inches (0.30607 cm)

C ----- Pu Alloy Core -----

C density = 105.136 grams/6.958542864 cc (analytic vol rounded to 9 decimals)

1 1 -15.108910307 &

(108 -109 111 -114 105 -106): & \$ full ht main +/- y body
 (107 -108 112 -113 105 -106): & \$ full ht main -x body
 (109 -110 112 -113 105 -106): & \$ full ht main +x body
 (-117 -108 113 105 -106): & \$ full height -x,+y corner
 (-119 109 113 105 -106): & \$ full height +x,+y corner
 (-121 -108 -112 105 -106): & \$ full height -x,-y corner
 (-123 109 -112 105 -106): & \$ full height +x,-y corner
 (101 -107 112 -113 115 -116): & \$ flat edge -x face
 (-125 -107 112 -113 -115): & \$ rounded lo edge -x face
 (-126 -107 112 -113 116): & \$ rounded hi edge -x face
 (-102 110 112 -113 115 -116): & \$ flat edge +x face
 (-127 110 112 -113 -115): & \$ rounded lo edge +x face
 (-128 110 112 -113 116): & \$ rounded hi edge +x face
 (-104 114 108 -109 115 -116): & \$ flat edge +y face
 (-129 114 108 -109 -115): & \$ rounded lo edge +y face
 (-130 114 108 -109 116): & \$ rounded hi edge +y face
 (103 -111 108 -109 115 -116): & \$ flat edge -y face
 (-131 -111 108 -109 -115): & \$ rounded lo edge -y face
 (-132 -111 108 -109 116): & \$ rounded hi edge -y face
 (117 -118 -108 113 115 -116): & \$ -x,+y corner face
 (119 -120 109 113 115 -116): & \$ +x,+y corner face
 (121 -122 -108 -112 115 -116): & \$ -x,-y corner face
 (123 -124 109 -112 115 -116): & \$ +x,-y corner face
 (-133 117 -108 113 -115): & \$ rnd lo edge -x,+y corner
 (-134 117 -108 113 116): & \$ rnd hi edge -x,+y corner
 (-135 119 109 113 -115): & \$ rnd lo edge +x,+y corner
 (-136 119 109 113 116): & \$ rnd hi edge +x,+y corner
 (-137 121 -108 -112 -115): & \$ rnd lo edge -x,-y corner
 (-138 121 -108 -112 116): & \$ rnd hi edge -x,-y corner
 (-139 123 109 -112 -115): & \$ rnd lo edge +x,-y corner
 (-140 123 109 -112 116): & \$ rnd hi edge +x,-y corner

u=1 imp:n=1

C ----- SS304 Sleeve and Plugs -----

C density = 24.765 grams/3.134781858 cc (analytic vol rounded to 9 decimals)

2 2 -7.90007124 &

(201 -204 207 -208 211 -212): & \$ flat +z face
 (201 -204 207 -208 215 -216): & \$ flat -z face
 (201 -204 213 -214 209 -210): & \$ flat +y face
 (201 -204 213 -214 205 -206): & \$ flat -y face
 (201 -204 208 214 217 -218): & \$ rounded +y,+z edge
 (201 -204 208 -213 219 -220): & \$ rounded +y,-z edge
 (201 -204 -207 214 221 -222): & \$ rounded -y,+z edge
 (201 -204 -207 -213 223 -224): & \$ rounded -y,-z edge
 (201 -202 208 214 -217): & \$ rnd +y,+z edge -x plug

```

(201 -202 208 -213 -219): & $ rnd +y,-z edge -x plug
(201 -202 208 -209 213 -214): & $ +y end -x plug
(201 -202 207 -208 212 -215): & $ main body -x plug
(201 -202 -207 206 213 -214): & $ -y end -x plug
(201 -202 -207 214 -221): & $ rnd -y,+z edge -x plug
(201 -202 -207 -213 -223): & $ rnd -y,-z edge -x plug
(203 -204 208 214 -217): & $ rnd +y,+z edge +x plug
(203 -204 208 -213 -219): & $ rnd +y,-z edge +x plug
(203 -204 208 -209 213 -214): & $ +y end +x plug
(203 -204 207 -208 212 -215): & $ main body +x plug
(203 -204 -207 206 213 -214): & $ -y end +x plug
(203 -204 -207 214 -221): & $ rnd -y,+z edge +x plug
(203 -204 -207 -213 -223) & $ rnd -y,-z edge +x plug
u=1 imp:n=1
C ----- Carbon Steel Spring -----
3 3 -7.82 (301 -302 -303 304 -305 -306): & $ -y arm, inner segment
(301 -302 303 -307 -308 -309): & $ +y arm, inner segment
(301 -302 -304 -310 -311 312): & $ -y arm, outer segment
(301 -302 307 -313 -314 315): & $ +y arm, outer segment
(301 -302 310 316 317 -318): & $ curled end, -y
(301 -302 313 319 320 -321) & $ curled end, +y
u=1 imp:n=1
4 0 #1 #2 #3 u=1 imp:n=1
c 1st layer
5 0 201 -204 205 -210 211 -216 u=2 imp:n=1 $void
6 0 #5 u=2 imp:n=1
7 0 201 -204 205 -210 211 -216 lat=1 u=3 imp:n=1
fill=-3:4 -2:3 0:0
2 2 2 2 2 2 2
2 1 1 1 1 1 2
2 1 1 1 1 1 2
2 1 1 1 1 1 2
2 1 1 1 1 1 2
2 2 2 2 2 2 2
8 0 #7 u=3 imp:n=1
9 0 -1 fill=3 u=7 imp:n=1
10 5 -0.967 1 u=7 imp:n=1
11 0 -44 fill=7 imp:n=1
c poly
12 5 -0.967 -2 imp:n=1 $poly
14 6 -2.7 -4 imp:n=1 $al
15 6 -2.7 -5 imp:n=1 $al bottom
16 5 -0.967 -10 imp:n=1 $poly, bottom 1"
17 like 12 but trcl=(0 0 0.80772) imp:n=1 $poly 2
19 like 11 but trcl=(0 0 0.80772) imp:n=1 $fuel 2
21 like 14 but trcl=(0 0 0.80772) imp:n=1 $Al 2
23 like 12 but trcl=(0 0 1.61544) imp:n=1 $poly 3
25 like 11 but trcl=(0 0 1.61544) imp:n=1 $fuel 3
27 like 14 but trcl=(0 0 1.61544) imp:n=1 $Al 3
33 like 12 but trcl=(0 0 2.42316) imp:n=1 $poly 4
35 like 11 but trcl=(0 0 2.42316) imp:n=1 $fuel 4
37 like 14 but trcl=(0 0 2.42316) imp:n=1 $Al 4
39 like 12 but trcl=(0 0 3.23088) imp:n=1 $poly 5
41 like 11 but trcl=(0 0 3.23088) imp:n=1 $fuel 5
43 like 14 but trcl=(0 0 3.23088) imp:n=1 $Al 5
45 like 12 but trcl=(0 0 4.0386) imp:n=1 $poly 6

```



```

47 like 11 but trcl=(0 0 4.0386) imp:n=1 $fuel 6
49 like 14 but trcl=(0 0 4.0386) imp:n=1 $Al 6
29 6 -2.7 -6 imp:n=1 $middle center
31 6 -2.7 -7 8 imp:n=1 $middle center
51 like 12 but trcl=(0 0 5.16382) imp:n=1 $poly 7
53 like 11 but trcl=(0 0 5.16382) imp:n=1 $fuel 7
55 like 14 but trcl=(0 0 5.16382) imp:n=1 $Al 7
57 like 12 but trcl=(0 0 5.97154) imp:n=1 $poly 8
59 like 11 but trcl=(0 0 5.97154) imp:n=1 $fuel 8
61 like 14 but trcl=(0 0 5.97154) imp:n=1 $Al 8
63 like 12 but trcl=(0 0 6.77926) imp:n=1 $poly 9
65 like 11 but trcl=(0 0 6.77926) imp:n=1 $fuel 9
67 like 14 but trcl=(0 0 6.77926) imp:n=1 $Al 9
69 like 12 but trcl=(0 0 7.58698) imp:n=1 $poly 10
71 like 11 but trcl=(0 0 7.58698) imp:n=1 $fuel 10
73 like 14 but trcl=(0 0 7.58698) imp:n=1 $Al 10
75 like 12 but trcl=(0 0 8.3947) imp:n=1 $poly 11
77 like 11 but trcl=(0 0 8.3947) imp:n=1 $fuel 11
79 like 14 but trcl=(0 0 8.3947) imp:n=1 $Al 11
81 like 12 but trcl=(0 0 9.20242) imp:n=1 $poly 12
83 like 11 but trcl=(0 0 9.20242) imp:n=1 $fuel 12
85 like 14 but trcl=(0 0 9.20242) imp:n=1 $Al 12
911 5 -0.967 -9 imp:n=1 $top poly
997 0 -3 #11 #12 #14 #15 #16 #17 #19 #21 #23 #25 #27 #29 #31
      #33 #35 #37 #39 #41 #43 #45 #47 #49 #51
      #53 #55 #57 #59 #61 #63 #65 #67 #69 #71 #73 #75
      #77 #79 #81 #83 #85
      #911
      imp:n=1
998 0 3 imp:n=0

c
1 rpp -17.5133 12.5095 -19.0712598 11.44276 -0.153035 0.153035 $fuel
44 rpp -20.0533 15.0495 -21.61126 13.98276 -0.153035 0.153035 $stray
2 rpp -20.0533 15.0495 -21.61126 13.98276 -0.654685 -0.178435 $poly,3/16" $tot = 0.80772
3 rpp -60 55 -61 54 -6 23
4 rpp -25.1333 20.1295 -26.69126 19.06276 -0.178435 -0.153035 $al
5 rpp -32.9819 27.9781 -34.2943 26.66575 -5.258435 -2.718435 $bottom Al
6 rpp -26.6319 21.6281 -27.9443 20.31575 4.191635 4.509135 $middle center
7 rpp -59.6519 54.6481 -60.9643 53.33575 1.969135 4.509135 $middle
8 rpp -26.6319 21.6281 -27.9443 20.31575 1.969135 4.509135 $middle inside
9 rpp -20.0533 15.0495 -21.61126 13.98276 9.355455 11.895455 $top poly 1"
10 rpp -20.0533 15.0495 -21.61126 13.98276 -2.718435 -0.654685 $bot poly 13/16"
C ----- carbon steel spring surfaces (minimum compression) -----
C
301 3 pz -0.0890775
302 3 pz 0.0890775
303 3 px 0.0
C -----
304 3 px -0.9707

305 3 p 0.0 -0.0269 0.0 -0.9707 -0.1470 -1.0 -0.9707 -0.1470 1.0
306 3 p 0.0 0.0 0.0 -0.9707 -0.1200 -1.0 -0.9707 -0.1200 1.0
C -----
307 3 px 0.9707
308 3 p 0.0 -0.0269 0.0 0.9707 -0.1470 -1.0 0.9707 -0.1470 1.0

```

```

309 3 p 0.0 0.0 0.0 0.9707 -0.1200 -1.0 0.9707 -0.1200 1.0
C -----
310 3 p -2.1839 -0.0664 0.0 -2.1773 -0.0003 -1.0 -2.1773 -0.0003 1.0
311 3 p -2.1799 -0.0269 0.0 -0.9707 -0.1470 -1.0 -0.9707 -0.1470 1.0
312 3 p -2.1773 -0.0003 0.0 -0.9707 -0.1200 -1.0 -0.9707 -0.1200 1.0
C -----
313 3 p 2.1839 -0.0664 0.0 2.1773 -0.0003 -1.0 2.1773 -0.0003 1.0
314 3 p 2.1799 -0.0269 0.0 0.9707 -0.1470 -1.0 0.9707 -0.1470 1.0
315 3 p 2.1773 -0.0003 0.0 0.9707 -0.1200 -1.0 0.9707 -0.1200 1.0
C -----
316 3 p -2.1839 -0.0664 0.0 -2.2478 -0.0840 -1.0 -2.2478 -0.0840 1.0
317 3 c/z -2.1839 -0.0664 0.0396875
318 3 c/z -2.1839 -0.0664 0.0663575
C -----
319 3 p 2.1839 -0.0664 0.0 2.2478 -0.0840 -1.0 2.2478 -0.0840 1.0
320 3 c/z 2.1839 -0.0664 0.0396875
321 3 c/z 2.1839 -0.0664 0.0663575
C -----
C ----- ss304 sleeve surfaces (adjusted dimensions) -----
C the analytic volume of these surfaces in cell 2 calculate to 3.134781858 cc
C -----
201 px -2.5019
202 px -2.2606
203 px 2.2606
204 px 2.5019
C -----
205 py -3.81425196
206 py -3.78587
207 py -3.7461825
208 py 3.7461825
209 py 3.78587
210 py 3.81425196
C -----
211 pz -0.153035
212 pz -0.12465304
213 pz -0.08496554
214 pz 0.08496554
215 pz 0.12465304
216 pz 0.153035
C -----
217 c/x 3.7461825 0.08496554 0.0396875
218 c/x 3.7461825 0.08496554 0.06806946
C -----
219 c/x 3.7461825 -0.08496554 0.0396875
220 c/x 3.7461825 -0.08496554 0.06806946
C -----
221 c/x -3.7461825 0.08496554 0.0396875
222 c/x -3.7461825 0.08496554 0.06806946
C -----
223 c/x -3.7461825 -0.08496554 0.0396875
224 c/x -3.7461825 -0.08496554 0.06806946
C -----
C ----- major core body surfaces (max dimensions, min radii) -----
C the analytic volume of these surfaces in cell 1 calculate to 6.958542864 cc
C -----
101 1 px -2.23901

```

```

102 1 px 2.23901
103 1 py -3.71221
104 1 py 3.71221
105 1 pz -0.10668
106 1 pz 0.10668
C ----- minor core body surfaces -----
107 1 px -2.159635
108 1 px -1.60401
109 1 px 1.60401
110 1 px 2.159635
C -----
111 1 py -3.632835
112 1 py -3.07721
113 1 py 3.07721
114 1 py 3.632835
C -----
115 1 pz -0.027305
116 1 pz 0.027305
C -----
117 1 c/z -1.60401 3.07721 0.555625
118 1 c/z -1.60401 3.07721 0.635
119 1 c/z 1.60401 3.07721 0.555625
120 1 c/z 1.60401 3.07721 0.635
121 1 c/z -1.60401 -3.07721 0.555625
122 1 c/z -1.60401 -3.07721 0.635
123 1 c/z 1.60401 -3.07721 0.555625
124 1 c/z 1.60401 -3.07721 0.635
C -----
125 1 c/y -2.159635 -0.027305 0.079375
126 1 c/y -2.159635 0.027305 0.079375
127 1 c/y 2.159635 -0.027305 0.079375
128 1 c/y 2.159635 0.027305 0.079375
C -----
129 1 c/x 3.632835 -0.027305 0.079375
130 1 c/x 3.632835 0.027305 0.079375
131 1 c/x -3.632835 -0.027305 0.079375
132 1 c/x -3.632835 0.027305 0.079375
C -----
133 1 tz -1.60401 3.07721 -0.027305 0.555625 0.079375 0.079375
134 1 tz -1.60401 3.07721 0.027305 0.555625 0.079375 0.079375
135 1 tz 1.60401 3.07721 -0.027305 0.555625 0.079375 0.079375
136 1 tz 1.60401 3.07721 0.027305 0.555625 0.079375 0.079375
137 1 tz -1.60401 -3.07721 -0.027305 0.555625 0.079375 0.079375
138 1 tz -1.60401 -3.07721 0.027305 0.555625 0.079375 0.079375
139 1 tz 1.60401 -3.07721 -0.027305 0.555625 0.079375 0.079375
140 1 tz 1.60401 -3.07721 0.027305 0.555625 0.079375 0.079375
C
C ---- pu alloy per Catherine 7/7/14 -----
C ----- 105.136 grams of alloy (sum)
m1 94239 -98.87 &
    94240 -4.697 &
    94241 -0.0032 &
    94242 -0.0049 &
    95241 -0.4021 &
    13027 -1.1584

```

```

C ---- ss304 per Huntsman 1 July 1983 -----
C ----- 24.765 grams of ss304 (sum)
m2 26000 -17.262 & $ added 1.002 to get proper sum
    24000 -4.57 &
    28000 -2.22 &
    25055 -0.42 &
    14000 -0.118 &
    42000 -0.079 &
    29000 -0.069 &
    6000 -0.016 &
    15031 -0.006 &
    16000 -0.005
C ---- carbon steel @ 7.82 g/cc -----
m3 26000 -0.994 &
    6000 -0.006
c ---- poly 0.967 g/cc -----
m5 1001 2
    6000 1
mt5 poly
m6 13027 -1.0
C -----
mode n
kcode 10000 1.0 97 1250
ksrc 0 0 0
tr1 0.0 -0.073659 0.0
tr3 0.000001 3.7856 0.0
*tr5 0 0 0 90 0 90 180 90 90 90 90 0
tr6 1.3 -1.3 0
C -----
c Neutron Groups
e0 1.00E-11 1.00E-10 5.00E-10 7.50E-10 1.00E-09 1.20E-09
    1.50E-09 2.00E-09 2.50E-09 3.00E-09 4.00E-09 5.00E-09 7.50E-09
    1.00E-08 2.53E-08 3.00E-08 4.00E-08 5.00E-08 6.00E-08
    7.00E-08 8.00E-08 9.00E-08 1.00E-07 1.25E-07 1.50E-07 1.75E-07
    2.00E-07 2.25E-07 2.50E-07 2.75E-07 3.00E-07 3.25E-07
    3.50E-07 3.75E-07 4.00E-07 4.50E-07 5.00E-07 5.50E-07 6.00E-07
    6.25E-07 6.50E-07 7.00E-07 7.50E-07 8.00E-07 8.50E-07
    9.00E-07 9.25E-07 9.50E-07 9.57E-07 1.00E-06 1.01E-06 1.02E-06
    1.03E-06 1.04E-06 1.05E-06 1.06E-06 1.07E-06 1.08E-06
    1.09E-06 1.10E-06 1.11E-06 1.12E-06 1.13E-06 1.14E-06 1.15E-06
    1.18E-06 1.20E-06 1.23E-06 1.25E-06 1.30E-06 1.35E-06
    1.40E-06 1.45E-06 1.50E-06 1.59E-06 1.68E-06 1.77E-06 1.86E-06
    1.94E-06 2.00E-06 2.12E-06 2.21E-06 2.30E-06 2.38E-06
    2.47E-06 2.57E-06 2.67E-06 2.77E-06 2.87E-06 2.97E-06 3.00E-06
    3.05E-06 3.15E-06 3.50E-06 3.73E-06 4.00E-06 4.75E-06
    5.00E-06 5.40E-06 6.00E-06 6.25E-06 6.50E-06 6.75E-06 7.00E-06
    7.15E-06 8.10E-06 9.10E-06 1.00E-05 1.15E-05 1.19E-05
    1.29E-05 1.38E-05 1.44E-05 1.51E-05 1.60E-05 1.70E-05 1.85E-05
    1.90E-05 2.00E-05 2.10E-05 2.25E-05 2.50E-05 2.75E-05
    3.00E-05 3.13E-05 3.18E-05 3.33E-05 3.38E-05 3.46E-05 3.55E-05
    3.70E-05 3.80E-05 3.91E-05 3.96E-05 4.10E-05 4.24E-05
    4.40E-05 4.52E-05 4.70E-05 4.83E-05 4.92E-05 5.06E-05 5.20E-05
    5.34E-05 5.90E-05 6.10E-05 6.50E-05 6.75E-05 7.20E-05
    7.60E-05 8.00E-05 8.02E-05 9.00E-05 1.00E-04 1.08E-04 1.15E-04
    1.19E-04 1.22E-04 1.86E-04 1.95E-04 2.08E-04 2.10E-04
    2.40E-04 2.85E-04 3.05E-04 5.50E-04 6.70E-04 6.83E-04 9.50E-04

```

```

1.15E-03 1.50E-03 1.55E-03 1.80E-03 2.20E-03 2.29E-03
2.58E-03 3.00E-03 3.74E-03 3.90E-03 6.00E-03 8.03E-03 9.50E-03
1.30E-02 1.70E-02 2.50E-02 3.00E-02 4.50E-02 5.00E-02
5.20E-02 6.00E-02 7.34E-02 7.54E-02 8.24E-02 8.50E-02 1.00E-01
1.28E-01 1.50E-01 2.00E-01 2.70E-01 3.30E-01 4.00E-01
4.20E-01 4.40E-01 4.70E-01 5.00E-01 5.50E-01 5.73E-01 6.00E-01
6.70E-01 6.79E-01 7.50E-01 8.20E-01 8.61E-01 8.75E-01
9.00E-01 9.20E-01 1.01E+00 1.10E+00 1.20E+00 1.25E+00 1.32E+00
1.36E+00 1.40E+00 1.50E+00 1.85E+00 2.35E+00 2.48E+00
3.00E+00 4.30E+00 4.80E+00 6.43E+00 8.87E+00 1.00E+01 1.28E+01
1.38E+01 1.46E+01 1.57E+01 1.73E+01 2.00E+01
f4:N (1<7<9<(11 19 25 35 41 47 53 59 65 71 77 83))
fm4 1 1 -6
sd4 6.958542864
print

```

TEX Pu Ta Dilution Experiment 10
 c ZPPR PANN plate model by Allan Krass
 c Array model and stack model by Soon Kim
 c
 C the outer dimensions of the PANN ZPR plate in this model come to
 C Length = 3.003348 inches (7.62850392 cm)
 C Width = 1.970 inches (5.0038 cm)
 C Height = 0.1205 inches (0.30607 cm)
 C ----- Pu Alloy Core -----
 C density = 105.1360 grams/6.958542864 cc (analytic vol rounded to 9 decimals)
 1 1 -15.108910307
 (108 -109 111 -114 105 -106): & \$ full ht main +/- y body
 (107 -108 112 -113 105 -106): & \$ full ht main -x body
 (109 -110 112 -113 105 -106): & \$ full ht main +x body
 (-117 -108 113 105 -106): & \$ full height -x,+y corner
 (-119 109 113 105 -106): & \$ full height +x,+y corner
 (-121 -108 -112 105 -106): & \$ full height -x,-y corner
 (-123 109 -112 105 -106): & \$ full height +x,-y corner
 (101 -107 112 -113 115 -116): & \$ flat edge -x face
 (-125 -107 112 -113 -115): & \$ rounded lo edge -x face
 (-126 -107 112 -113 116): & \$ rounded hi edge -x face
 (-102 110 112 -113 115 -116): & \$ flat edge +x face
 (-127 110 112 -113 -115): & \$ rounded lo edge +x face
 (-128 110 112 -113 116): & \$ rounded hi edge +x face
 (-104 114 108 -109 115 -116): & \$ flat edge +y face
 (-129 114 108 -109 -115): & \$ rounded lo edge +y face
 (-130 114 108 -109 116): & \$ rounded hi edge +y face
 (103 -111 108 -109 115 -116): & \$ flat edge -y face
 (-131 -111 108 -109 -115): & \$ rounded lo edge -y face
 (-132 -111 108 -109 116): & \$ rounded hi edge -y face
 (117 -118 -108 113 115 -116): & \$ -x,+y corner face
 (119 -120 109 113 115 -116): & \$ +x,+y corner face
 (121 -122 -108 -112 115 -116): & \$ -x,-y corner face
 (123 -124 109 -112 115 -116): & \$ +x,-y corner face
 (-133 117 -108 113 -115): & \$ rnd lo edge -x,+y corner
 (-134 117 -108 113 116): & \$ rnd hi edge -x,+y corner
 (-135 119 109 113 -115): & \$ rnd lo edge +x,+y corner
 (-136 119 109 113 116): & \$ rnd hi edge +x,+y corner
 (-137 121 -108 -112 -115): & \$ rnd lo edge -x,-y corner
 (-138 121 -108 -112 116): & \$ rnd hi edge -x,-y corner
 (-139 123 109 -112 -115): & \$ rnd lo edge +x,-y corner
 (-140 123 109 -112 116): & \$ rnd hi edge +x,-y corner
 u=1 imp:n=1
 C ----- SS304 Sleeve and Plugs -----
 C density = 24.765 grams/3.134781858 cc (analytic vol rounded to 9 decimals)
 2 2 -7.90007124 &
 (201 -204 207 -208 211 -212): & \$ flat +z face
 (201 -204 207 -208 215 -216): & \$ flat -z face
 (201 -204 213 -214 209 -210): & \$ flat +y face
 (201 -204 213 -214 205 -206): & \$ flat -y face
 (201 -204 208 214 217 -218): & \$ rounded +y,+z edge
 (201 -204 208 -213 219 -220): & \$ rounded +y,-z edge
 (201 -204 -207 214 221 -222): & \$ rounded -y,+z edge
 (201 -204 -207 -213 223 -224): & \$ rounded -y,-z edge
 (201 -202 208 214 -217): & \$ rnd +y,+z edge -x plug
 (201 -202 208 -213 -219): & \$ rnd +y,-z edge -x plug

```

(201 -202 208 -209 213 -214): & $ +y end -x plug
(201 -202 207 -208 212 -215): & $ main body -x plug
(201 -202 -207 206 213 -214): & $ -y end -x plug
(201 -202 -207 214 -221): & $ rnd -y,+z edge -x plug
(201 -202 -207 -213 -223): & $ rnd -y,-z edge -x plug
(203 -204 208 214 -217): & $ rnd +y,+z edge +x plug
(203 -204 208 -213 -219): & $ rnd +y,-z edge +x plug
(203 -204 208 -209 213 -214): & $ +y end +x plug
(203 -204 207 -208 212 -215): & $ main body +x plug
(203 -204 -207 206 213 -214): & $ -y end +x plug
(203 -204 -207 214 -221): & $ rnd -y,+z edge +x plug
(203 -204 -207 -213 -223) & $ rnd -y,-z edge +x plug
u=1 imp:n=1
C ----- Carbon Steel Spring -----
3 3 -7.82 (301 -302 -303 304 -305 -306): & $ -y arm, inner segment
(301 -302 303 -307 -308 -309): & $ +y arm, inner segment
(301 -302 -304 -310 -311 312): & $ -y arm, outer segment
(301 -302 307 -313 -314 315): & $ +y arm, outer segment
(301 -302 310 316 317 -318): & $ curled end, -y
(301 -302 313 319 320 -321) & $ curled end, +y
u=1 imp:n=1
4 0 #1 #2 #3 u=1 imp:n=1
c 1st layer
5 0 201 -204 205 -210 211 -216 u=2 imp:n=1 $void
6 0 #5 u=2 imp:n=1
7 0 201 -204 205 -210 211 -216 lat=1 u=3 imp:n=1
fill=-3:4 -2:3 0:0
2 2 2 2 2 2 2
2 1 1 1 1 1 2
2 1 1 1 1 1 2
2 1 1 1 1 1 2
2 1 1 1 1 1 2
2 2 2 2 2 2 2
8 0 #7 u=3 imp:n=1
9 0 -1 fill=3 u=4 imp:n=1
10 5 -0.967 1 u=4 imp:n=1
11 0 -44 fill=4 imp:n=1
c Ta lattice
501 7 -16.69 501 -502 503 -504 505 -506 u=5 imp:n=1
502 0 #501 u=5 imp:n=1
503 0 501 -502 503 -504 505 -506 u=6 imp:n=1
504 0 #503 u=6 imp:n=1
505 0 501 -502 503 -504 505 -506 lat=1 u=7 imp:n=1
fill=-2:3 -3:4 0:0
6 6 6 6 6
6 5 5 5 5 6
6 5 5 5 5 6
6 5 5 5 5 6
6 5 5 5 5 6
6 5 5 5 5 6
6 5 5 5 5 6
6 6 6 6 6
506 0 #505 imp:n=1 u=7
507 0 -507 fill=7 u=8 imp:n=1 $Ta layer
508 5 -0.967 507 u=8 imp:n=1
509 0 -508 fill=8 imp:n=1

```

```

c    poly
12  5 -0.967 -2  imp:n=1 $poly
14  6 -2.7  -4  imp:n=1 $al
15  6 -2.7  -5  imp:n=1 $al bottom
16  5 -0.967 -10 imp:n=1 $bot poly 1"
c
17  like 12 but trcl=(0 0 3.0278324) imp:n=1 $poly 2
18  like 509 but trcl=(0 0 3.0278324) imp:n=1 $Ta 2
19  like 11 but trcl=(0 0 3.0278324) imp:n=1 $fuel 2
21  like 14 but trcl=(0 0 3.0278324) imp:n=1 $Al 2
23  like 12 but trcl=(0 0 6.0556648) imp:n=1 $poly 3
24  like 509 but trcl=(0 0 6.0556648) imp:n=1 $Ta 3
25  like 11 but trcl=(0 0 6.0556648) imp:n=1 $fuel 3
27  like 14 but trcl=(0 0 6.0556648) imp:n=1 $Al 3
33  like 12 but trcl=(0 0 9.0834972) imp:n=1 $poly 4
34  like 509 but trcl=(0 0 9.0834972) imp:n=1 $Ta 4
35  like 11 but trcl=(0 0 9.0834972) imp:n=1 $fuel 4
37  like 14 but trcl=(0 0 9.0834972) imp:n=1 $Al 4
39  like 12 but trcl=(0 0 12.1113296) imp:n=1 $poly 5
40  like 509 but trcl=(0 0 12.1113296) imp:n=1 $Ta 5
41  like 11 but trcl=(0 0 12.1113296) imp:n=1 $fuel 5
43  like 14 but trcl=(0 0 12.1113296) imp:n=1 $Al 5
29  6 -2.7 -6  imp:n=1 $middle center
31  6 -2.7 -7 8  imp:n=1 $middle center
45  like 12 but trcl=(0 0 15.482062) imp:n=1 $poly 6
46  like 509 but trcl=(0 0 15.482062) imp:n=1 $Ta 6
47  like 11 but trcl=(0 0 15.482062) imp:n=1 $fuel 6
c 49 like 14 but trcl=(0 0 15.482062) imp:n=1 $Al 6
50  like 12 but trcl=(0 0 18.509894) imp:n=1 $poly 7
51  like 509 but trcl=(0 0 18.509894) imp:n=1 $Ta 7
52  like 11 but trcl=(0 0 18.509894) imp:n=1 $fuel 7
53  like 14 but trcl=(0 0 18.509894) imp:n=1 $Al 7
55  like 12 but trcl=(0 0 21.537727) imp:n=1 $poly 8
56  like 509 but trcl=(0 0 21.537727) imp:n=1 $Ta 8
57  like 11 but trcl=(0 0 21.537727) imp:n=1 $fuel 8
58  like 14 but trcl=(0 0 21.537727) imp:n=1 $fuel 8
59  like 12 but trcl=(0 0 24.565559) imp:n=1 $Al 9
63  like 509 but trcl=(0 0 24.565559) imp:n=1 $Ta 9
65  like 11 but trcl=(0 0 24.565559) imp:n=1 $fuel 9
67  like 14 but trcl=(0 0 24.565559) imp:n=1 $Al 9
69  like 12 but trcl=(0 0 27.593392) imp:n=1 $Al 10
73  like 509 but trcl=(0 0 27.593392) imp:n=1 $Ta 10
75  like 11 but trcl=(0 0 27.593392) imp:n=1 $fuel 10
77  like 14 but trcl=(0 0 27.593392) imp:n=1 $Al 10
79  like 12 but trcl=(0 0 30.621224) imp:n=1 $Al 11
83  like 509 but trcl=(0 0 30.621224) imp:n=1 $Ta 11
85  like 11 but trcl=(0 0 30.621224) imp:n=1 $fuel 11
87  like 14 but trcl=(0 0 30.621224) imp:n=1 $Al 11
91  like 12 but trcl=(0 0 33.649056) imp:n=1 $Al 12
92  like 509 but trcl=(0 0 33.649056) imp:n=1 $Ta 12
93  like 11 but trcl=(0 0 33.649056) imp:n=1 $fuel 12
94  like 14 but trcl=(0 0 33.649056) imp:n=1 $Al 12
997 0 -3 #11 #12 #14 #15 #16 #509 #17 #18 #19 #21 #23 #24 #25 #27
    #33 #34 #35 #37 #39 #40 #41 #45 #46 #47 #43 #50 #51
    #52 #53 #55 #56 #57 #58 #59 #63 #65 #67
    #69 #73 #75 #77 #79 #83 #85 #87 #29 #31

```



```

#91 #92 #93 #94
imp:n=1
998 0 3 imp:n=0

c
1 rpp -17.5133 12.5095 -19.0712598 11.44276 -0.153035 0.153035 $fuel
44 rpp -20.0533 15.0495 -21.61126 13.98276 -0.153035 0.153035 $tray
2 rpp -20.0533 15.0495 -21.61126 13.98276 0.309397 2.849397 $poly,1"
3 rpp -60 55 -61 54 -6 42
4 rpp -25.1333 20.1295 -26.69126 19.06276 -0.178435 -0.153035 $al
5 rpp -32.9819 27.9781 -34.2943 26.66575 -5.258435 -2.718435 $bottom Al
6 rpp -26.6319 21.6281 -27.9443 20.31575 14.962 15.2795 $middle center
7 rpp -59.6519 54.6481 -60.9643 53.33575 12.7395 15.2795 $middle
8 rpp -26.6319 21.6281 -27.9443 20.31575 12.7395 15.2795 $middle
10 rpp -20.0533 15.0495 -21.61126 13.98276 -2.718435 -0.178435 $bottom poly 1"
c
501 px -2.501902
502 px 5.099404
503 py -3.814248
504 py 1.251833
505 pz 0.153035
506 pz 0.309397
507 rpp -17.70451 12.70071 -19.01249 11.38399 0.153035 0.309397 $Ta
508 rpp -20.0533 15.0495 -21.61126 13.98276 0.153035 0.309397 $Ta-poly
C ----- carbon steel spring surfaces (minimum compression) -----
C
301 3 pz -0.0890775
302 3 pz 0.0890775
303 3 px 0.0
C -----
304 3 px -0.9707
305 3 p 0.0 -0.0269 0.0 -0.9707 -0.1470 -1.0 -0.9707 -0.1470 1.0
306 3 p 0.0 0.0 0.0 -0.9707 -0.1200 -1.0 -0.9707 -0.1200 1.0
C -----
307 3 px 0.9707
308 3 p 0.0 -0.0269 0.0 0.9707 -0.1470 -1.0 0.9707 -0.1470 1.0
309 3 p 0.0 0.0 0.0 0.9707 -0.1200 -1.0 0.9707 -0.1200 1.0
C -----
310 3 p -2.1839 -0.0664 0.0 -2.1773 -0.0003 -1.0 -2.1773 -0.0003 1.0
311 3 p -2.1799 -0.0269 0.0 -0.9707 -0.1470 -1.0 -0.9707 -0.1470 1.0
312 3 p -2.1773 -0.0003 0.0 -0.9707 -0.1200 -1.0 -0.9707 -0.1200 1.0
C -----
313 3 p 2.1839 -0.0664 0.0 2.1773 -0.0003 -1.0 2.1773 -0.0003 1.0
314 3 p 2.1799 -0.0269 0.0 0.9707 -0.1470 -1.0 0.9707 -0.1470 1.0
315 3 p 2.1773 -0.0003 0.0 0.9707 -0.1200 -1.0 0.9707 -0.1200 1.0
C -----
316 3 p -2.1839 -0.0664 0.0 -2.2478 -0.0840 -1.0 -2.2478 -0.0840 1.0
317 3 c/z -2.1839 -0.0664 0.0396875
318 3 c/z -2.1839 -0.0664 0.0663575
C -----
319 3 p 2.1839 -0.0664 0.0 2.2478 -0.0840 -1.0 2.2478 -0.0840 1.0
320 3 c/z 2.1839 -0.0664 0.0396875
321 3 c/z 2.1839 -0.0664 0.0663575
C
C ----- ss304 sleeve surfaces (adjusted dimensions) -----
C the analytic volume of these surfaces in cell 2 calculate to 3.134781858 cc

```

```

C
201 px -2.5019
202 px -2.2606
203 px 2.2606
204 px 2.5019
C -----
205 py -3.81425196
206 py -3.78587
207 py -3.7461825
208 py 3.7461825
209 py 3.78587
210 py 3.81425196
C -----
211 pz -0.153035
212 pz -0.12465304
213 pz -0.08496554
214 pz 0.08496554
215 pz 0.12465304
216 pz 0.153035
C -----
217 c/x 3.7461825 0.08496554 0.0396875
218 c/x 3.7461825 0.08496554 0.06806946
C -----
219 c/x 3.7461825 -0.08496554 0.0396875
220 c/x 3.7461825 -0.08496554 0.06806946
C -----
221 c/x -3.7461825 0.08496554 0.0396875
222 c/x -3.7461825 0.08496554 0.06806946
C -----
223 c/x -3.7461825 -0.08496554 0.0396875
224 c/x -3.7461825 -0.08496554 0.06806946
C
C ----- major core body surfaces (max dimensions, min radii) -----
C the analytic volume of these surfaces in cell 1 calculate to 6.958542864 cc
C
101 1 px -2.23901
102 1 px 2.23901
103 1 py -3.71221
104 1 py 3.71221
105 1 pz -0.10668
106 1 pz 0.10668
C ----- minor core body surfaces -----
107 1 px -2.159635
108 1 px -1.60401
109 1 px 1.60401
110 1 px 2.159635
C -----
111 1 py -3.632835
112 1 py -3.07721
113 1 py 3.07721
114 1 py 3.632835
C -----
115 1 pz -0.027305
116 1 pz 0.027305
C -----
117 1 c/z -1.60401 3.07721 0.555625

```

118 1 c/z -1.60401 3.07721 0.635
 119 1 c/z 1.60401 3.07721 0.555625
 120 1 c/z 1.60401 3.07721 0.635
 121 1 c/z -1.60401 -3.07721 0.555625
 122 1 c/z -1.60401 -3.07721 0.635
 123 1 c/z 1.60401 -3.07721 0.555625
 124 1 c/z 1.60401 -3.07721 0.635
 C -----
 125 1 c/y -2.159635 -0.027305 0.079375
 126 1 c/y -2.159635 0.027305 0.079375
 127 1 c/y 2.159635 -0.027305 0.079375
 128 1 c/y 2.159635 0.027305 0.079375
 C -----
 129 1 c/x 3.632835 -0.027305 0.079375
 130 1 c/x 3.632835 0.027305 0.079375
 131 1 c/x -3.632835 -0.027305 0.079375
 132 1 c/x -3.632835 0.027305 0.079375
 C -----
 133 1 tz -1.60401 3.07721 -0.027305 0.555625 0.079375 0.079375
 134 1 tz -1.60401 3.07721 0.027305 0.555625 0.079375 0.079375
 135 1 tz 1.60401 3.07721 -0.027305 0.555625 0.079375 0.079375
 136 1 tz 1.60401 3.07721 0.027305 0.555625 0.079375 0.079375
 137 1 tz -1.60401 -3.07721 -0.027305 0.555625 0.079375 0.079375
 138 1 tz -1.60401 -3.07721 0.027305 0.555625 0.079375 0.079375
 139 1 tz 1.60401 -3.07721 -0.027305 0.555625 0.079375 0.079375
 140 1 tz 1.60401 -3.07721 0.027305 0.555625 0.079375 0.079375
 C

C ---- pu alloy per Catherine 7/7/14 -----
 C ----- 105.136 grams of alloy (sum)
 m1 94239 -98.87 &
 94240 -4.697 &
 94241 -0.0032 &
 94242 -0.0049 &
 95241 -0.4021 &
 13027 -1.1584
 C ---- ss304 per Huntsman 1 July 1983 -----
 C ----- 24.765 grams of ss304 (sum)
 m2 26000 -17.262 & \$ added 1.002 to get proper sum
 24000 -4.57 &
 28000 -2.22 &
 25055 -0.42 &
 14000 -0.118 &
 42000 -0.079 &
 29000 -0.069 &
 6000 -0.016 &
 15031 -0.006 &
 16000 -0.005
 C ---- carbon steel @ 7.82 g/cc -----
 m3 26000 -0.994 &
 6000 -0.006
 c ---- poly 0.967 g/cc -----
 m5 1001 2
 6000 1
 mt5 poly
 m6 13027 -1.0

```

c   Ta, 16.69
m7  73181 0.99988
    73180 0.00012
C -----
mode n
kcode 10000 1.0 97 1250
ksrc 0 0 0
tr1  0.0   -0.073659 0.0
tr3  0.000001 3.7856  0.0
*tr5 0 0 0 90 0 90 180 90 90 90 90 0
tr6  1.3 -1.3 0
C -----
C -----
c Neutron Groups
e0  1.00E-11 1.00E-10 5.00E-10 7.50E-10 1.00E-09 1.20E-09
    1.50E-09 2.00E-09 2.50E-09 3.00E-09 4.00E-09 5.00E-09 7.50E-09
    1.00E-08 2.53E-08 3.00E-08 4.00E-08 5.00E-08 6.00E-08
    7.00E-08 8.00E-08 9.00E-08 1.00E-07 1.25E-07 1.50E-07 1.75E-07
    2.00E-07 2.25E-07 2.50E-07 2.75E-07 3.00E-07 3.25E-07
    3.50E-07 3.75E-07 4.00E-07 4.50E-07 5.00E-07 5.50E-07 6.00E-07
    6.25E-07 6.50E-07 7.00E-07 7.50E-07 8.00E-07 8.50E-07
    9.00E-07 9.25E-07 9.50E-07 9.57E-07 1.00E-06 1.01E-06 1.02E-06
    1.03E-06 1.04E-06 1.05E-06 1.06E-06 1.07E-06 1.08E-06
    1.09E-06 1.10E-06 1.11E-06 1.12E-06 1.13E-06 1.14E-06 1.15E-06
    1.18E-06 1.20E-06 1.23E-06 1.25E-06 1.30E-06 1.35E-06
    1.40E-06 1.45E-06 1.50E-06 1.59E-06 1.68E-06 1.77E-06 1.86E-06
    1.94E-06 2.00E-06 2.12E-06 2.21E-06 2.30E-06 2.38E-06
    2.47E-06 2.57E-06 2.67E-06 2.77E-06 2.87E-06 2.97E-06 3.00E-06
    3.05E-06 3.15E-06 3.50E-06 3.73E-06 4.00E-06 4.75E-06
    5.00E-06 5.40E-06 6.00E-06 6.25E-06 6.50E-06 6.75E-06 7.00E-06
    7.15E-06 8.10E-06 9.10E-06 1.00E-05 1.15E-05 1.19E-05
    1.29E-05 1.38E-05 1.44E-05 1.51E-05 1.60E-05 1.70E-05 1.85E-05
    1.90E-05 2.00E-05 2.10E-05 2.25E-05 2.50E-05 2.75E-05
    3.00E-05 3.13E-05 3.18E-05 3.33E-05 3.38E-05 3.46E-05 3.55E-05
    3.70E-05 3.80E-05 3.91E-05 3.96E-05 4.10E-05 4.24E-05
    4.40E-05 4.52E-05 4.70E-05 4.83E-05 4.92E-05 5.06E-05 5.20E-05
    5.34E-05 5.90E-05 6.10E-05 6.50E-05 6.75E-05 7.20E-05
    7.60E-05 8.00E-05 8.02E-05 9.00E-05 1.00E-04 1.08E-04 1.15E-04
    1.19E-04 1.22E-04 1.86E-04 1.95E-04 2.08E-04 2.10E-04
    2.40E-04 2.85E-04 3.05E-04 5.50E-04 6.70E-04 6.83E-04 9.50E-04
    1.15E-03 1.50E-03 1.55E-03 1.80E-03 2.20E-03 2.29E-03
    2.58E-03 3.00E-03 3.74E-03 3.90E-03 6.00E-03 8.03E-03 9.50E-03
    1.30E-02 1.70E-02 2.50E-02 3.00E-02 4.50E-02 5.00E-02
    5.20E-02 6.00E-02 7.34E-02 7.54E-02 8.24E-02 8.50E-02 1.00E-01
    1.28E-01 1.50E-01 2.00E-01 2.70E-01 3.30E-01 4.00E-01
    4.20E-01 4.40E-01 4.70E-01 5.00E-01 5.50E-01 5.73E-01 6.00E-01
    6.70E-01 6.79E-01 7.50E-01 8.20E-01 8.61E-01 8.75E-01
    9.00E-01 9.20E-01 1.01E+00 1.10E+00 1.20E+00 1.25E+00 1.32E+00
    1.36E+00 1.40E+00 1.50E+00 1.85E+00 2.35E+00 2.48E+00
    3.00E+00 4.30E+00 4.80E+00 6.43E+00 8.87E+00 1.00E+01 1.28E+01
    1.38E+01 1.46E+01 1.57E+01 1.73E+01 2.00E+01
f4:N (1<7<9<(11 19 25 35 41 47 52 57 65 75 85 93))
fm4 1 1 -6
sd4 6.958542864
print

```

Appendix B: Design Drawings

(Provided as separate PDFs)

Appendix C: Separation Distance Study for Estimating Critical Configurations

A series of MCNP calculations has been performed to investigate the effect of assembly separation for Pu ZPPR experiments without tantalum and for experiments diluted with tantalum. The modeled experiment configuration consists of half of the total number of fuel plate layers placed above the aluminum upper support platen, and the other half below the support platen. The distance between the aluminum support platen and the top of the lower half fuel plate layers was varied to study the separation effect. Figure C.1 shows a screen capture in the YZ direction for a case, bl_1_6g of Table C-1. This configuration is composed of six fuel plate layers with 1" thick polyethylene plates (shown in green). The separation distance of this configuration is 1", and the calculated $k_{\text{eff}} \pm \sigma$ was 0.9671 ± 0.0003 .

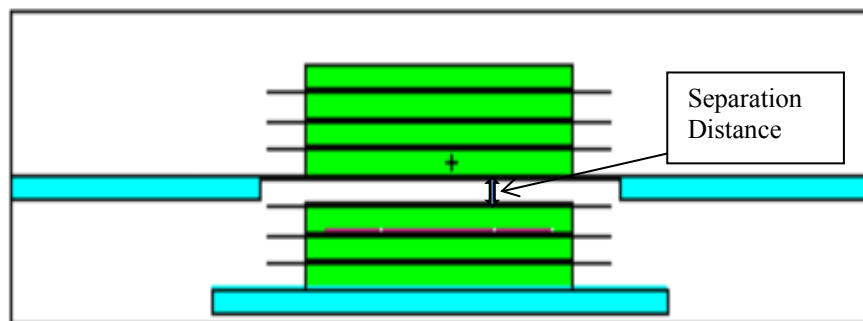


Figure C.1. MCNP Model of an Experimental Configuration Showing Separation between Two Half Assemblies.

Five different experimental configurations were selected for the study. These are the fuel plate layers with 0", 1/16", 3/16", 7/16" and 1" thick polyethylene plates. Number of critical or above critical configuration was iteratively determined and the half bottom fuel assembly was lowered by 0.125", 0.25", 0.5", and/or 1" until the system became subcritical. Table C-1 summarizes MCNP results for configurations without tantalum. Results indicate that Δk_{eff} reduction for a separation distance of 0.125" is about 0.0125. For the last case of Table 1 (1" polyethylene case), a critical configuration is achieved with 0.5" separation between the two half assemblies.

ZPPR experiments diluted with tantalum for the five different polyethylene thicknesses were also analyzed. Table C-2 summarizes MCNP results. Because the calculated k_{eff} s are critical for 0", 1/16", 3/16", and 7/16" polyethylene cases, additional calculations were not performed. For 1" polyethylene case, the separation distance was varied by 0.125" and increased to 0.25".

Calculated Δk_{eff} for the separation distance of 0.125" was about 0.005, which was less than a half of the case without tantalum. This is due to more thermalized neutron spectrum with introduction of tantalum that has significant thermal absorption property. Note that the number of fuel layers required to make a critical configuration diluted with tantalum is twice (12) the number (6) of fuel plate layers of the case without tantalum.

Table C-1: k_{eff} versus Assembly Separation Distance for Varying Polyethylene Plate Thickness for Cases without Ta.

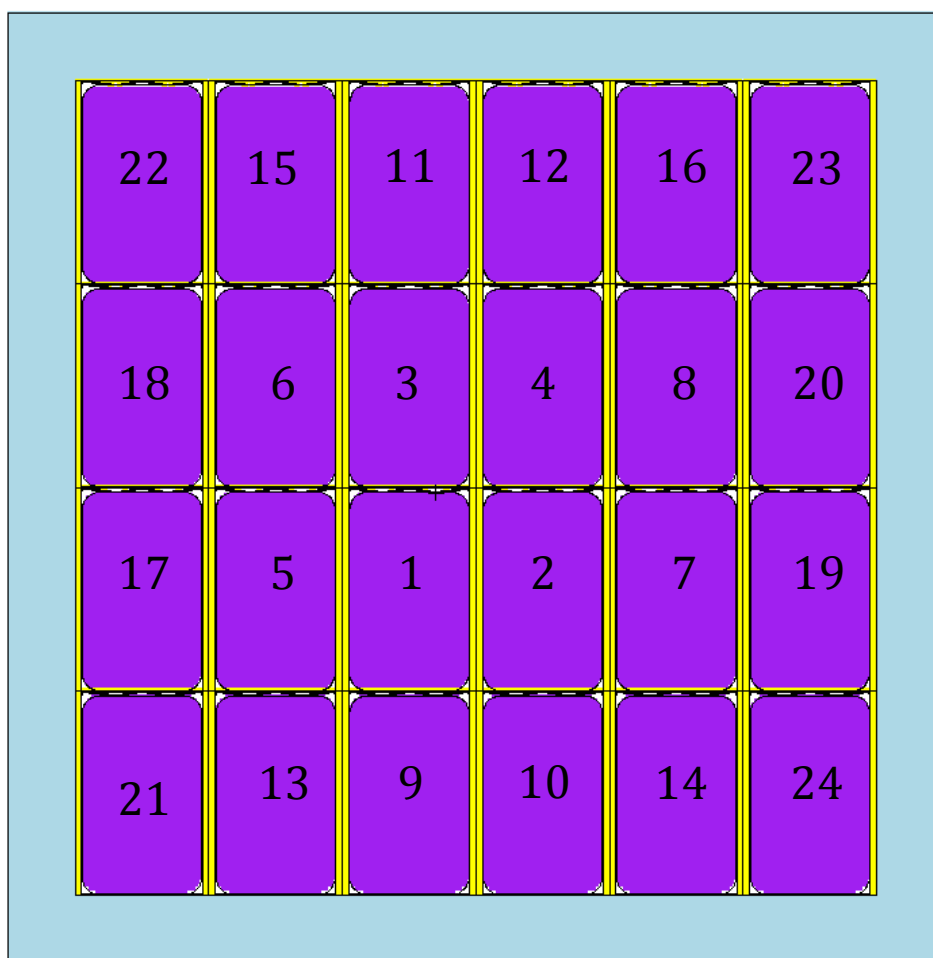
Polyethylene Plate Thickness	Case ID	Separation Distance (Inches)	$k_{\text{eff}} \pm \sigma$
0	bl_0_21c	0	1.0298 ± 0.0002
	bl_0_21d	0.125	1.0162 ± 0.0003
	bl_0_21e	0.25	1.0031 ± 0.0002
	bl_0_21f	0.5	0.9786 ± 0.0002
1/16"	bl_116_17c	0	1.0115 ± 0.0003
	bl_116_17d	0.125	0.9992 ± 0.0003
	bl_116_17e	0.25	0.9864 ± 0.0003
3/16"	bl_316_12c	0	1.0115 ± 0.0003
	bl_316_12d	0.125	0.9992 ± 0.0003
	bl_316_12e	0.25	0.9864 ± 0.0003
7/16"	bl_716_8c	0	1.0240 ± 0.0003
	bl_716_8d	0.125	1.0115 ± 0.0003
	bl_716_8e	0.25	0.9914 ± 0.0003
	bl_716_8f	0.5	0.9746 ± 0.0003
1"	bl_1_6c	0	1.0548 ± 0.0003
	bl_1_6d	0.125	1.0427 ± 0.0003
	bl_1_6e	0.25	1.0299 ± 0.0003
	bl_1_6f	0.5	1.0069 ± 0.0003
	bl_1_6g	1	0.9671 ± 0.0003

Table C-2: k_{eff} versus Assembly Separation Distance for Varying Polyethylene Plate Thickness for Cases with Ta.

Polyethylene Plate Thickness	Case ID	Separation Distance (Inches)	$k_{\text{eff}} \pm \sigma$
0	ta_0_26cc	0	1.0048 ± 0.0002
1/16"	ta_116_30cc	0	1.0050 ± 0.0002
3/16"	ta_316_29c	0	1.0002 ± 0.0002
7/16"	ta_716_18c	0	1.0036 ± 0.0003
1"	ta_1_12cc	0	1.0110 ± 0.0002
	ta_1_12d	0.125	1.0059 ± 0.0003
	ta_1_12e	0.25	1.0004 ± 0.0003

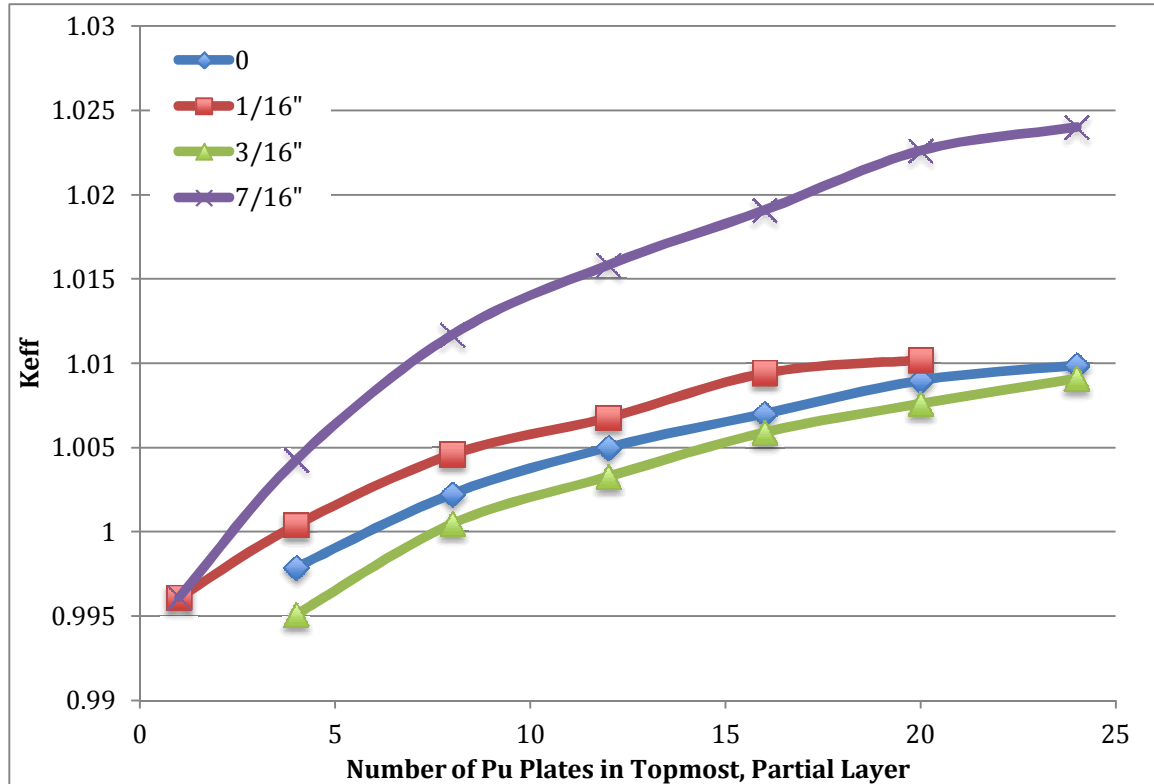
Appendix D: Partial Layer Study for Estimating Critical Configurations

A series of MCNP calculations has been performed to determine if just critical configurations could be constructed with partial layers on top of the TEX experimental stacks. The MCNP models reported in Section 4.1 was modified for these calculations by varying the number of plutonium plates present in the top layer of the experiment. The modeled experiment configurations consist of full Plutonium layers for each layer except the topmost layer. For the top layer, individual Pu plates were added to determine the critical plate number in the pattern shown in Figure D-1. Aluminum plates, “blanks,” were modeled in place of the missing plutonium plates. The top 1” reflector was modeled.

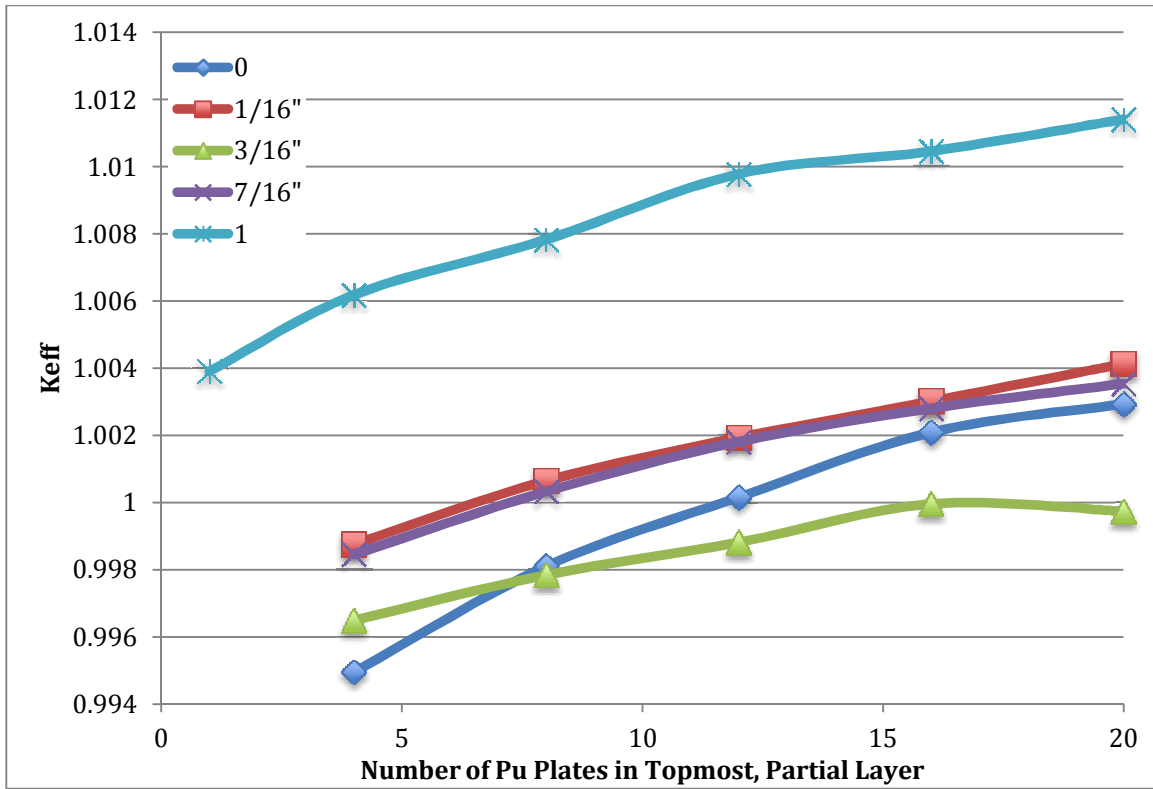


The results of the calculations indicate that just critical ($k_{\text{eff}} = 1$) configurations can be created using partial topmost layers of plutonium in all cases except for the 1" of moderator cases, both with and without tantalum diluents. Instead, these cases can be made just critical either by adding a little thicker upper reflector or separation distance between the two halves.

Figures D-2 and D-3 show the partial layer results for the baseline and tantalum-diluted cases.



D-2: K_{eff} versus Number of Plates in Topmost Partial Plutonium Layer for Plutonium Baseline Experiments.



D-3: K_{eff} versus Number of Plates in Topmost Partial Plutonium Layer for Plutonium Experiments Diluted with Tantalum.